Sound transmission through ceilings from air terminal devices in the plenum: final report

Warnock, A. C. C.

https://doi.org/10.4224/20338214

National Research Council Canada
Conseil national de recherches Canada

NRC · CNRC

Sound Transmission Through Ceilings from Air Terminal Devices in the Plenum

Warnock, A.C.C.

RP-755

A version of this paper was published as :
ASHRAE TC2.6, Final Report RP755
January, 1997

Abstract / Résumé

ASHRAE TC2.6

Final Report RP755

Sound Transmission Through Ceilings from Air Terminal Devices in the Plenum

January 1997

A.C.C. Warnock

Acoustics, IRC

National Research Council Canada.

Table of Contents.

List of Figures.

List of Tables.

1. Introduction.

HVAC sources in ceiling plenums are often major contributors to the noise level in occupied spaces below. Duct work or devices in the plenum, such as Variable Air Volume (VAV) boxes, are typical sources of such noise. The radiated sound passes through the ceiling, often only a few centimeters from the device, and enters the room below. This transmission occurs in addition to sound transmission along ducts and consequent radiation from air supply outlets.

At the beginning of this project the situation with respect to this problem was as follows:

1. There was no standard test method for rating the ability of ceiling materials to reduce the transmission of sound from HVAC components in plenums.
2. It was known that transmission loss results obtained in reverberation room tests according to ASTM E90 [1] did not apply to this situation because of the close coupling between the source and the ceiling panels and the absence of a diffuse sound field in typical plenums.
3. There was no consistent body of information providing designers with typical sound attenuation values for common ceiling types with typical ventilation openings.
4. ARI standard 885-90 [2] provided a method to calculate the sound levels in a room below a plenum containing a sound source. The standard includes a "Plenum/Ceiling Effect" table for use when predicting sound radiation from VAV terminals installed above some typical ceilings. The information used to prepare the standard was provided by a few manufacturers, but it did not form a consistent set based on a standard test procedure or accepted method of measurement.

ASHRAE RP-755 was initiated to investigate the transmission of sound through different ceiling types from different sources with the intent of providing more reliable design information to deal with sound transmission through ceilings close to HVAC devices. The development of the need for this project is discussed further in Section 4.

2. Summary of the investigation.

2.1 Terminal Types.

The aim of project RP755 was to measure the sound pressure level generated in a room below different ceiling types by five types of air terminal units. The terminal types were originally

1. An air-to-air ceiling induction unit
2. A VAV shutoff unit
3. A bypass VAV unit
4. A series flow fan-powered VAV unit
5. A parallel flow fan-powered VAV unit

After some preliminary work, the monitoring committee decided to drop the third unit, the bypass VAV unit, from the list.

To provide a simple and more convenient reference source with good repeatability, a metal box containing two loudspeakers radiating random noise was also used as a source above the ceiling. Two of these VAV simulators were used. One was positioned near the middle of the room, close to the devices begin tested. The second was added late in the project at NRC's initiative and was placed in one corner of the plenum.

At the request of the monitoring committee, a length of unlined duct was introduced to the plenum. This had two loudspeakers mounted internally at one end to generate noise within the duct.

2.2 Standard measurements on each sound source in the RAT room

For each source the sound power was measured in the room acoustics test room (RAT room) in accordance with ANSI S12.31 [3] and ARI 880 [4]. Measurements of power were made using the direct method (measurement of sound pressure level and reverberation time) and the substitution technique (comparison with a reference sound source – an Acculab RSS).

2.3 Ceiling panel types used

Five ceiling panel types were tested supported on a standard T-bar grid. The types were

1. 13 mm gypsum board
2. 50 mm thick vinyl-faced fiberglass
3. 50 mm thick vinyl-faced fiberglass, with an aluminum foil backing
4. 16 mm thick regular mineral fiber tiles

5. 16 mm thick light weight mineral fiber tiles

Toward the end of the project NRC added a 16 mm thick glass fiber tile to the set. In each case the ceiling tiles were simply laid in the T-bar grid; no clips or other devices were used to hold them down.

2.4 Standard reverberation room measurements on each ceiling type.

For each ceiling type the following standard measurements were made in NRC's reverberation rooms:

1. Sound transmission loss according to ASTM E90 with the specimen mounted in a T-bar support system as it was in the test room.
2. Sound absorption according to ASTM C423 [5] with the specimen mounted on an E400 frame as described in ASTM E795 [6] (400 mm air space). For each specimen, except the gypsum board, the specimen was tested twice. Once with the normally-exposed face up and once with it down.
3. Ceiling insertion loss (CIL) by the ASTM draft test method as described in Section 12.

2.5 Routine Measurements in the RAT room.

Each source was installed in the plenum in the RAT room. The sound pressure levels generated by each source in combination with each ceiling type were measured in the room below. As well, each time a ceiling was installed in the RAT room for testing, the sound pressure levels generated in the room by the simulators, the duct and the Acculab reference sound source (RSS), the reverberation times in the room and the spatial attenuation (sound pressure level as a function of distance) from a nominally omni-directional source were measured.

2.6 Additional investigations in the RAT room

2.6.1 Effect of plenum edge absorption.

For most of the testing, the vertical surfaces of the plenum were lined with 100 mm of sound absorptive foam. To examine the effects of changing the sound absorptive properties of the ceiling plenum, a lining of 300 mm thick glass fiber was installed for some measurements and the standard set of measurements in the RAT room were carried out. In all cases the ceiling of the plenum was unlined.

2.6.2 Effect of ceiling openings

The effects of openings in the ceiling were investigated by cutting slots in one set of ceiling tiles and moving the slots to different positions in the room. For each slot position, the sound pressure level in the room was measured. In addition to these slots, a

lighting fixture with an integral air diffusion slot was installed as requested by the monitoring committee, and the changes in room sound pressure level as a result of transmission through it were measured.

2.6.3 Effect of gap between the device and the ceiling.

To establish the importance of gaps between the device and the rear face of the ceiling, the VAV simulator source was installed at several distances from the back face of the A755B ceiling tiles, and sound pressure levels in the room measured.

2.6.4 Effect of room size.

One wall of the RAT room is movable. For a few measurements the room length was increased to investigate the effects of this parameter.

2.6.5 Effect of carpet and wall absorption.

Under normal testing conditions, the RAT room did not have a carpet on the floor; it would have interfered with movement of the microphone system. To examine the effects of additional absorption in the RAT room, a carpet and absorbing wall panels were added for some of the measurements.

3. Major Findings.

This section summarizes the major findings in the report. To a large extent, it is assumed that the reader is already familiar with the project and the area of study. More detailed information can be found in the main body of the report.

The six ceiling types tested are described in more detail in Chapter 6. Throughout the report, coded versions of the tile names are used for brevity. The correspondence between the codes and the type of tile is given in Table 3-1.

Table 3-1: Codes used to identify ceiling types.

Code	Ceiling panel type
A895	16 mm thick Armstrong type 895 Fireguard mineral fiber tiles
A755B	16 mm thick Armstrong type 755B Minaboard mineral fiber tiles
G13	13 mm vinyl-faced gypsum board
FGvin	50 mm thick glass fiber tile with perforated vinyl face
FGTL	50 mm thick glass fiber tile with perforated vinyl face and metal foil backing
A2910	16 mm thick Armstrong type A2910 random fissure perforated glass fiber tiles

The difference between the sound power, L_w, of a given device placed in the plenum and the average sound pressure level, $<L_p>$, in the room below measures the combination of the "plenum/ceiling effect" and the average "space effect". These terms are defined in ARI 885 [2] as

> *Plenum/Ceiling Effect*: The difference between the octave band sound power level from the source located in the plenum/ceiling cavity and the sound power level transmitted to the occupied space.
>
> *Space Effect*: The difference between the octave band sound power level entering the occupied space and the resulting octave band sound pressure level at a specific point in an occupied space.

3.1 Ceiling attenuations.

To see the average L_w - $<L_p>$ for each type of ceiling tile, the attenuations for all the sources used were averaged. The resulting graph is shown in Figure 3-1. The interesting

feature of this graph is the small differences between tiles with the exception of the G13 and A2910 tiles.

The result for the G13 tiles perhaps is in itself somewhat surprising. One might have expected that these heavier tiles would have given much lower levels in the room than the other lighter tiles. The conclusion drawn from this research work is that for most of the tiles used, the dominant path through the ceiling is the leakage between the edges of the tiles and the T-bars. For the mineral fiber and glass fiber tiles there will be different relative amounts of sound power transmitted due to leakage, absorption on the rear face and at the edges, and transmission through the body of the tile. The results show that for the mineral fiber tiles and the thick glass fiber tiles the type is not too important.

The light A2910 tiles provide little attenuation through the body of the tile at high frequencies and for the gypsum board tiles, there is no sound absorbing material to offset the effects of the leaks around the edges of the tiles. These two types of tiles are quite different from the others but are perhaps not typical of products used below air terminal units.

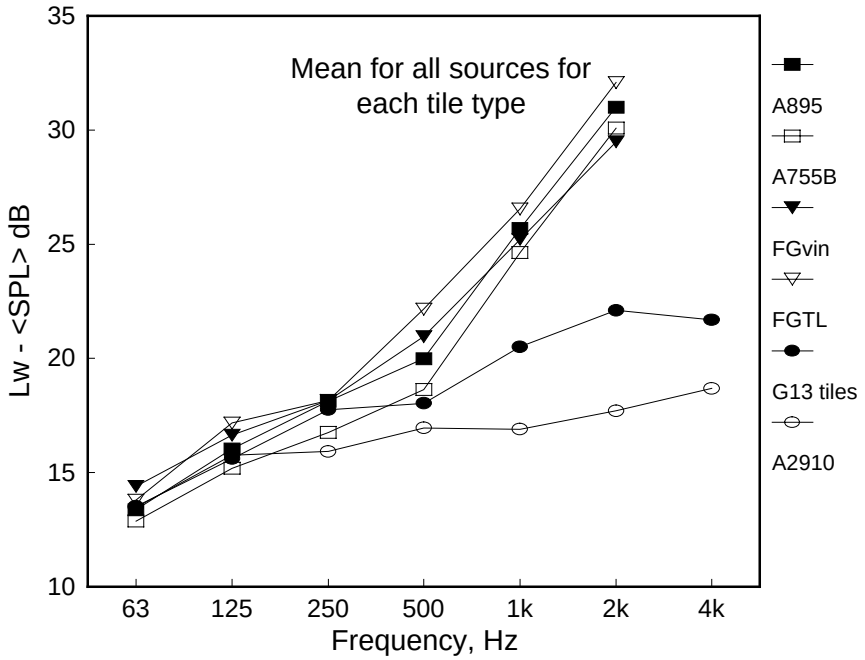

Figure 3-1: Average of L_w - $<L_p>$ for all sources for each type of ceiling tile.

One conclusion that can be drawn from this result is that since most normal tiles give about the same result, there is little point in creating a test procedure to rate the effectiveness of ceiling tiles as attenuators of sound from air terminal units. The sound powers of the devices tested all decreased fairly rapidly as frequency increased. So, even the poor attenuation of the G13 and A2910 tiles at high frequencies is not likely to be important. On the other hand, different mounting systems for the tiles give more attenuation so it may still be deemed advisable to create a test procedure.

3.2 Ceiling Attenuation compared with ARI 885 values.

The attenuations measured for the different ceiling types, do not agree well with those predicted from values given in ARI 885. The values given in ARI 885 in the table for Ceiling/Plenum effect do not include any attenuation for propagation in the room below, so they were corrected according to the standard using the mean distance from the microphones to the source and the room volume as parameters in the Schultz [7] expression. This allows direct comparisons with the measured data which are shown in Figure 3-2 to Figure 3-4. The best agreement is for the 16 mm thick mineral fiber tiles, but even there, the differences are rather large.

The data in ARI 885 for gypsum board are for a solid sheet, not tiles as were tested in this project. To provide some estimate of what might have been measured if a solid ceiling had been used, the measured G13 data were adjusted using the data measured in the E90 tests for the taped and un-taped installation of the G13 tiles (See Chapter 9.3). The differences between the transmission loss values for the taped installation and the un-taped installation were added to the values measured in the RAT room for the un-taped tiles. The adjusted values are still not as high as those given in the ARI 885 guide. The same procedure was followed using the second set of CIL data (See Chapter 12). The resulting curve is not very different from that derived using the E90 results.

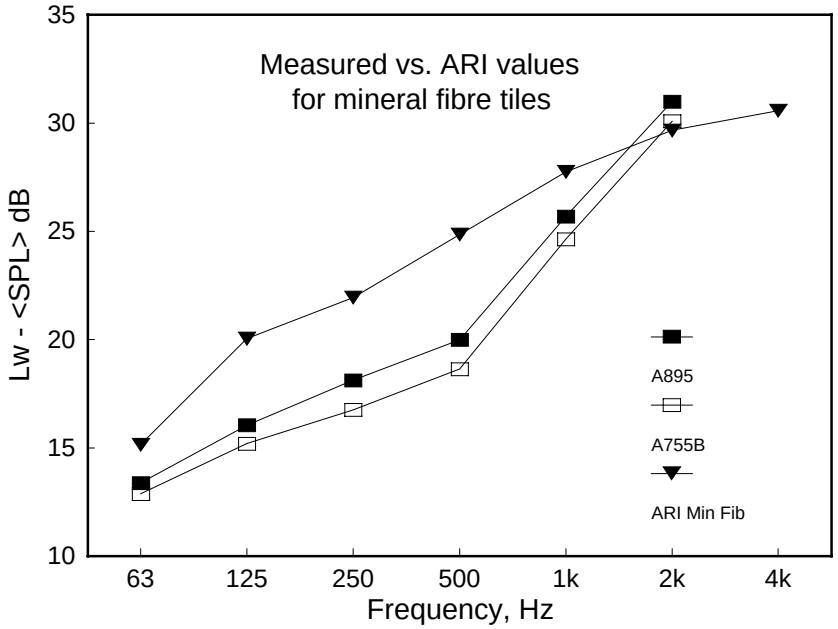

Figure 3-2: Sound power minus average room sound pressure level for measured cases and ARI 885 values — mineral fiber tiles.

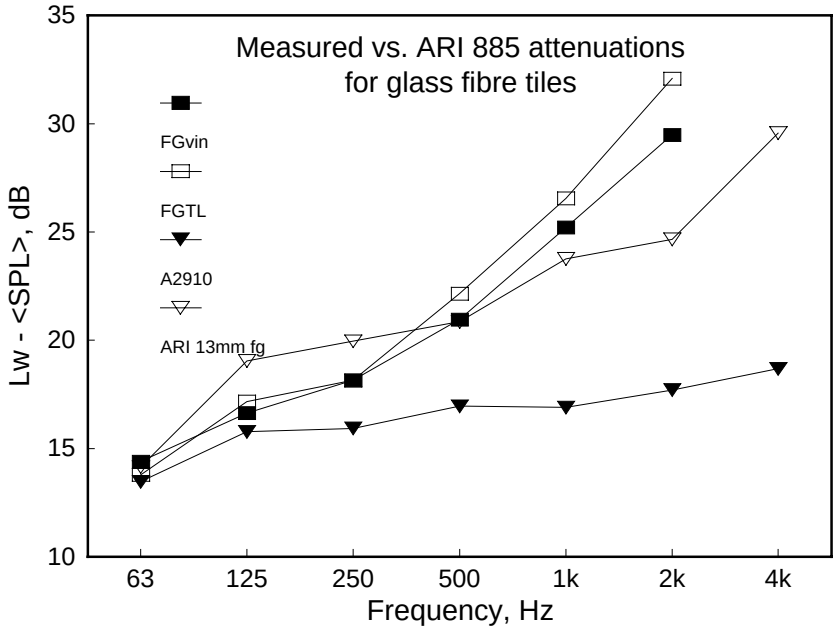

Figure 3-3: Sound power minus average room sound pressure level for measured cases and ARI 885 values — glass fiber tiles.

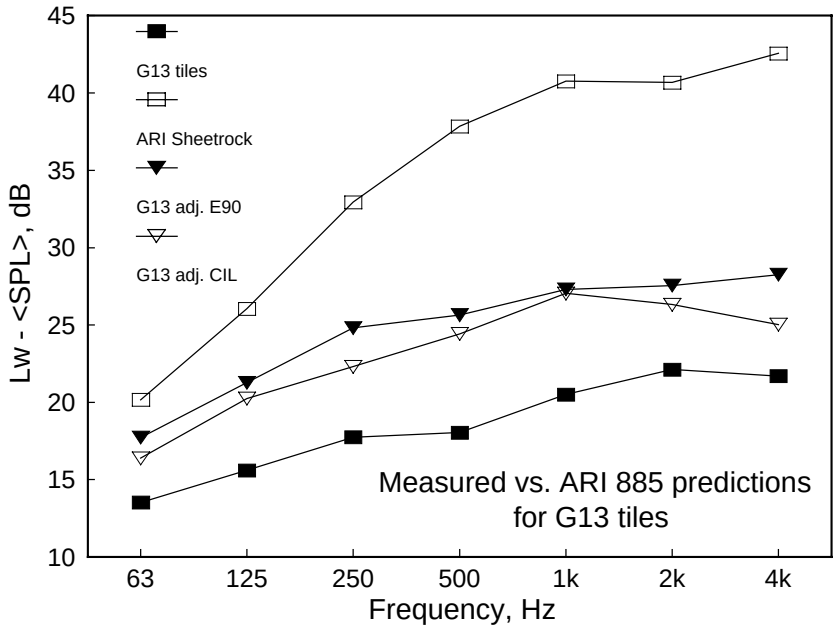

Figure 3-4: Sound power minus average room sound pressure level for measured cases and ARI 885 values — gypsum board tiles.

3.3 Differences between sources.

Figure 3-5 shows for each source the average attenuation for all the ceiling types used. If the sound power emitted by the device were not altered by the presence of the ceiling, if

the attenuation provided by the ceiling were constant, and if there were no interaction between the device and the ceiling, then all of these curves would be approximately the same. There are, however, quite significant differences at and below 250 Hz among the devices. The conclusion to be drawn from this graph is that the coupling between the ceiling tiles and the source influences the sound power radiated into the room below the ceiling. This makes it difficult to accurately predict the sound pressure level in the room below using only sound power levels for the device measured under standard conditions in a reverberation room or a hemi-anechoic space and some fixed insertion loss values for the ceiling tiles.

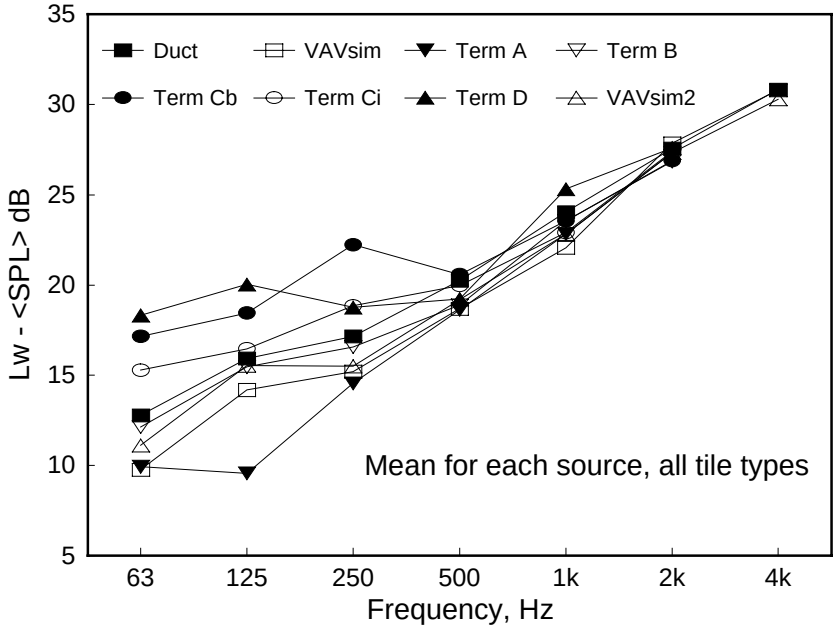

Figure 3-5: Average of L_w - $<L_p>$ for all ceilings for each type of source.

3.4 Dependence of ceiling attenuation on source area.

Examination of the data collected revealed a fairly strong correlation between the effective ceiling attenuation and the area of the surface of the source closest to the ceiling. As the area increased, so did the ceiling attenuation. This correlation explains much of the scatter at low frequencies in Figure 3-5. No physical model or analytical expression has been found to explain this dependence. The most that can be said is that the ceiling interacts with the lower face of the terminal unit so as to decrease the power radiated from that face. The empirical model developed is embodied in the following equation:

$$SPL(f) = Power(f) - Attenuation(f) + Slope(f) \times (Area - 0.83).$$

where the term 0.83 is an empirical constant determined from the measured data, and

SPL(f) is the average sound pressure level in the room, dB,

Power(f) is the power emitted by the terminal unit when tested according to

standards, dB

Attenuation(f) is the nominal attenuation of the ceiling tiles, dB,

Slope(f) is the slope of the regression of attenuation on area, dB/m^2 ,

Area is the area of the lower face of the terminal unit, m^2,

f is the mid-band frequency of the octave band, Hz.

The values of *slope* found from experiment are given in Table 3-2, together with the standard error (SE) of the estimate of sound pressure level and the square of correlation coefficient for measured versus predicted level.

Table 3-2: Parameters for empirical model for predicting average room sound pressure level from device power, ceiling attenuation and device face area.

Frequency, Hz	63	125	250	500	1k	2k	4k
Slope, dB/m^2	4.4	4.1	2.5	0	0	0	0
SE, dB	1.7	1.9	2.2	1.3	1.3	1.2	2.4
r squared	0.90	0.97	0.96	0.99	0.99	0.99	0.98

3.5 Spatial attenuation.

When a nominally omni-directional source was placed in the room *below* the ceiling, the attenuation of sound with distance in the room was approximately 3 dB/distance doubling (dB/dd), that is to say the sound pressure level had a 10 log *r* dependence as suggested by the Schultz [7] formula. At each frequency, however, the attenuation with distance depended on the reciprocal of the room reverberation time. Additionally, the spatial attenuation showed a dependence on the absorption coefficient measured for the ceiling tiles according to ASTM C423 in the NRC reverberation room. This is not surprising since the ceiling tiles were the only significant sound-absorbing elements in the room. There is no dependence on absorption in the Schultz formula. The dependence found in this work, while quite clear, is not very important relative to other factors.

When the source was *above* the ceiling in the plenum, the sound field in the room below varied very little with distance from the source; the Schultz formula does not apply. Except at 2000 and 4000 Hz, the attenuation is less than 1 dB/dd. ARI 885 specifies the use of the Schultz formula and so is inaccurate in this respect.

3.6 Environmental Adjustment Factor.

The environmental effect specified by ARI 885 to allow for the difference between free-field and reverberant room sound power measurements, seems somewhat too large. This conclusion rests on the experimental work presented later and the work done by Vorländer [8, 9]. Slightly lower values are suggested in Section 4.4.

3.7 Effect of Plenum and Room absorption.

Placing 100 mm of sound absorbing foam on the four vertical surfaces of the plenum reduced the sound pressure levels in the room below by as much as 6 dB from 125 to 1000 Hz. Replacing the foam with 300 mm thick glass fiber batts further reduced the levels by about 1 dB at and above 250 Hz. At 63 and 125 Hz the reductions were about 4 dB. A carpet on the floor and twelve FGvin ceiling tiles to the walls further reduced sound pressure levels by about 2 dB at frequencies above 250 Hz.

The normal condition of the room during tests was with 100 mm foam on the plenum surfaces and no carpet or wall absorbers. Thus the ceiling attenuations found in this work can be considered to be conservative for heavily furnished rooms or plenums containing large amounts of sound absorbing material.

3.8 ARI 885 recommendations.

Based on the work in this project, Section 18 provides recommended procedures to calculate the sound pressure level in a room below a terminal unit. These same procedures should be incorporated into the relevant ASHRAE publications.

3.9 Ceiling Attenuation and Standard Ceiling Test Procedures.

This work has shown that insertion losses for ceiling systems cannot readily be obtained from standard measurements in reverberation rooms or two-room facilities using existing standards. As mentioned above, there seems little point in introducing a special test for this situation since most commonly used tiles, with some exceptions, will give about the same attenuation. As well, because of the uncertain amount of leakage through the ceiling systems and the additional leakage due to air-supply devices, the insertion losses for different installations of the same tiles will vary somewhat. This conclusion might not be valid for tiles with improved support systems that significantly reduced leakage around the tile edges.

4. Background.

The focus of this research project was on the interactions between terminal units (positioned above and close to a lay-in ceiling), the ceiling panels themselves, the plenum and the room below. The aim was to improve methods of predicting sound pressure levels in the room below the ceiling from known physical quantities and standard acoustical measurements of the elements involved. There is almost no information in the acoustical literature dealing directly with this situation, although some studies are partially relevant. To meet the need for a prediction scheme, standard ARI 885 was developed using the best information available at the time. A major goal of this research project was to evaluate the methods used in ARI 885 and suggest improvements where necessary.

4.1 Relevant research.

Around 1980, with the increasing popularity and use of variable air-volume terminal boxes, noise problems associated with them became more prominent. A major portion of the roaring noise experienced in a room comes from the casing-radiation of the terminal boxes and duct break-out from these units located in the ceiling plenum. In a study sponsored by ARI, Blazier [10] identified some of the reasons why noise problems were being experienced in the field with the application of these boxes.

Blazier found that measured values of sound power level for nine variable air-volume terminal boxes did not agree well with the data available from manufacturer's catalogs; measured values were on average about 7 dB below catalog values in all octave bands from 125 Hz to 4 kHz with standard deviations as high as 10 dB. (See Figure 4-1)

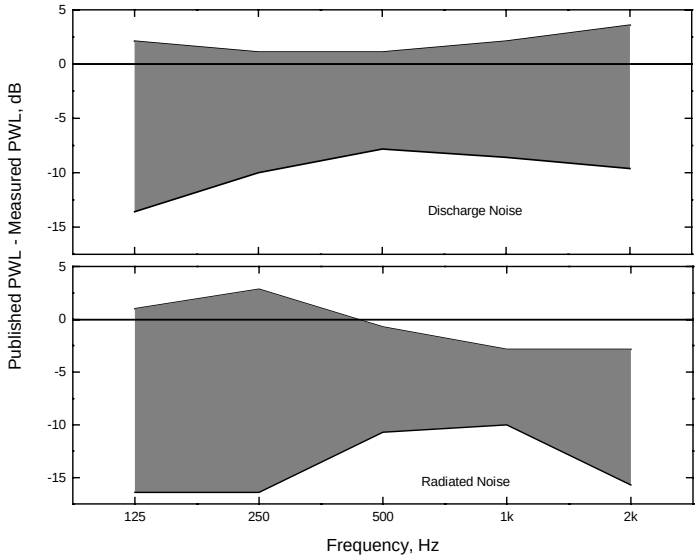

Figure 4-1: Blazier's comparison of measured sound power data with catalog data for nine variable air-volume terminal boxes. The measured values lay within the shaded areas.

To complicate matters further, the insertion loss to be used to account for the presence of the ceiling tiles was not well known. As defined in ARI 885, the plenum/ceiling effect refers to the reduction in sound power level transmitted to the occupied space caused by the presence of the plenum/ceiling. Prior to the existence of Standard 885, the common practice was to subtract 10 dB from the level of the casing-radiated noise to account for the transmission loss of the ceiling. According to Blazier [11], this step, compounded by subtracting 10 dB at all frequencies to account for the room-effect (discussed below), could lead to under-estimating the room sound pressure level by 10-12 dB. Blazier presented data, reproduced in Figure 4-2, that showed values for ceiling insertion loss much lower than 10 dB and very little difference between types of ceiling tiles.

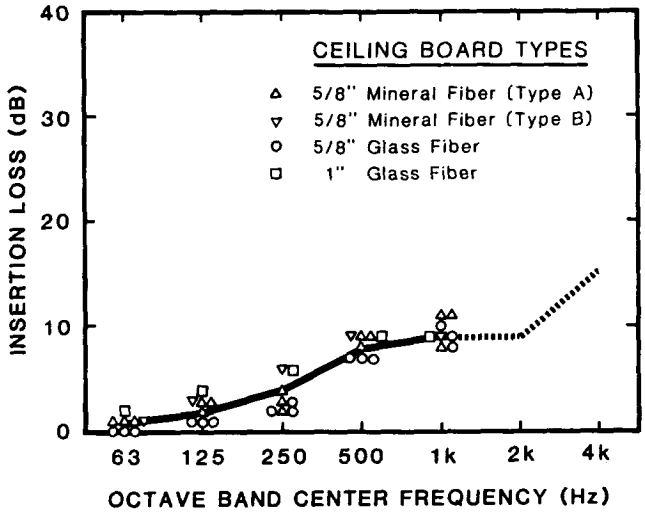

Figure 4-2: Blazier's measurements of insertion loss for different types of ceiling tile.

Another problem identified by Blazier was the uncertainty when converting from sound power level to sound pressure level in normal rooms. Calculation procedures based on Diffuse Field Theory of sound propagation in rooms [12] are clearly not applicable in a modern office building. Due to the presence of absorbing ceilings, scattering objects, and floor coverings, the sound field is not likely to be diffuse. Blazier presented measurements of the reduction of sound pressure level with distance from a source. There was poor agreement with diffuse field theory and no sign of a reverberant field being developed. The practice in use at the time of converting to mean room sound pressure level by subtracting 10 dB from the sound power level was clearly not adequate to account for the effect of the room and its contents. In too many cases this approach failed.

In ASHRAE research project, RP-339, Schultz [7] investigated the conversion from sound power level to sound pressure level in the room in some detail. After reviewing the existing literature dealing with sound propagation in non-Sabine spaces (spaces not

satisfying the requirements of diffuse field theory), he concluded that none of the available theories was satisfactory for typical dwellings or offices. Schultz collected an extensive set of experimental data in rooms ranging in volume from 322 to 40,000 ft^3, with most between 1,100 and 3,000 ft^3, and a range of furnishing from nearly bare to normal. Based on this data, he developed a simple empirical formula that was subsequently incorporated into the ASHRAE Handbook and used in ARI 885. Schultz' formula is

$$L_p = L_w - 10\log r - 5\log V - 3\log f + K$$

where L_p is the sound pressure level in dB re 20 μPa
L_w is the sound power level in dB re 1 pW
r is the shortest distance from the noise source to the receiver
V is the volume of the room
f is the mid-band frequency for the octave band of interest, and
K is a constant equal to 25 when r, and V are in feet and cubic feet respectively and equal to 12 when r, and V are in metres and cubic metres

Many were surprised that there was no explicit term in this equation to account for the amount of sound absorption in the room. It should be remembered that this equation is a fit to measured data and has specified limited application.

Industry Standard ARI 885 [2] was developed to provide a consistent method for predicting sound pressure levels in a room below a ceiling with a plenum containing air-handling devices. In an overview of this standard, Ebbing and Waeldner [13] identified two key items as possible barriers to the production and acceptance of the standard. They are (1) the uncertainties associated with the ceiling and plenum effect and (2) the tolerance or prediction uncertainty that could be achieved. So far, there are only two published reports [14, 15] showing comparison between predictions and measurements in mock-up conditions.

The transfer functions in ARI 885 for the ceiling materials were estimated from measurements of sound attenuation obtained by several manufacturers. The sources were fan boxes with areas around 1 m^2 and the plenums were about 3 ft deep. The rooms where the measurements were made had volumes in the range 22,000 to 25,000 ft^3.

A substantial amount of sound transmission data is available for different ceiling types measured according to ASTM E1414 in a two-room facility. Despite considerable work in the area [16, 17, 18, 19, 20], no acceptable method has been developed for estimating the random-incidence single-pass transmission loss as determined in a reverberation room suite from these double-pass data. A recent, rather complicated paper gives the most thorough treatment yet [21]. In his concluding remarks, the author notes that his analytical model is simplified with respect to a real suspended ceiling; the model uses a homogeneous plate for the ceiling. The author also shows the significant differences in

measured sound transmission that can arise for mineral fiber tiles that differ only in their mounting systems (Figure 4-3).

There has been no work to link double-pass data to the case under study here where the source is very close to the ceiling tiles. In any case, the validity of using double-pass data for formulating the plenum/ceiling effect is questionable because there are no source/plenum and source/ceiling interaction effects.

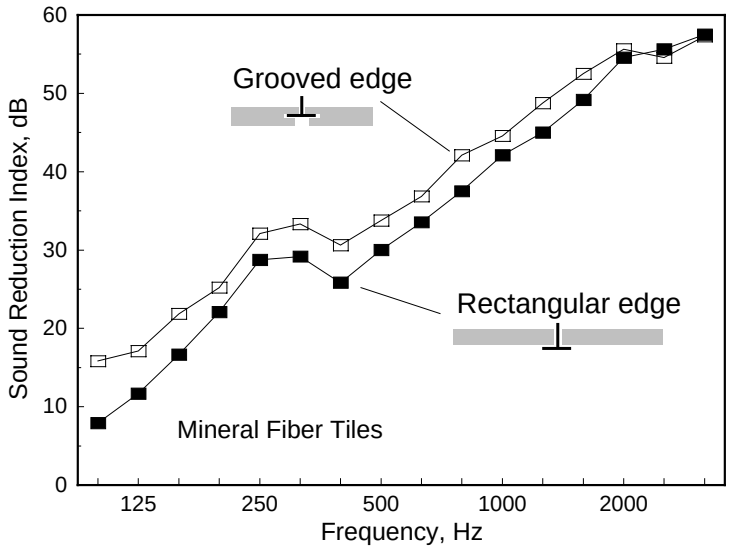

Figure 4-3: Measured sound transmission loss of suspended ceilings made from compressed mineral fiber board, differing only in their mounting systems [21].

4.2 Close-fitting acoustical enclosures

Conventional sound transmission loss theory and measurement applies to sound transmission between rooms or through enclosures when the volume of the source of noise in the enclosure is small relative to the enclosure volume and the source is not close to the enclosure. When these conditions are not satisfied, then transmission loss values for the enclosure walls determined in reverberant rooms in accordance with ASTM E90, will give misleading estimates of the enclosure insertion loss.

Two phenomena are important when the source of sound is close to the surface of an enclosure. First the enclosure can load the source and alter the emitted sound power. To what extent this occurs will depend on the internal impedance of the source. Second, resonances in the air space between the source and the enclosure can lead to large changes in the insertion loss.

Fairly detailed reviews of the research work done on close-fitting enclosures can be found in some handbooks [22, 23]. Since most of the work is only partially relevant to the problem addressed in this work, only a short overview is given here.

Attempts to model close-fitting enclosures probably started with Jackson's one-dimensional model [24, 25] which assumed infinite flat surfaces. Junger extended this theory [26], modeling the enclosure wall and the source surface as finite surfaces. Air loading of the panel and coincidence effects were also included. Tweed and Tree [27] evaluated these theoretical models and another model by Vér [28]. They concluded from their measurements that all of these models were inadequate for design purposes. A further refinement to the one-dimensional models was subsequently proposed by Tweed and Tree [29] which gave better agreement at low frequencies. However, their predictions are characterized by severe resonance effects, since damping was not included. Oldham and Hillarby [30, 31] proposed yet another theory, not applicable to the plenum/ceiling situation, for small, close-fitting enclosures with panel dimensions of less than 1 m.

The simple model proposed by O'Keefe and Stewart [32] assumed that the insertion loss was equal to the wall transmission loss minus the sound pressure level increase resulting from the presence of standing waves. Comparisons with experimental results obtained by the authors are fairly good but the model is not useful for air-terminals in plenums. The small spaces typically encountered between the terminal and the ceiling should, according to the theory, only lead to differences from random-incidence TL values at and above $c/2d$, where c is the speed of sound and d is the cavity depth. For spaces around 50 mm, this frequency is around 6 kHz thus the theory says there should be no difference from E90 results below 6 kHz. This not in agreement with what was observed in this project and other work.

Some of the important parameters that determine the insertion loss for a free-standing, close-fitting enclosure are listed in reference [23] and repeated here. If the enclosure is well sealed, then the insertion loss depend on (1) the thickness, size, and material of the enclosure wall; (2) the edge conditions of the wall plates and their loss factors; (3) the vibration pattern of the machine surface; (4) the average thickness of the air gap between the enclosure surface and the radiating device; and (5) the type of sound absorbing material in the gap. Measured data from [33] show that increasing mass or thickness of the enclosure or the air gap between it and the radiating surface increases insertion loss. Sound absorbing material in the airspace reduces the effect of resonances in the airspace and substantially increases the insertion loss above 1 kHz.

Byrne et al. [34] presented a one-dimensional model for a free-standing enclosure, also discussed in [23], that incorporates the effects of enclosure mass, sound absorbing material in the cavity and the depth of the cavity. The model does not allow for possible changes in radiation efficiency due to the interaction of the radiating device and the enclosure.

It is doubtful that any of the above theories can be applied on its own for predicting the plenum/ceiling effect. Many of them did not consider damping within the enclosure and none directly address the issue of a noise source very close to an extended surface that bounds an absorptive, cluttered and shallow plenum. An additional complication is that, as will be seen, real ceilings usually have significant sound leaks. A successful model

would have to combine the effects of a close-fitting barrier (the ceiling), including changes in radiation efficiency, and the complicated path for sound from the device into the plenum (certainly a non-diffuse field) and then through the ceiling with its plethora of service and ventilation openings and leaks.

4.3 ASTM E33 research.

In the early 80s, ASTM committee E33 was asked to look at the problem of measuring the sound transmission through ceiling tiles from air terminal devices close to the rear face of the tiles. A task group was formed and concluded that the most convenient method of test was to mount the tiles in a frame similar to the E400 mount described in ASTM E795 [6]. This approach was thought to have the advantage that tests could be carried out in any existing reverberation room. The source was to be a metal box containing loudspeakers to simulate a VAV device. Several members of the task group made measurements relevant to the problem. Methods differed in detail but the ceiling insertion loss was presented as the difference in sound power or sound pressure level with and without the test ceiling in place.

At NRC we found that the values of ceiling insertion loss (CIL) depended quite strongly on source position and whether the supporting frame was lined or not. In each case the insertion loss was much less than the transmission loss measured according to ASTM E90 (Figure 4-4).

The dependence on frame lining was not so strong when the ceiling tiles were fairly transparent. The result in Figure 4-5 is for an ASTM reference absorption specimen which consists of panels of glass fiber 50 mm thick.

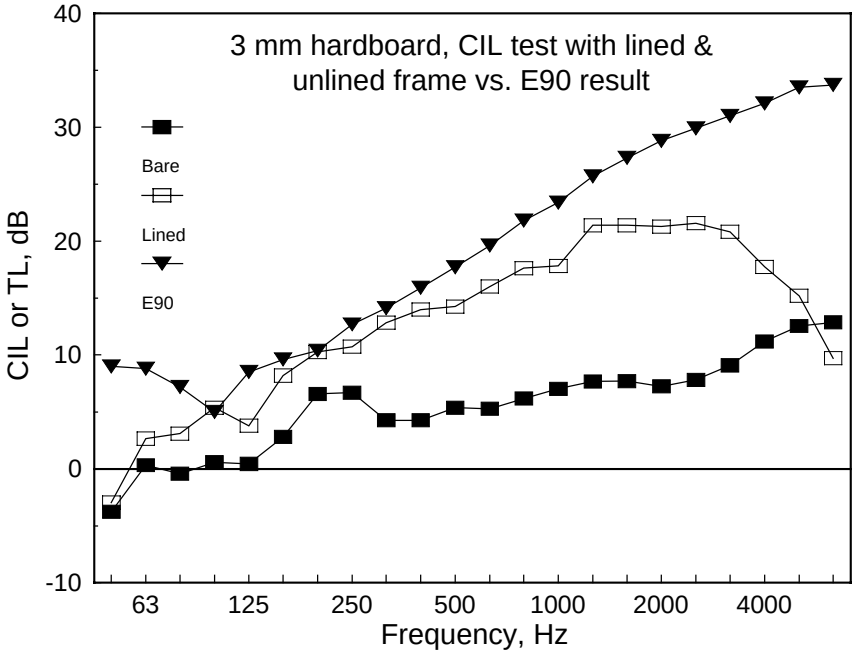

Figure 4-4 Ceiling insertion loss for 3 mm masonite with the E400 frame unlined and lined with 50 mm thick absorbing foam. The E90 transmission loss is shown also.

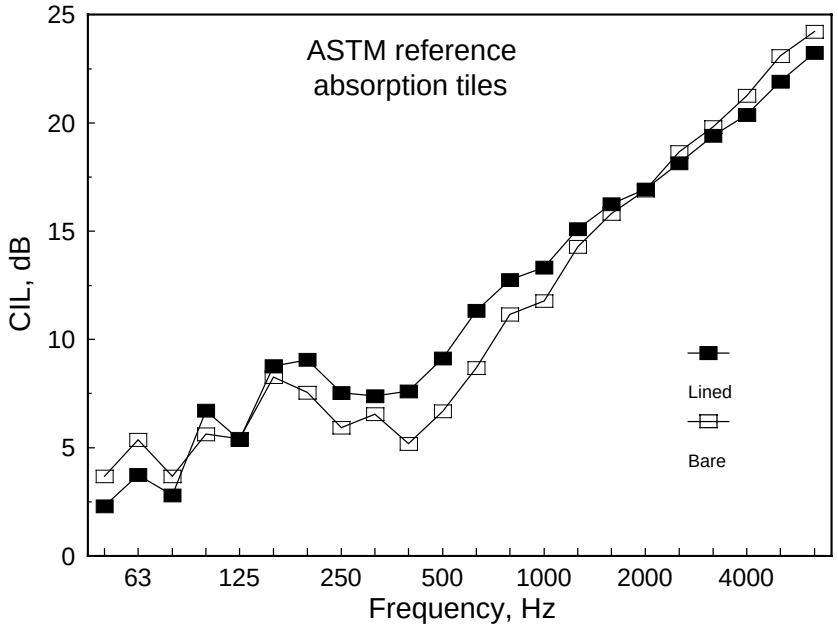

Figure 4-5: Ceiling insertion loss for ASTM reference absorption specimen (50mm thick glass fiber tiles). In one case the E400 frame is bare, in the other it is lined with 50 mm of sound absorbing foam.

Walker [35] measured transmission from a VAV simulator mounted between floor joists supporting a ceiling suspended in a T-bar system. The floor joists were mounted between the rooms of a floor test facility so it was possible to measure conventional transmission loss according to ASTM E336. (The laboratory did not quite qualify for making E90

measurements.) As well, by covering the floor above the simulator it was possible to simulate a 30-inch deep plenum. The results obtained are shown in Figure 4-6. Any effects of the plenum are limited to frequencies below 500 Hz and are in any event, not large except at 125 Hz. Again the conventional transmission loss result overpredicts the ceiling attenuation.

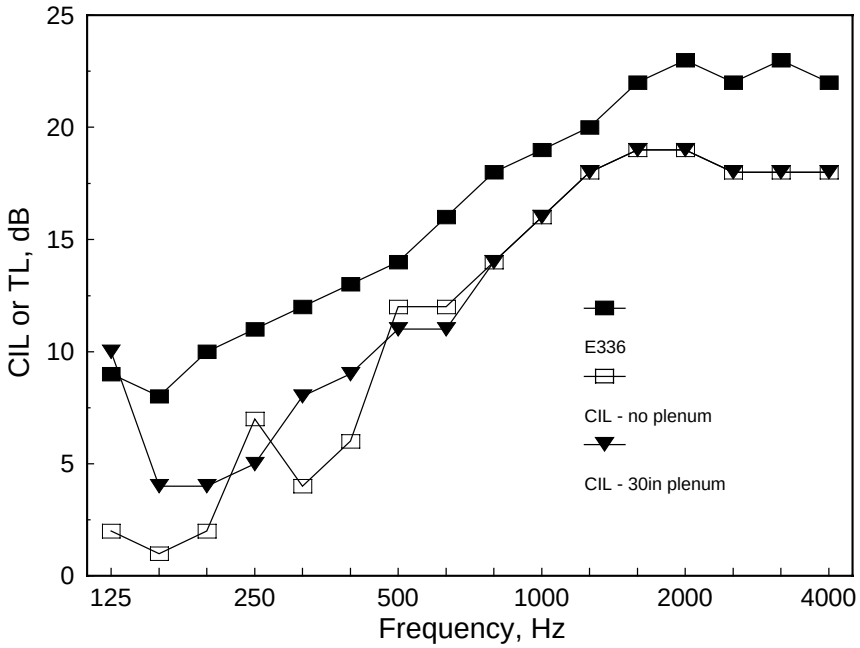

Figure 4-6: Ceiling insertion loss obtained by Walker for mineral fiber tiles with and without an upper plenum surface in place.

Walker also measured the effect of changing the distance from the source to the rear surface of the ceiling tiles. His results are in Figure 4-7 and show that he found no significant effect due to increasing this distance.

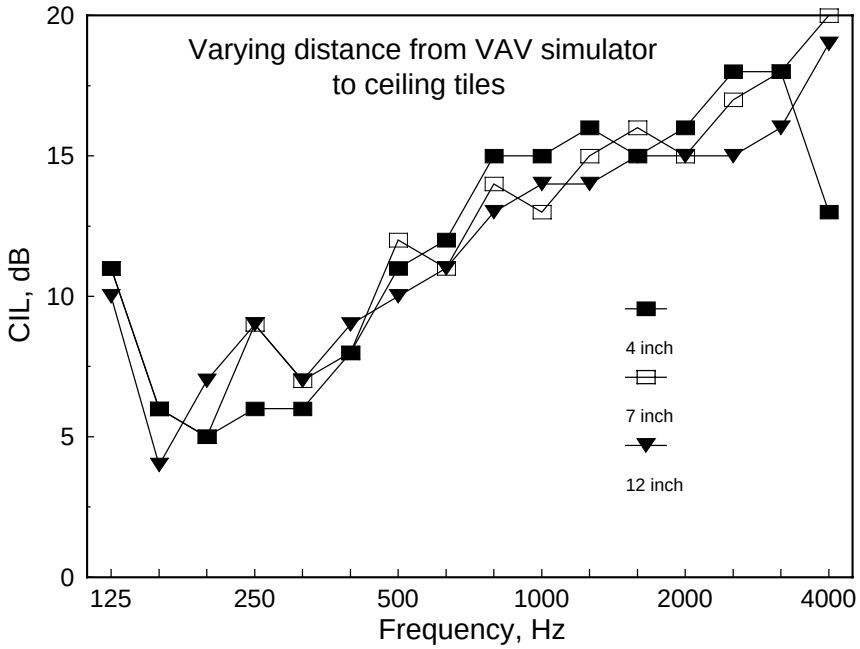

Figure 4-7: Changing the distance from the source to the surface of the ceiling tiles. Data from Walker.

Bay [36] measured the difference in radiated noise from a VAV box through five types of ceiling panels. The VAV box was mounted inside an E400 mounting that was unlined. The ceiling types were placed in the E400 mounting and the levels measured in the reverberation room. The ceiling tiles measured included

1. a ½-inch thick mineral board weighing 0.84 lb/ft^2
2. a 5/8-inch thick mineral board weighing 0.94 lb/ft^2
3. a 5/8-inch thick glass fiber tile weighing 0.15 lb/ft^2
4. a 1.5-inch thick, foil-backed fiberglass tile weighing 0.5 lb/ft^2
5. a 1.5-inch thick fiberglass tile weighing 0.75 lb/ft^2.

The data are presented as insertion losses in Figure 4-8. The differences between types of tile are not very large.

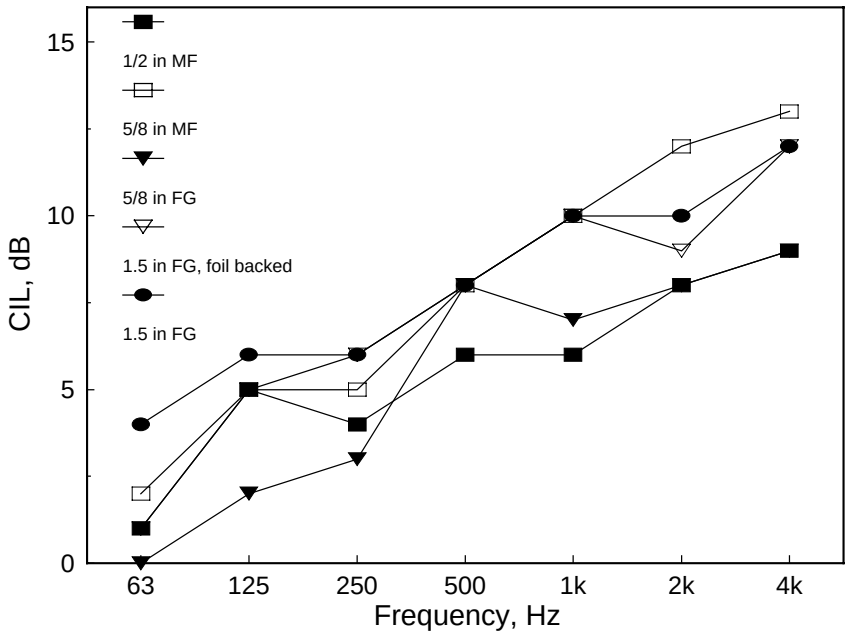

Figure 4-8: Ceiling insertion losses measured by Bay.

Some measurements provided to the ASTM task group by Watson [37] gave some information about the effect of absorption in the plenum space. His measurements were made in a room measuring about 30 x 15 ft with a slab to slab height of 11 ft. The suspended ceiling was installed 9 ft above the floor. Levels due to an air terminal unit above the ceiling were measured in the room below with the vertical plenum faces bare and reflective and with two adjacent surfaces lined with 6 inches of glass fiber. Watson's results are shown in Figure 4-9.

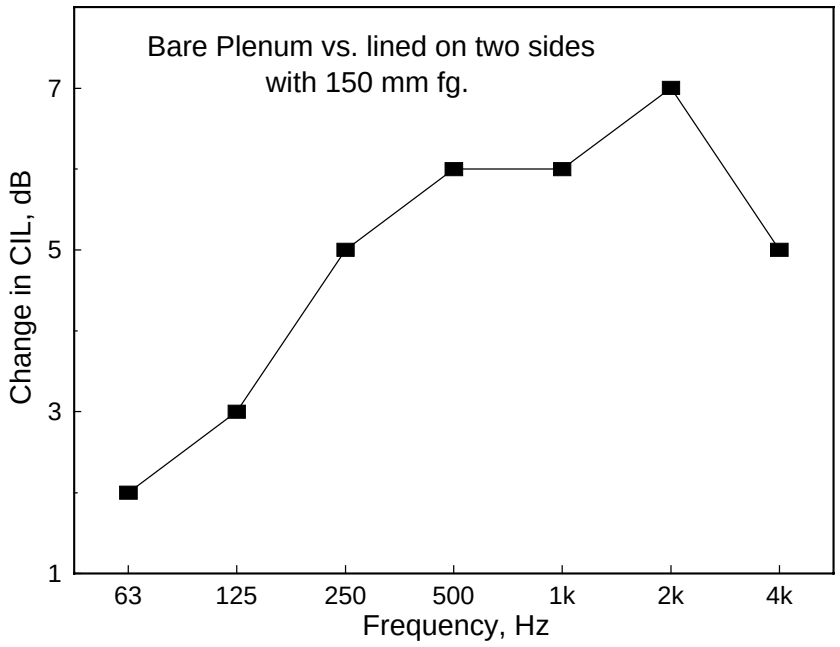

Figure 4-9: Change in ceiling insertion loss caused by lining two adjacent faces of the plenum.

On the basis of all of this work, a draft test method was created by the E33 task group to evaluate the attenuation of ceiling tiles when a simulated VAV source was close to the tiles. The draft test method was intended to take the research findings into account as far as possible. Briefly, a metal box measuring 300 x 600 x 900 mm is placed inside a frame that measures 2.44 x 3.05 m by 500 mm high and that is lined on its inner faces with sound absorbing material. The frame supports the ceiling tiles. The metal box contains two loudspeakers, each driven by a separate noise generator and power amplifier channel, and simulates an air terminal box. The upper surface of the metal box is 50 mm from the rear face of the ceiling panels. The sound power from this source placed in four positions inside the frame is measured with and without a ceiling specimen in place in the frame. The difference in sound power between the two measurements gives a spectrum called the ceiling insertion loss (CIL). This procedure was meant to simulate actual installation of air terminal devices and to rank ceiling panels for their effectiveness in preventing the transmission of sound from such devices. It was not clear, however, that the results from the proposed test could be used to predict what would happen in a real situation. More extensive research was needed, hence project RP755.

4.4 Environmental Adjustment factor.

An issue that must be dealt with when predicting sound pressure levels in a room is the "environmental adjustment factor". The sound power measured for a source placed on the floor of a hemi-anechoic space is generally found to be greater at low frequencies than that for the same source placed on the floor of a reverberation room. This difference is attributed to the different impedance presented to the source by the reverberation room. There are few modes in the room at low frequencies, thus less power is transferred to the room sound field. A great deal of work has been done to study the causes of the difference between the two methods. For this report, the causes are not important. It is only the magnitude of the difference that is immediately relevant for making predictions of sound pressure levels in rooms.

When air terminal devices are tested according to ARI 880, a reference sound source is used to generate sound pressure levels in the room. The differences between these levels and those generated by the device under test are added to the power levels of the reference source to get the power of the device under test. This is the substitution technique. Adherence to this procedure means that the power levels found by following ARI 880 are equivalent to free-field power levels, assuming that both sources are influenced by the room in the same way.

When devices are installed in real rooms, it is expected that the power level emitted at low frequencies will also be reduced because of the influence of the room. The question to be answered is, "How much should the power levels be reduced?"

The recent work by Vorländer and Raabe [8, 9] showed that the difference between free field and reverberant room power is strongly influenced by measurement procedures. Sound power levels measured in reverberant rooms using the direct technique increased when the decay range used to determine reverberation time was decreased. Increasing the radius of the scan used to determine the sound power in a hemi-anechoic space reduced the values of sound power at low frequency. A summary graph extracted from this work is shown in Figure 4-10.

Two sets of measurements are available from the IRC acoustics laboratory that can be used to estimate the environmental adjustment factor. The power of our standard ILG source has been measured in our anechoic room with an added reflecting floor as well as in the M27 reverberation room. The Acculab RSS used in this work was supplied with a set of the manufacturer's hemi-free field power data for another RSS unit of the same type. It is supposed that the difference between these RSS units is comparatively small; the free-field power of our RSS has not yet been measured. The RSS power was measured in three of our reverberation rooms. The differences between the reverberant sound powers and the hemi-free field powers are shown in Figure 4-11 in one-third octave bands. The same data are shown in octave bands and compared to the ARI 885 environmental adjustment factor in Figure 4-12. Also shown in the figure are the differences between curves 4 and 1 and between 3 and 2 from Vorländer and Raabe's work.

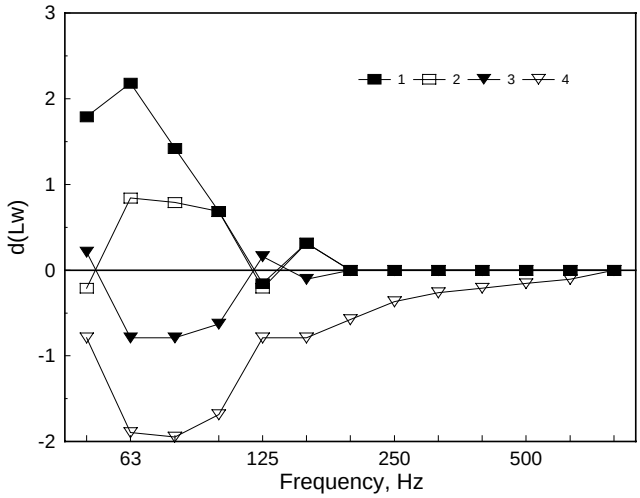

Figure 4-10: Graph from reference [8] showing the disparity between hemi-anechoic and reverberation room determinations of sound power for different measurement conditions. Curve 1 – hemi-free field measurements using a 1.5 m radius; Curve 2 - hemi-free field measurements using a 2 m radius; Curve 3 - reverberation room measurements using a 15 dB range to determine decay rate; and Curve 4 -- reverberation room measurements using a 30 dB range to determine decay rate. d(Lw) is the difference relative to the grand mean.

For a given device, if sound power data are determined from hemi-free field measurements or measurements in a reverberation room using the substitution technique,

then an environmental correction is undoubtedly appropriate when predicting levels in rooms. On the basis of the information presented here, the values specified in ARI 885 seem to be too large. Until changes are made to the governing standards to more precisely define measurement procedures, it may be assumed that the data obtained in the NRC facilities and by Vorländer will be typical of those in other laboratories. More appropriate values for the environmental correction estimated from the data given here are presented in Table 4-1.

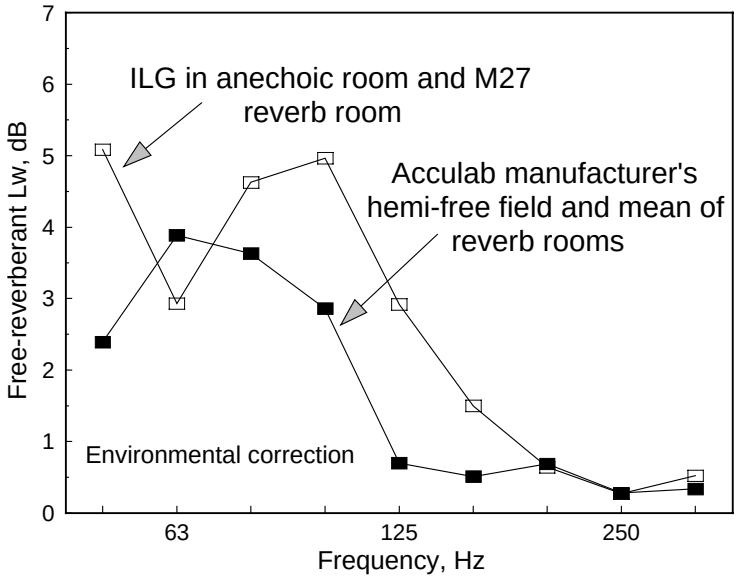

Figure 4-11: Difference between manufacturer's hemi-free field power data and the average of the reverberant room data for the Acculab RSS and between anechoic and reverberant room power for the ILG RSS – one-third octave bands.

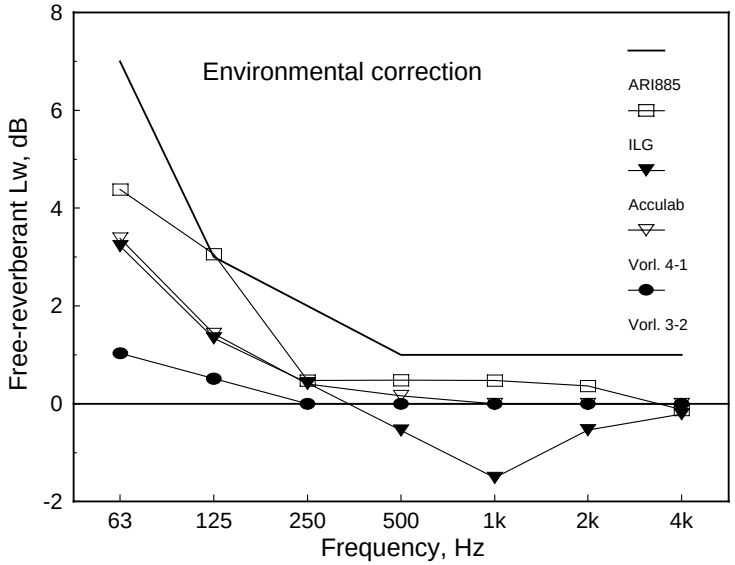

Figure 4-12: Environmental correction for two sources measured at NRC, data from reference [8] and the ARI 885 values.

Table 4-1: Recommended environmental correction.

Octave Band Frequency, Hz							
63	125	250	500	1k	2k	4k	8k
4	2	1	0	0	0	0	0

4.5 Summary of ARI 885.

ARI 885 provides transfer functions for three types of ceiling tile. These transfer functions include the effect of absorption of the ceiling tile and plenum absorption and allow the calculation of an effective sound power transmitted through the ceiling from a sound source located in the ceiling cavity. The table of transfer functions applies to ceilings with typical penetrations and light fixtures. It applies to either wide (over 30 ft), or lined ceiling plenums, at least 3 feet deep with no penetration directly under the source.

ARI 885 covers many more situations than the restricted cases investigated here, so only a part of the document is directly relevant to this research. The general steps specified in ARI 885 to calculate the sound pressure levels in a room are:

1. Obtain the sound power level for the source of noise
2. Identify the sound paths to be considered
3. Determine the attenuation for each path
4. Combine the energy from each path to determine the overall sound pressure level.

Before the sound power levels are used, the environmental adjustment factor (Section 4.4) must be applied to the levels.

The parts of ARI 885-90 relevant to this research project are those dealing with the Plenum/Ceiling Effect, the Space Effect, and the Environmental Effect. Measurements were made to study the first two effects but none were made specifically to study the environmental effect although relevant information was collected and has been presented already.

4.5.1 Plenum/Ceiling Cavity Effect.

To calculate the sound power level transmitted through a ceiling from a sound source located in the plenum, transfer functions are provided. The transfer functions include the effect of the absorption of the ceiling tile and the plenum absorption. Data are provided for only three types of tile and are reproduced in Table 4-2

Table 4-2 Plenum/Ceiling Cavity Effect: Values to be subtracted from sound power of device to get sound power transmitted through the ceiling.

	Octave Band Frequency, Hz						
	63	125	250	500	1k	2k	4k
Type 1: Fiberglas Tile 1/2" thick, 6 lb/ft^3	4	8	8	8	10	10	14
Type 2: Mineral Fiber Tile 5/8" thick, 35 lb/ft^3	5	9	10	12	14	15	15
Type 3: Sheet Rock 5/8" thick	10	15	21	25	27	26	27

4.5.2 Space Effect

The calculation of the sound pressure level at a point in a room is done using the Schultz [7] equation given earlier in Section 4.1.

4.5.3 Environmental Effect

The values specified in ARI 885 to be subtracted from the sound power data to account for the environmental effect are reproduced in Table 4-3.

Table 4-3: Environmental Adjustment factor in ARI 885

Octave Band Frequency, Hz							
63	125	250	500	1k	2k	4k	8k
7	3	2	1	1	1	1	1

5. The NRC test facilities.

5.1 The RAT room.

The room acoustics test (RAT) room, where the measurements were made, is a rectangular parallelepiped 4.71 m wide and 3.6 m high. One end wall can be moved to allow changes in length. The maximum length is about 11 m. For most of the experiments, the length was set at 9.2 m giving a room volume of 156 m^3. The T-bar system for supporting tiles was installed so the distance from the supporting surface of the T-bar to the true ceiling of the room was 740 mm. Plenum depths were thus 13 to 50 mm less than this depending on the tile thickness.

The RAT room walls, floor and ceiling are split near the middle of the room. Each section of the room is independently supported on steel springs. This allows the room to be divided into two rooms, isolated from each other by an additional partition built over the split. When the dividing partition does not extend to the roof of the room but leaves the plenum open, the two rooms formed are used for testing according to ASTM E1414 [38]. The two rooms are identified as the East room and the West room. Their dimensions are given in Table 5-1. The partition separating the two rooms measured 4.74 x 2.8 m and had an area of 13.24 m^2. A schematic showing the principal features of the room is given in Figure 5-1. Other views of the room are given later.

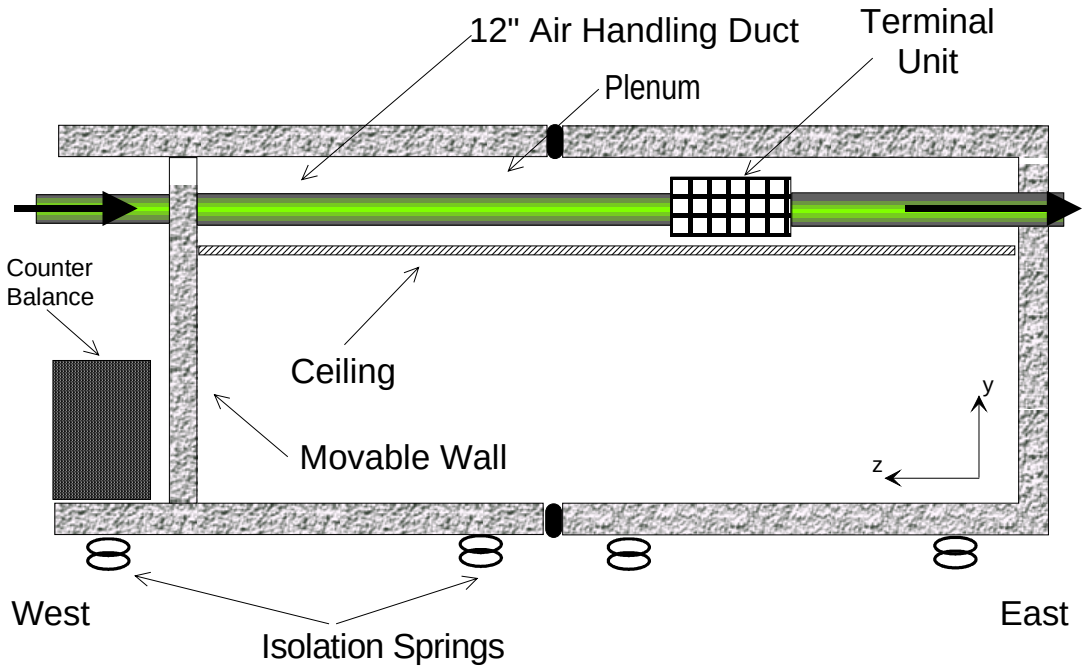

Figure 5-1: Cross-section through the RAT room showing major features and air-handling system.

Table 5-1: Dimensions of East and West RAT rooms when used for E1414 tests.

	East Room	West Room
Ceiling height, m	2.8	2.79
Width, m	4.73	4.74
Length, m	4.46	4.52
Volume, m^3	59.1	59.8

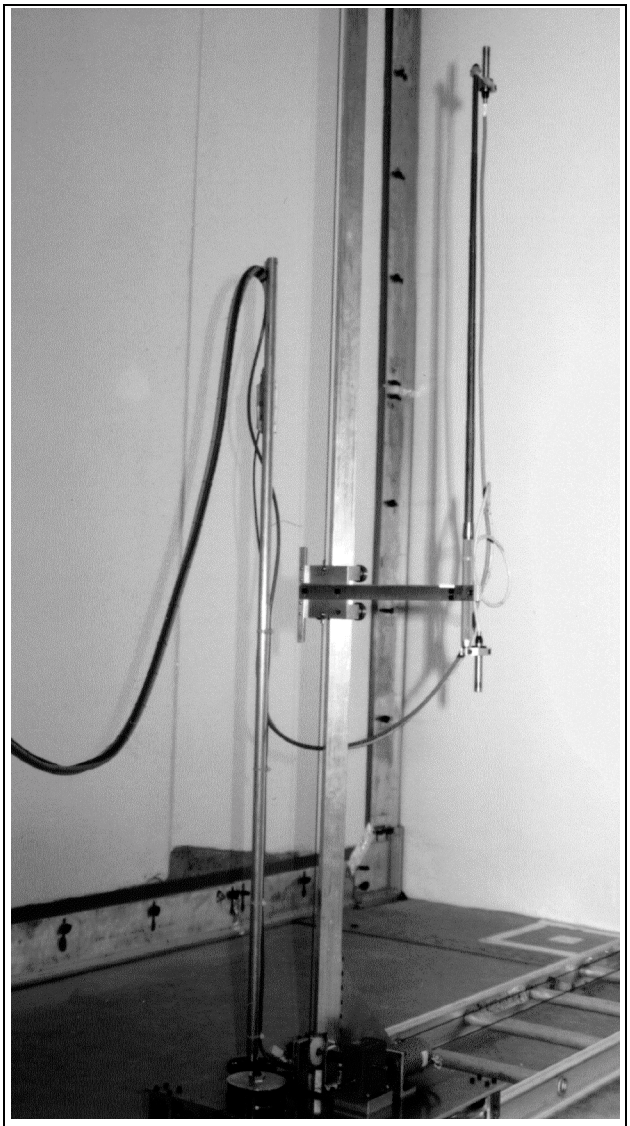

Figure 5-2: View of the ladder system used to move the microphones.

5.1.1 Diffusers.

Early in the measurement series, it became apparent that the reverberation times in the RAT room were too long despite the amount of sound absorbing material contributed by the ceiling. This was not unexpected because of the lack of scattering and diffusing elements in the room. To provide some scattering, 8 sheets of 16 mm gypsum board measuring 1.22 x 1.22 m were hung on the walls or placed on the floor and inclined against the walls. These diffusing panels were present for measurements in the main series looking at the effects of ceiling type and sound source type.

5.1.2 Movable microphone system.

Two microphone systems were used in the RAT room. One system used a pair of microphones mounted 1 metre apart on a movable rod. The rod moves vertically along a pole. The pole moves horizontally along a ladder. This assembly allows the pair of microphones to be positioned under computer control anywhere on a plane. The ladder supporting the pole assembly can be moved to different planes in the room. A view of the system is shown in Figure 5-2.

The second microphone “system” consisted of a single microphone on a stand that was moved manually to marked positions on the floor and set to different heights.

5.1.3 Background noise in the RAT room.

The RAT room is situated in a busy laboratory where construction work generates sporadic noise. Measured background noise levels inevitably show variations from minute to minute and day to day. Obvious noise intrusions could be heard by the operator or seen on the real-time-analyser screen. Some intrusions could be less obvious to the ear. It would be unrealistic to believe that background levels, measured from necessity up to an hour after the measurement of device levels, could be used to correct the device levels. Background noise measurements were made frequently and the mean value at each frequency was used to reject measured device levels if, on inspection, they were considered too close to background. No attempts were made to correct levels. This approach led to the rejection of much of the data from the terminal units at 4 kHz. This frequency is of little concern and attenuations there can be determined with sufficient accuracy from the measurements made using the simulators. For reference, the background noise in the RAT room is shown in Figure 5-3 as a box and whisker plot.

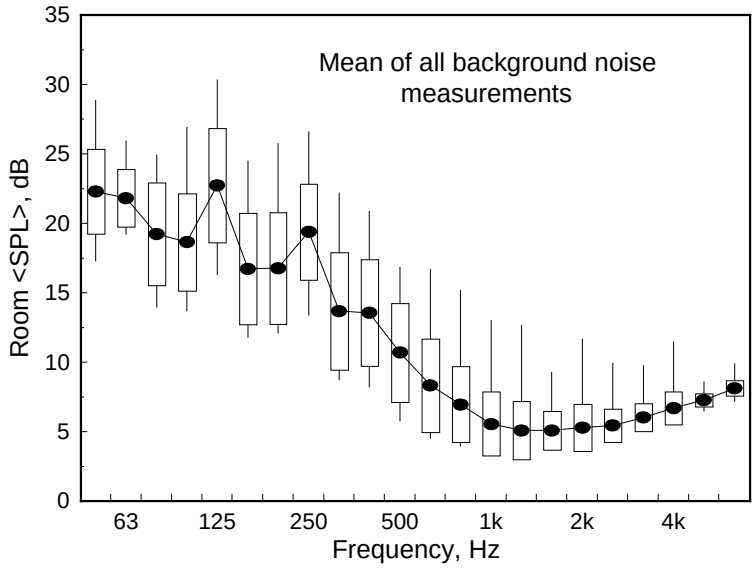

Figure 5-3: Mean of means of all background noise measurements. The boxes represent the mean ± one standard deviation, the whiskers show minimum and maximum values measured and the solid dots show the grand mean.

5.1.4 The air supply fan.

Initially a 16-inch diameter fan driven by a d.c. supply was intended to be used in the air supply unit. Initial tests with this fan showed that it was unable to deliver the required quantity of air. A more powerful 15-inch fan, which did have the capacity was used instead. The speed of this fan was controlled by a digital controller visible in Figure 5-4.

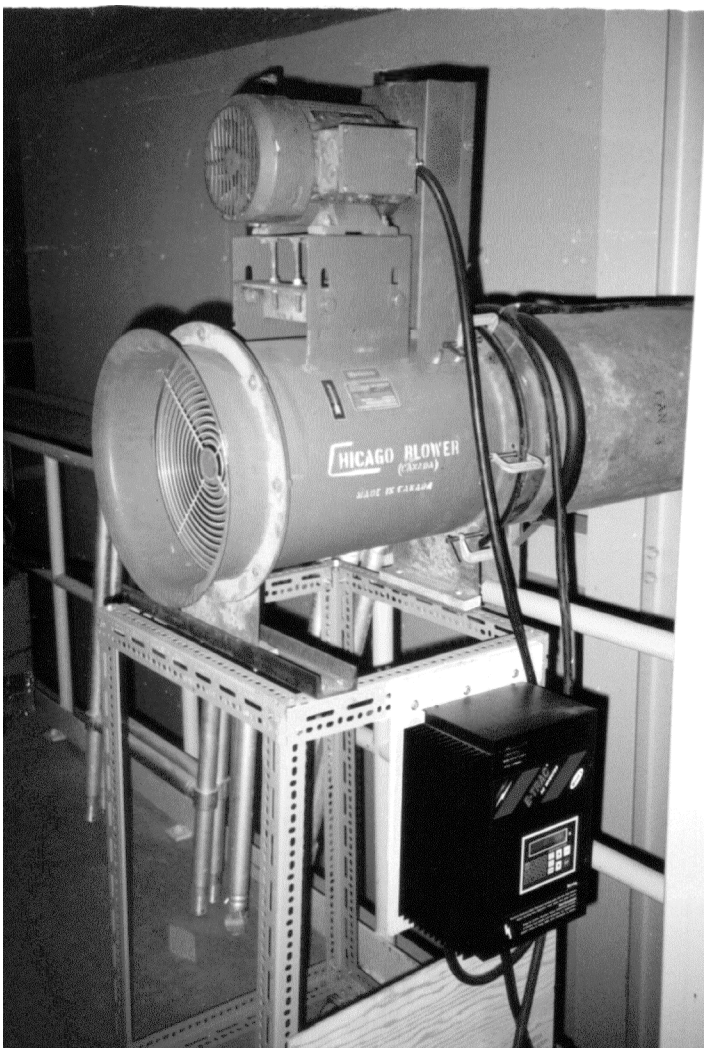

Figure 5-4: A view of the supply fan with its electronic controller.

5.1.5 The duct system.

The general layout of the ducts in the room is shown in Figure 5-5. The supply fan was positioned at one end of an 8.8 m long section of 16-inch diameter spiral duct. To avoid interfering with flow measurements, the first 5.6 m was unlined, the remaining section was lined with 25 mm thick glass fiber duct liner. The flow measuring station was at the south end of this duct. Plenum box P1 measured 2.14 x 0.616 x 0.76 m and was lined with 50 mm of glass fiber duct liner. The outlet from plenum P1 was 1.45 m above the inlet and connected to Plenum P2 through a 2.59 m long section of 16-inch diameter lined spiral duct. Plenum P2 measured 1.84 x 1.84 x 1.02 m high and was also lined with 50 mm of glass fiber.

The outlet from P2 and the supply to the terminal unit under test was along nominal 12-inch diameter plastic sewer pipe (The internal diameter was 296 mm). The pipe material

was 4 mm thick and had 11 mm high ridges at intervals of 30 mm along its length. Pressure taps were inserted where needed in this pipe.

Exhaust air left through plenum P3. Plenum P3 measured 0.605 x 1.26 x 2.44 m and was lined with 50 mm of acoustical foam. It was fitted with a pair of silencers in parallel at the output.

When it was necessary to supply air to the space above the ceiling in the RAT room, it entered through plenum P4. Plenum P4 measured 0.64 x 1.22 x 2.44 m and was lined with 50 mm of acoustical foam. It was also fitted with silencers at the inlet.

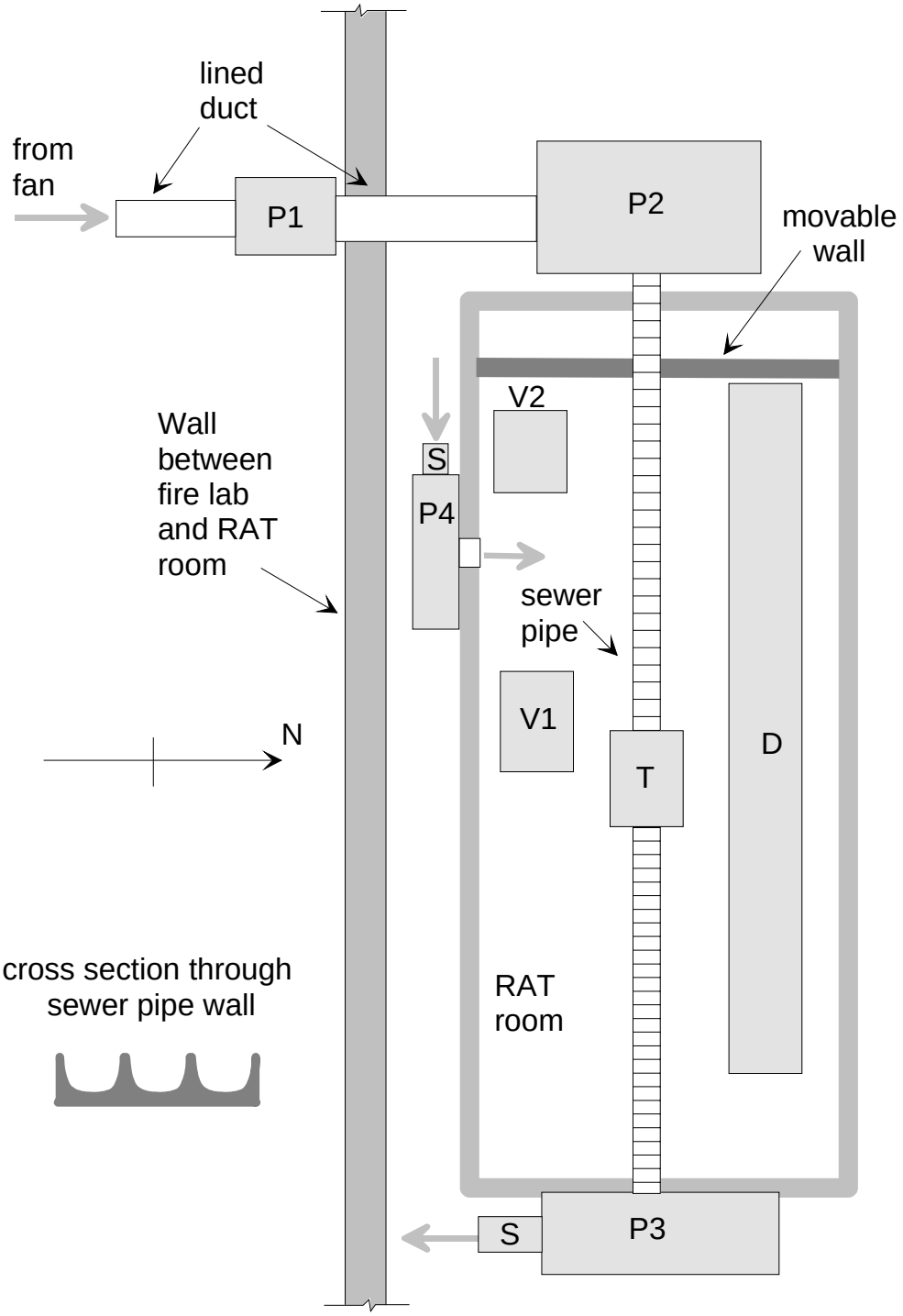

Figure 5-5: Plan view of the RAT room showing the layout of the air supply and duct system (not to scale). P1, P2, P3, P4 are lined plenums, V1 and V2 are the VAV simulator boxes. T is the air terminal device under test and D is the large duct. The loudspeakers were at the west end of the duct. The gray arrows represent air flows. S are sound attenuators.

5.1.6 Measurements of flow rate.

Air velocity through the duct system was measured using averaging tubes. The readout from these tubes was calibrated using a pitot tube scan. Pressure differences at the averaging tubes and at various positions in the system were measured using an electronic micromanometer type AP2705 by DP Measurement Ltd., Oxford, England.

5.1.7 Background noise from fan system.

The sound pressure levels in the room were measured with no terminal device in place, only a continuous length of sewer pipe. The measured levels are shown in Figure 5-6. Except at high frequencies the background noise in the RAT room was negligible during these measurements.

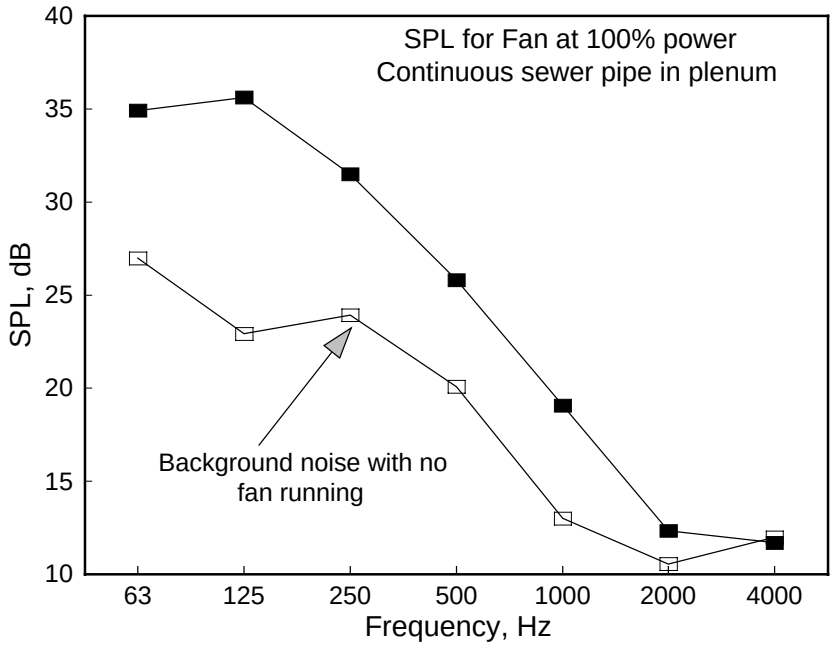

Figure 5-6: Measured sound pressure levels with a continuous length of sewer pipe in the room. The A755B ceiling was installed.

5.2 M59 floor test facility

This facility was used to measure ceiling insertion loss and sound transmission loss of ceiling tiles. The facility comprises two reverberation rooms with a removable frame for supporting floor/ceiling specimens [39]. Each room has a volume of 175 m^3 and is fitted with fixed diffusing panels and with four loudspeakers, each with its own noise generator and amplifier. Microphones in each room are mounted on booms that are moved by stepping motors controlled by the testing computer. Nine microphone positions are used in each room. The test opening measures 3.8 x 4.7 m.

For measurement of sound transmission loss according to ASTM E90, the ceiling boards were mounted in a T-bar system between the two rooms. The measurement of ceiling insertion loss was done in the lower room as described in Section 11.7.

5.3 M27 reverberation room.

The 250 m^3 room in building M27 was used for some sound power measurements and measurements of sound absorption coefficients. The room is a rectangular parallelepiped and is equipped with a rotating diffuser and a computer-controlled movable microphone. Nine microphone positions are used in this room.

6. Sound sources used in the RAT room.

6.1 Terminal units.

Four terminal units were used. They are described below. All units were operated without using automatic controls.

6.1.1 Terminal unit A.

Terminal A was a single duct, variable volume unit, TITUS model ESV 3000. Air flow was controlled by a single circular damper that was set manually to give the required flow conditions. Standard conditions were an inlet static pressure drop of 374 Pa (1.5 inches of water) with a flow of 2000 ft/minute. For some tiles the unit was operated with an inlet pressure drop of 625 Pa and a flow of 1580 ft/minute. The unit measured 15” wide x 16” high x 15.5” long. A view of the installed unit, seen from the south-east corner of the RAT room is shown below. The mid-point of the lower face of the unit was at room co-ordinates (2, 2.97, 3.83). The lower face was 170 mm above the bottom of the T-bars.

6.1.2 Terminal unit B.

Terminal B was a constant volume, fan-powered unit from Anemostat, type JCV 3310 1HA 4024 HAR. The unit measured 32” wide x 58½” long x 16” high. A view of terminal B from the north east corner of the RAT room is shown below. The mid-point of the lower face of the unit was at room co-ordinates (1.9, 3.0, 3.0). The lower face was 200 mm above the bottom of the T-bars.

6.1.3 Terminal unit C.

Terminal unit C was a variable volume, fan-powered unit. It was an FV Bypass Terminal from York International Corporation, unit type HVFB2 F, control code 9311DB0, blower part no. 35-01009-000, motor part no. 31-02012-006 [.333 HP 7.0 FLA]. The unit measured 49” wide x 34” long x 14” high. The view of this unit is from below and slightly toward the south-west corner of the room. The mid-point of the lower face of the unit was at room co-ordinates (1.59, 3.05, 3.83). The lower face was 205 mm above the bottom of the T-bars.

6.1.4 Terminal unit D.

Terminal unit D was a Titus HIEP pressure independent induction unit. It measured 47 5/8" wide x 72" long x 16" high. This unit is seen below from the north-west corner of the RAT room. The large duct source, described later, is also visible as is the simulator, VAVsim1. The mid-point of the lower face of the unit was at room co-ordinates (2, 2.98, 3.2). The lower face was 180 mm above the bottom of the T-bars.

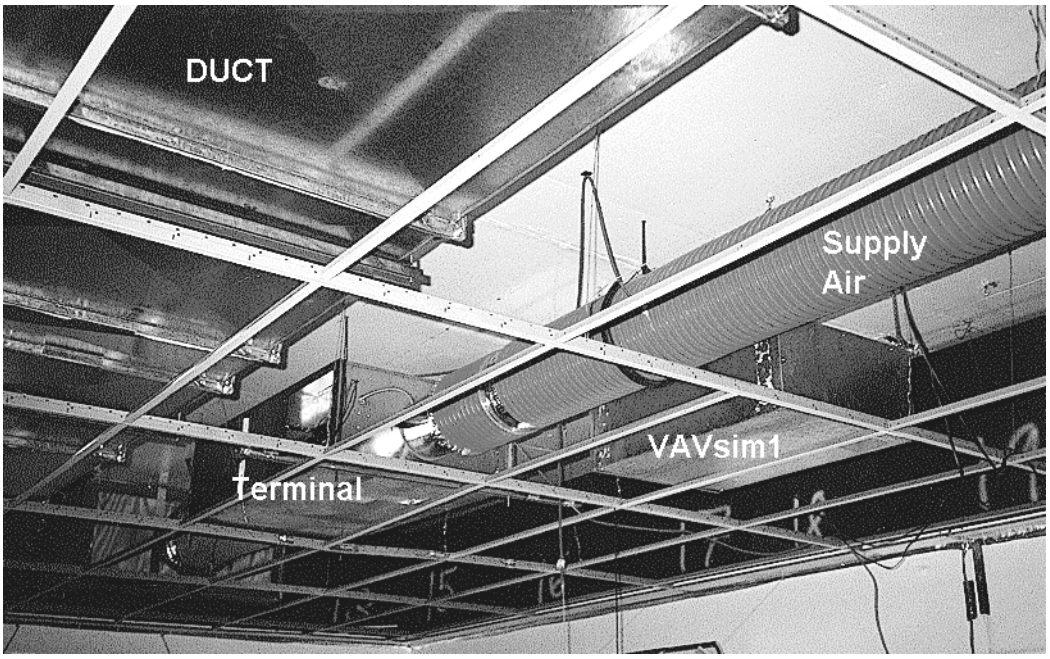

Adapters were constructed as needed to change from the 12-inch diameter sewer pipes used in the air supply system to the inlet and outlet attachments on the units.

6.2 Simulated Air Terminal sources.

6.2.1 VAV simulators.

The simulated air terminal unit is a metal box measuring 300 x 600 x 900 mm. The metal was 24 Ga. galvanized steel. Two elliptical car loudspeakers are mounted facing in opposite directions on a 13 mm thick plywood panel at the mid-plane of the box (See Figure 6-1). Each is fed by its own noise generator and amplifier. This unit can be seen close to the terminal units in the views just above.

Two of these devices were used during the measurements. In the main part of the series of measurements, they are denoted VAVsim1 and VAVsim2. The mid-point of the lower face of VAVsim1 was at room co-ordinates (1.52, 2.88, 3.2). The lower face was 75 mm above the bottom of the T-bars. The mid-point of the lower face of VAVsim2 was at

room co-ordinates (2.0, 2.88, 8.16). The lower face was 75 mm above the bottom of the T-bars.

An earlier version of VAVsim1 was called Box A. It was used in some early experiments but the loudspeakers were accidentally destroyed and could not be replaced with identical units.

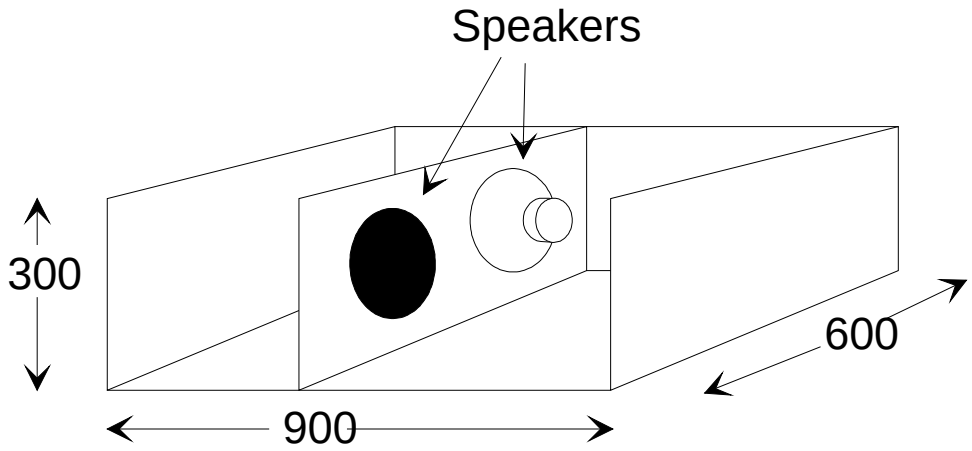

Figure 6-1: View of an air terminal simulator with the top and one side removed. The central panel is made of 13 mm plywood. Dimensions are in mm.

6.2.2 Duct simulator.

At the request of the monitoring committee, a length of duct was installed down one side of the room (See Figure 5-2). The duct was 7.7 m long with cross-section measuring 457 x 1219 mm. It was formed from 20 Ga. steel. A pair of car loudspeakers, powered by separate noise generators and amplifiers, were installed at the West end of the duct. The east end was faced with a layer of glass fiber batts about 300 mm thick to reduce reflections. The lower face of the duct was 140 mm above the lower face of the T-bars.

6.3 Other Sources

6.3.1 Accculab reference sound source.

The Acculab RSS-500 is a vertically-oriented, centrifugal fan with a 305 mm diameter fan wheel. The rotational speed was chosen by the manufacturer so that troublesome tones associated with the blade passage frequency occurred below 25 Hz. The source is shown in Figure 6-2

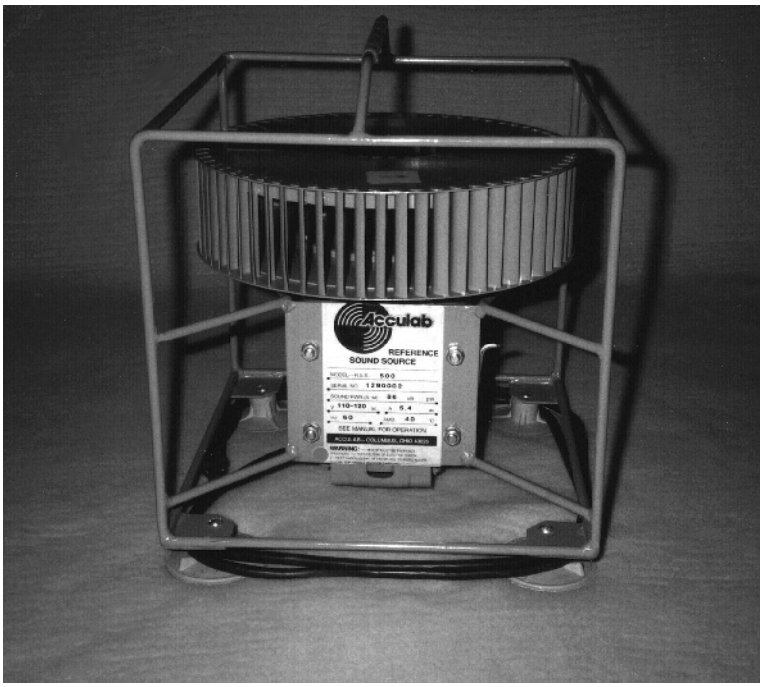

Figure 6-2: The Acculab reference sound source used in the project.

6.3.2 Dodecahedral source.

The source that was finally selected for drawaway measurements in the room was a dodecahedral array. The 12 loudspeakers (100 mm diameter units from Bose) were powered from a single noise generator and power amplifier. Early in the project the drawaway curves obtained with this unit were compared with those from a horn driver loaded with a thin tube. The sound radiating from the end of the tube should be a good approximation to a point source. The agreement between the two sources was deemed satisfactory and the dodecahedral source was used for the main series of measurements. A photograph of the source is shown in Figure 6-3. Note that the microphone ladder is not in the position used for drawaway measurements in this picture.

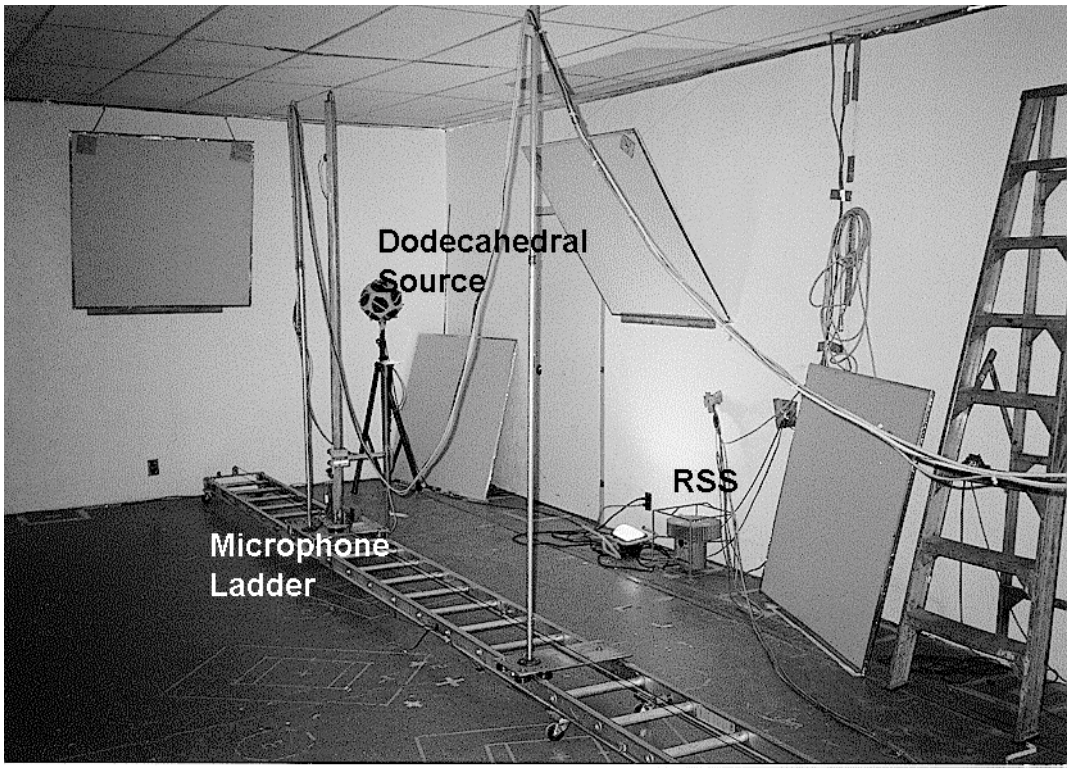

Figure 6-3: Dodecahedral source used in drawaway experiments.

6.4 Sound power of terminal units and other sources.

6.4.1 Powers measured in RAT room.

Sound power was measured in the RAT room using the direct and substitution methods. The sound pressure levels and the reverberation times measured as described in Sections 7.1 and 7.3 were used as the input data for the calculations. Using the direct technique, the sound power of a source in a reverberation room is given by [3]

$$L_W = L_p - 10\log\frac{T}{T_0} + 10\log\frac{V}{V_0} + 10\log\left(1 + \frac{\lambda S}{8V}\right) + 10\log\frac{B}{100} - 14 \quad \text{dB}$$

where
- L_W is the sound power level of the source under test, dB re 1 pW
- L_p is the mean sound pressure level in the room, dB re 20 μPa
- T is the reverberation time in the room, s
- T_0 is 1 second
- V is the volume of the room, m^3
- V_0 is 1 m^3
- λ is the wavelength of sound at the mid-band frequency of the 1/3 octave band, m
- S is the total surface area of the room, m^2
- B is the barometric pressure in kPa.

For the substitution technique, the reference source was the Acculab Fan. Sound pressure levels produced by the fan were compared with those generated by the source to be measured. The reference values of sound power for the fan were taken as the results measured in the 250 m^3 room in M27. Using the substitution technique, the sound power is given by

$$L_W = L_p + C_{Wr} - L_{pr}$$

where L_W is the sound power level of the source under test, dB re 1 pW
L_p is the mean sound pressure level in the room due to the source under test, dB re 20 μPa
L_{Wr} is the sound power level of the reference sound source, dB re 1 pW
L_{pr} is the mean sound pressure level in the room due to the reference sound source, dB re 20 μPa

For completeness, the measured power levels are tabulated in Table 6-1 and Table 6-2.

The hemi-free field sound power levels provided with NRC's Acculab RSS did not actually belong to the NRC source; they were for another unit of the same type. It is reasonable to assume that power levels of the two reference sound sources will be approximately the same. However, the sound power values used in calculations of the ceiling attenuation were those measured in our large reverberation room using the direct method.

In the RAT room measurements of sound power using the substitution technique, the hemi-free field data supplied by the manufacturer were used. There were systematic differences between the results from the two methods and these are plotted in Figure 6-4. These differences are examples of the environmental effect. At low frequencies the reduced sound power in the RAT room can be attributed to the lack of modes there. Around 1 kHz, the difference is attributed to either inadequate spatial sampling in the original hemi-free field measurements or possibly to differences between the NRC RSS and the unit to which the power data actually apply.

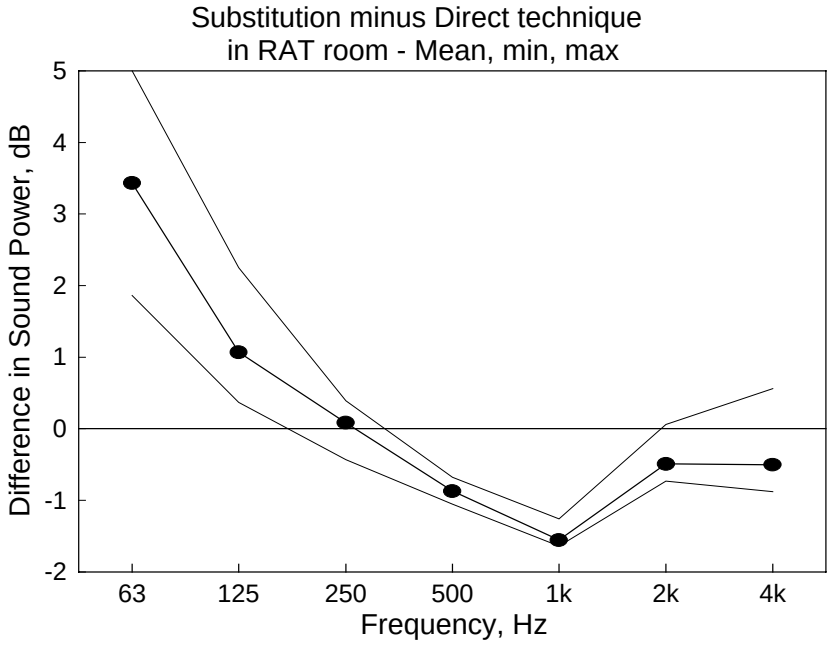

Figure 6-4: Average difference in sound powers measured in the RAT room using the direct and substitution techniques.

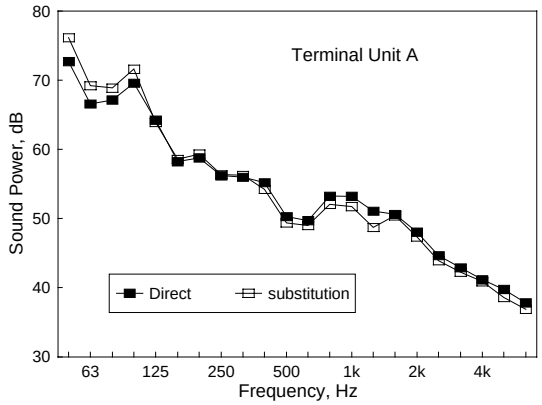

Figure 6-5 Power of the single duct VAV terminal unit, Terminal A, measured in the RAT room – Standard operation .

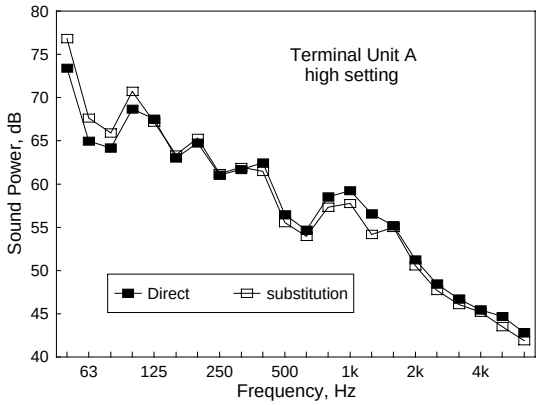

Figure 6-6 Power of the single duct VAV terminal unit, Terminal A, measured in the RAT room – High operation .

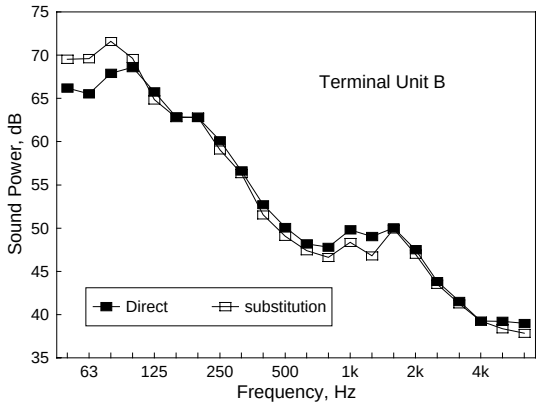

Figure 6-7 Power of Terminal B measured in the RAT room

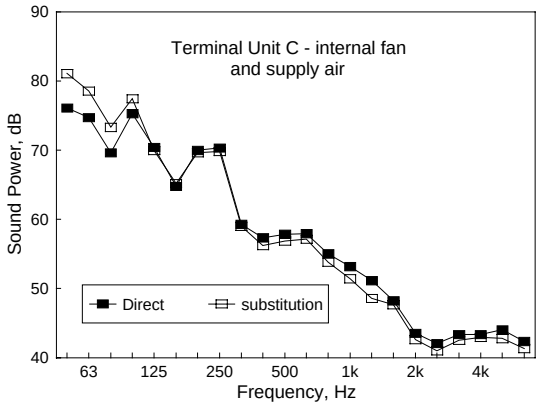

Figure 6-8 Power of Terminal C measured in the RAT room, internal fan and supply air both on.

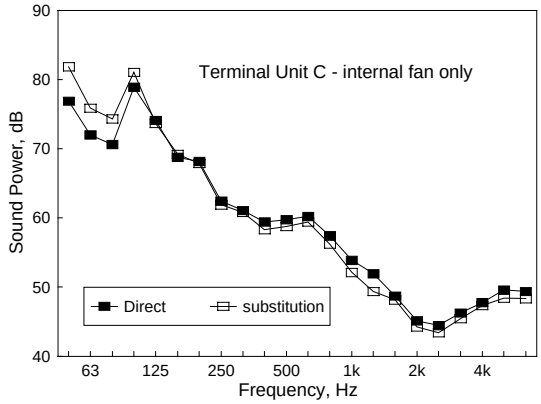

Figure 6-9 Power of Terminal C measured in the RAT room, internal fan only

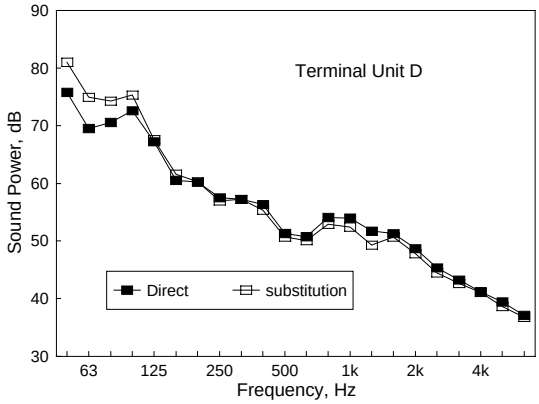

Figure 6-10 Power of Terminal D measured in the RAT room

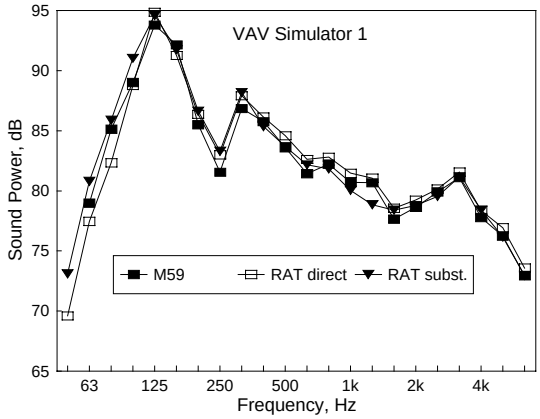

Figure 6-11: Power of VAV simulator source 1 measured in the RAT room and in the lower M59 reverberation room.

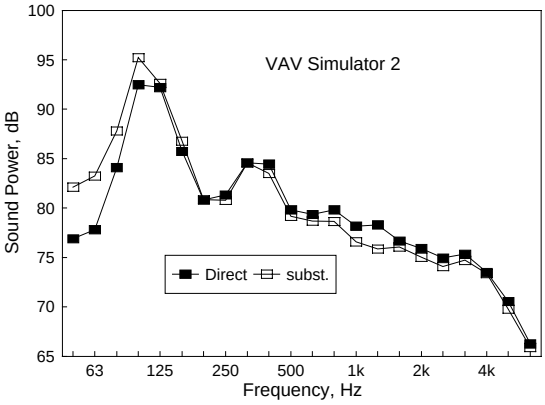

Figure 6-12: Power of VAV simulator source 2 measured in the RAT room.

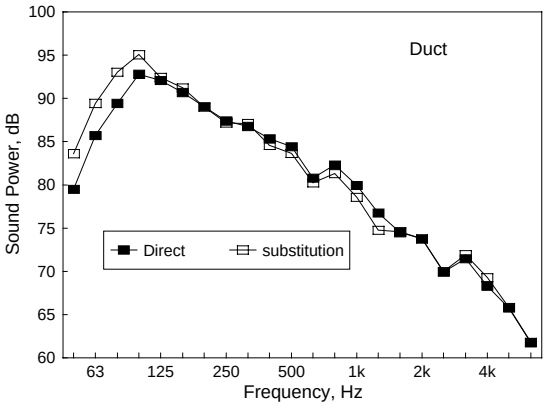

Figure 6-13 Power of the large duct source measured in the RAT room.

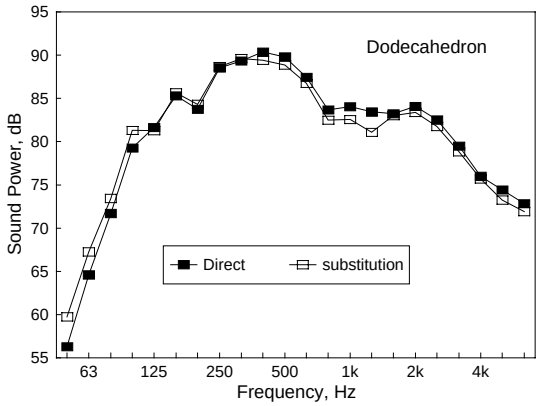

Figure 6-14 Power of the dodecahedral source measured at one end of the RAT room.

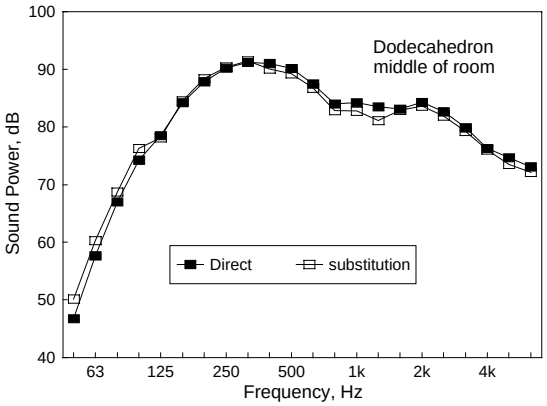

Figure 6-15 Power of the dodecahedral source measured in the middle of the RAT room.

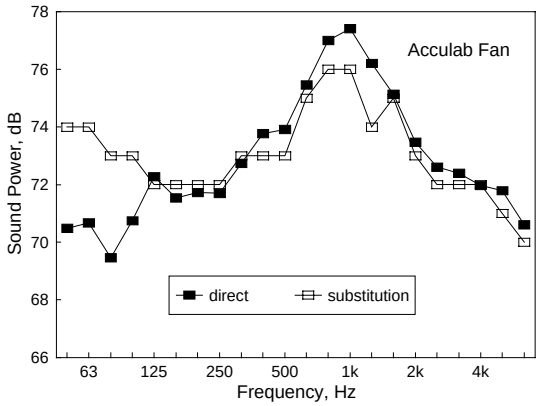

Figure 6-16 Power of the Acculab fan reference sound source measured in the RAT room.

6.4.2 Powers measured in Reverberant rooms.

The sound power for the reference Acculab sound source was also measured in the 250 m^3 room in M27. These data were taken as the reference values. It was measured in the RAT room before and after the installation of the large duct. It was also measured, for interest, in the two rooms comprising the floor suite in M59. All these data are shown in Figure 6-17. While it has little to do with the main goal of the project, it is interesting to see that agreement between the results for the reverberation rooms is good except below 100 Hz where the range in levels is about 3 dB in each band. The high frequency data for the upper room in M59 points to a possible problem to be resolved in that room.

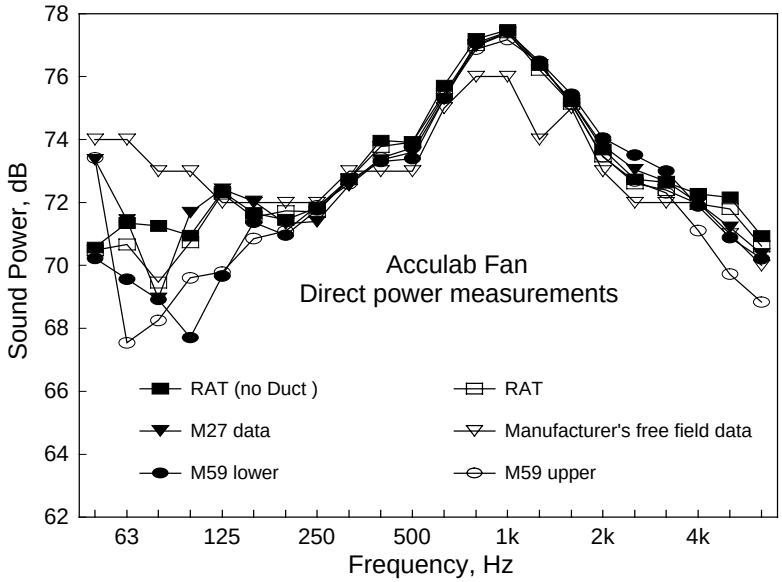

Figure 6-17: Sound power for the Acculab fan using the direct method in two RAT room conditions, in the M27 reverberation room, and in both M59 reverberation rooms. The manufacturer's hemi-free-field data for a similar unit is also shown.

Table 6-1: Sound power levels measured in the RAT room using the direct method.

	Terminal Units						Simulators				No Duct		
Freq. (Hz)	A	A high	B	C both	C int.	D	VAV sim1	VAV sim2	Duct	Dodec	VAV sim1	Fan	Dodec Mid
50	72.7	73.4	66.2	76.1	76.9	75.8	69.6	76.9	79.5	56.3	67.9	70.6	46.7
63	66.6	65.0	65.5	74.7	72.0	69.5	77.5	77.8	85.7	64.6	76.7	71.4	57.7
80	67.1	64.2	67.9	69.6	70.6	70.6	82.3	84.1	89.4	71.7	81.5	71.3	67.0
100	69.6	68.7	68.6	75.3	78.9	72.6	88.8	92.5	92.8	79.3	89.1	71.0	74.2
125	64.2	67.5	65.8	70.4	74.1	67.2	94.9	92.2	92.1	81.6	93.8	72.4	78.5
160	58.2	63.0	62.9	64.8	68.8	60.5	91.3	85.7	90.7	85.3	91.1	71.7	84.2
200	58.8	64.7	62.8	70.0	68.2	60.2	86.4	80.8	89.0	83.8	85.8	71.4	87.9
250	56.2	61.0	60.1	70.3	62.4	57.5	83.0	81.3	87.4	88.5	83.5	71.8	90.2
315	56.0	61.7	56.6	59.3	61.1	57.2	87.9	84.6	86.8	89.3	88.0	72.7	91.2
400	55.2	62.4	52.7	57.3	59.4	56.3	86.1	84.5	85.3	90.4	86.6	74.0	91.0
500	50.3	56.4	50.1	57.8	59.7	51.3	84.6	79.8	84.4	89.8	85.1	73.9	90.2
630	49.7	54.7	48.2	57.9	60.2	50.8	82.6	79.4	80.8	87.4	83.1	75.7	87.5
800	53.3	58.5	47.8	55.0	57.4	54.1	82.8	79.8	82.3	83.7	83.2	77.2	84.0
1000	53.2	59.2	49.8	53.2	53.9	54.0	81.5	78.2	79.9	84.0	81.8	77.5	84.2
1250	51.1	56.5	49.0	51.2	52.0	51.7	81.1	78.3	76.7	83.4	81.2	76.4	83.5
1600	50.6	55.2	50.0	48.2	48.7	51.3	78.5	76.7	74.5	83.2	78.7	75.2	83.1
2000	48.1	51.2	47.5	43.5	45.1	48.7	79.2	75.9	73.8	84.1	79.5	73.7	84.3
2500	44.6	48.4	43.8	42.1	44.5	45.3	80.1	75.0	69.9	82.5	80.1	72.7	82.6
3150	42.9	46.7	41.5	43.4	46.3	43.2	81.6	75.3	71.4	79.5	81.5	72.6	79.9
4000	41.2	45.4	39.2	43.4	47.8	41.2	78.4	73.5	68.3	76.0	78.3	72.3	76.3
5000	39.8	44.7	39.2	44.0	49.6	39.4	76.9	70.6	65.8	74.4	76.8	72.2	74.7
6300	37.8	42.8	39.0	42.4	49.4	37.1	73.6	66.3	61.8	72.8	73.3	70.9	73.1

Table 6-2: Sound powers measured using the substitution technique.

	Terminal Units						Simulators				No Duct	
Freq. (Hz)	A	A high	B	C both	C int.	D	VAV sim1	VAV sim2	Duct	Dodec	VAV sim1	Dodec Mid
50	75.5	76.1	76.8	69.5	81.1	81.9	73.1	82.1	83.6	59.7	70.7	50.2
63	66.7	69.2	67.6	69.6	78.6	75.9	80.8	83.3	89.4	67.2	76.8	60.3
80	64.8	68.9	65.9	71.6	73.3	74.3	85.9	87.8	93.0	73.4	79.2	68.8
100	70.3	71.6	70.7	69.6	77.5	81.1	91.0	95.2	95.1	81.3	89.8	76.3
125	64.3	63.9	67.2	64.8	70.0	73.7	94.6	92.6	92.4	81.3	93.9	78.1
160	58.6	58.6	63.4	62.8	65.2	69.2	91.7	86.8	91.2	85.6	91.5	84.5
200	58.6	59.3	65.3	62.8	69.7	67.9	86.6	80.9	89.0	84.3	85.7	88.4
250	55.8	56.4	61.2	59.0	69.8	61.9	83.3	80.8	87.2	88.7	83.1	90.4
315	55.8	56.3	61.9	56.3	59.0	60.8	88.2	84.6	87.1	89.6	87.8	91.5
400	54.6	54.2	61.5	51.5	56.2	58.3	85.4	83.5	84.6	89.4	86.0	90.0
500	50.0	49.4	55.5	49.1	56.9	58.8	83.7	79.2	83.6	88.9	84.8	89.2
630	49.3	49.0	53.9	47.4	57.1	59.4	82.2	78.7	80.2	86.7	82.7	86.7
800	53.0	52.1	57.3	46.6	53.8	56.2	81.8	78.6	81.3	82.5	83.0	82.8
1000	53.1	51.7	57.8	48.3	51.4	52.1	80.1	76.6	78.5	82.6	81.7	82.7
1250	51.1	48.7	54.2	46.8	48.6	49.4	78.8	75.9	74.7	81.1	81.2	81.1
1600	50.6	50.4	55.0	49.9	47.7	48.2	78.4	76.1	74.6	83.0	78.7	82.9
2000	48.2	47.4	50.5	47.0	42.6	44.2	78.8	75.0	73.8	83.4	79.6	83.6
2500	45.0	43.9	47.7	43.5	41.0	43.4	79.5	74.1	70.0	81.8	80.4	81.9
3150	42.9	42.2	46.1	41.2	42.6	45.5	81.2	74.7	71.9	78.8	81.6	79.2
4000	40.9	40.9	45.2	39.2	42.9	47.3	78.4	73.4	69.3	75.7	78.1	76.0
5000	38.8	38.6	43.5	38.4	42.8	48.4	76.1	69.8	65.8	73.2	75.8	73.5
6300	37.3	36.9	41.9	37.8	41.3	48.3	73.0	65.9	61.8	71.9	72.7	72.1

Table 6-3: Sound powers measured in other rooms and manufacturer's hemi-free field data for a unit of the same type as the NRC RSS.

	Acculab Fan				VAVsim1
	Hemi-free	M59 lower	M59 upper	M27	M59
50	74	70.2	73.4	73.4	
63	74	69.6	67.5	71.4	79.0
80	73	68.9	68.3	69.0	85.1
100	73	67.7	69.6	71.7	89.0
125	72	69.7	69.8	72.4	93.8
160	72	71.4	70.9	72.0	92.1
200	72	71.0	71.1	71.3	85.5
250	72	71.8	71.9	71.4	81.5
315	73	72.7	72.6	72.5	86.9
400	73	73.3	73.4	73.4	85.8
500	73	73.4	73.7	73.6	83.6
630	75	75.3	75.4	75.3	81.4
800	76	77.1	76.9	77.0	82.2
1000	76	77.4	77.2	77.4	80.7
1250	74	76.5	76.4	76.4	80.7
1600	75	75.4	75.1	75.2	77.6
2000	73	74.1	73.4	73.8	78.6
2500	72	73.5	72.7	73.0	79.9
3150	72	73.0	72.3	72.7	81.1
4000	72	71.9	71.1	72.0	77.8
5000	71	70.9	69.7	71.2	76.2
6300	70	70.2	68.8	70.4	72.9

7. Standard measurement procedures in the RAT room.

All measurements in all rooms were performed in essentially the same way. Computer programs control the movement of microphones, the switching of sound systems and the collection of spectral information. Some manual intervention is required in some cases, mostly in the RAT room.

The analyzer used was a Norsonics NE830. Microphones were B&K 13 mm diffuse field microphones type 4166**.**

7.1 Sound pressure levels in the room.

To measure sound pressure levels in the RAT room, two positions of the microphone ladder were used. These were at x = 1.6 and x = 3.2 m. At each x ladder position, the lower microphone was 0.9 m above the floor and the upper microphone was 1.9 m above the floor. Nine positions along the ladder were used. These had z coordinates of 0.6, 1.5, 2.5, 3.5, . . 8.5 m. There were 36 microphone positions in total. The integration time at each position was 32 s.

7.1.1 Repeatability of sound pressure level measurements

The VAVsim1 source provided a means of checking the repeatability of the measurements. It was in place throughout the series, so several measurements were made with it as the source for each ceiling tile. In addition, some measurements were repeated using terminal A. The large duct was also in position for much of the series and repeat measurements were made with it as the source for each ceiling tile. The mean standard deviations are shown in Figure 7-1. Most variation occurred at low frequencies where standard deviations for a specific tile of around 2 dB were found. These were generally found to be due to one single unusual measurement with no apparent explanation for the discrepancy. However, the repeatability was deemed to be good enough for the purpose of the project.

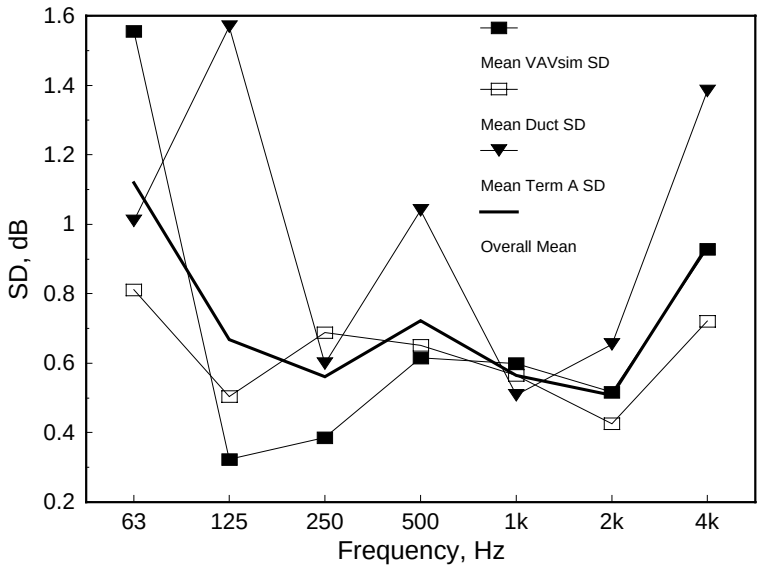

Figure 7-1: Mean standard deviations for sound pressure level measurements.

7.2 Drawaway measurements.

It has been well established that in typical rooms, the decay of sound pressure level with distance from a source does not agree with diffuse-field, reverberant room theory. A plot of sound pressure level vs. distance is here called a drawaway curve. The transition from the direct or near field decaying at 6 dB per distance doubling to the reverberant field with a constant level is not observed. In particular, drawaway curves in the room at low frequencies do not show monotonic decreases in level with distance; the relative lack of room modes leads to strong oscillatory behavior as shown in Figure 7-2.

To measure the reduction in sound pressure level with distance from a source in the RAT room, a dodecahedral source was placed in the south-east corner of the room with the approximate center of the source at the point (0.76, 1.45, 0.47). The microphone ladder was placed at an angle in the room running from the north-west corner to the source. Data were collected at both microphones. The upper microphone was at a height of 1.6 m above the floor.

The dodecahedral source contains twelve 10 mm diameter loudspeakers mounted on the faces of an aluminum dodecahedron. At the high end of the spectrum, the loudspeaker sources used initially were suspected of beaming the sound too much. Different sources were tried, including a long copper pipe driven by a horn driver. This was expected to be a very good approximation to a point source at all frequencies but was unsuitable for the project because it did not emit enough low frequency power. After some comparisons the dodecahedral source was selected for regular use. It is powerful enough and has a radiation pattern that is uniform enough at all frequencies. Some comparisons between dodecahedral and horn driver/pipe results are shown in Figure 7-3 to Figure 7-5.

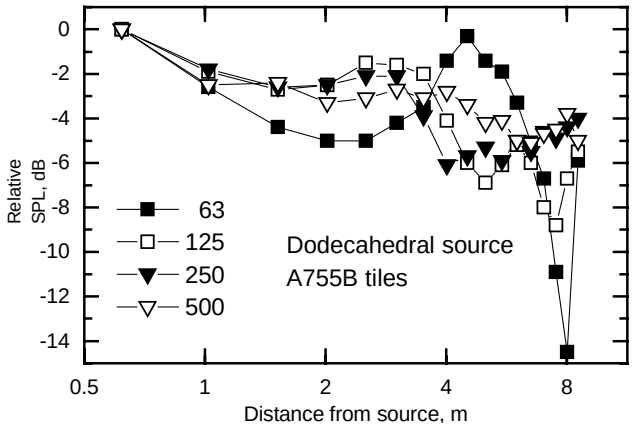

Figure 7-2 : Drawaway curves at low frequencies under A755B tiles.

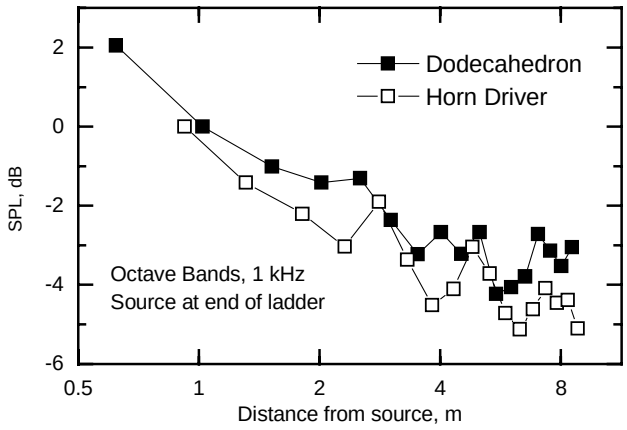

Figure 7-3: Comparison of drawaway curves for the dodecahedral source and the horn driver/pipe source at 1 kHz

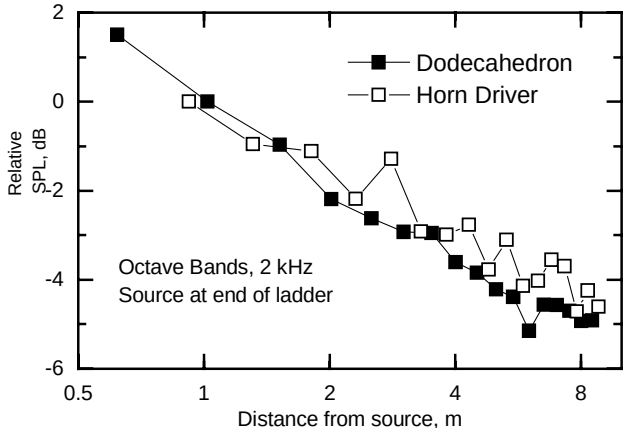

Figure 7-4: Comparison of drawaway curves for the dodecahedral source and the horn driver/pipe source at 2 kHz

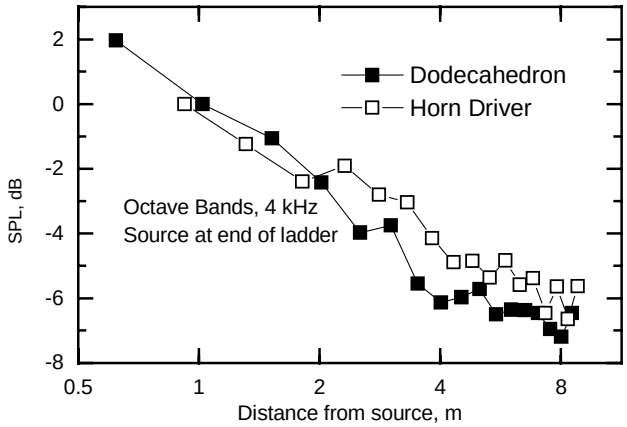

Figure 7-5: Comparison of drawaway curves for the dodecahedral source and the horn driver/pipe source at 4 kHz

7.2.1 Repeatability of drawaway measurements.

As with the sound pressure level measurements, measurements of sound pressure level vs. distance from the dodecahedral source were repeated throughout the series, each time a particular ceiling type was installed. As Figure 7-6 shows, the measurements show most variation in the highest and lowest bands. At low frequencies, the very concept of a drawaway measurement in a room of this size makes little sense. The room sound pressure level shows a strong modal response. Changes in room temperature might account for a lot of the variation at low frequency. At high frequencies, the variations can be attributed to changes in temperature and humidity. These quantities are not controlled in the room and measurements were made in all seasons.

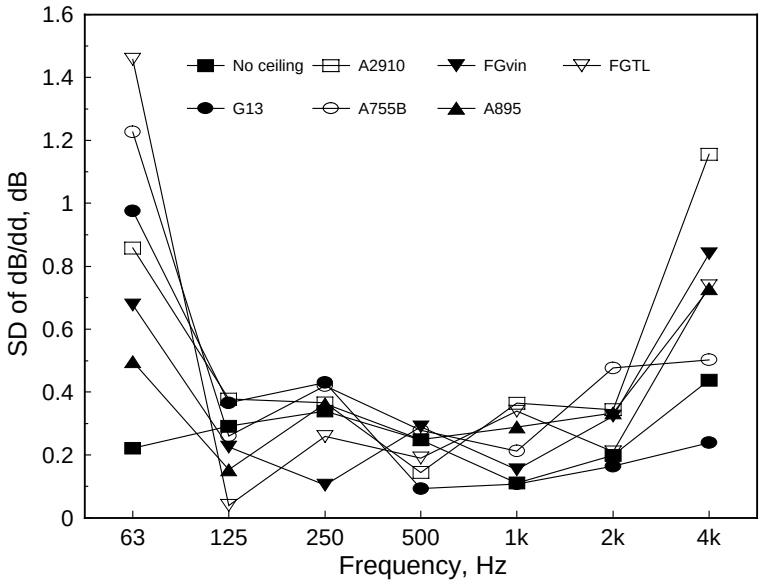

Figure 7-6: Standard deviations for drawaway measurements.

7.3 Reverberation Times.

Reverberation times were measured in the room using two loudspeakers in diagonally opposite corners as noise sources. The speakers were supplied with pink noise and the same diagonal position of the microphone ladder that was used for drawaway measurements was used. Seventeen microphone positions were used. At each position, the NE830 RTA collected 10 decays and formed an average of the decays at each frequency. The ensemble was passed to the computer and a straight line was fitted to the first 25 dB of the decay in each one-third octave band.

7.3.1 Repeatability of reverberation times.

Repeat measurements of reverberation time showed very low variability when ceiling tiles were installed (Figure 7-7). The measurements of the empty room show much more variation because the empty room was continually being varied by the addition of different terminal units and changes to the ductwork. The variations in the case of the gypsum board tiles can be explained by variations in room temperature and humidity; air absorption is a more significant factor when most of the room surfaces are hard.

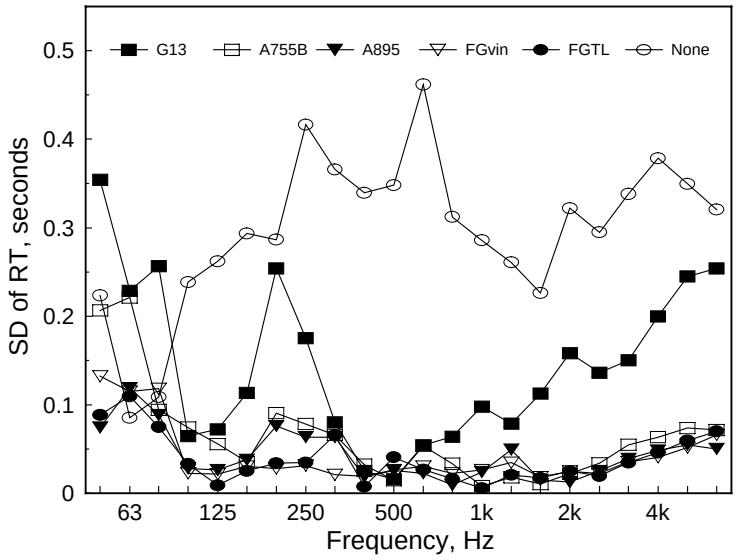

Figure 7-7: Repeatability for measurements of reverberation time.

8. RAT room reverberation times.

For the standard conditions with 100 mm of foam lining the plenum, and eight fixed diffusing panels, the average reverberation times obtained with each ceiling are given in Table 8-1. These data are also plotted in Figure 8-8 and Figure 8-9.

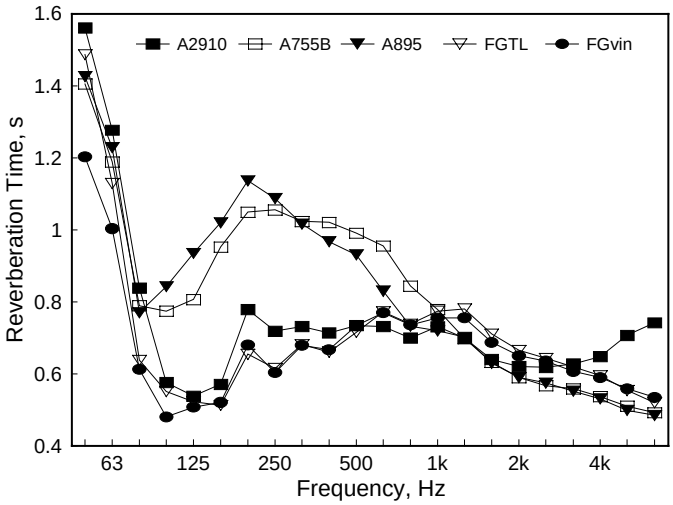

Figure 8-8: Reverberation times under normal test conditions: 100 mm foam lining the plenum and diffusers in the room – absorptive ceilings.

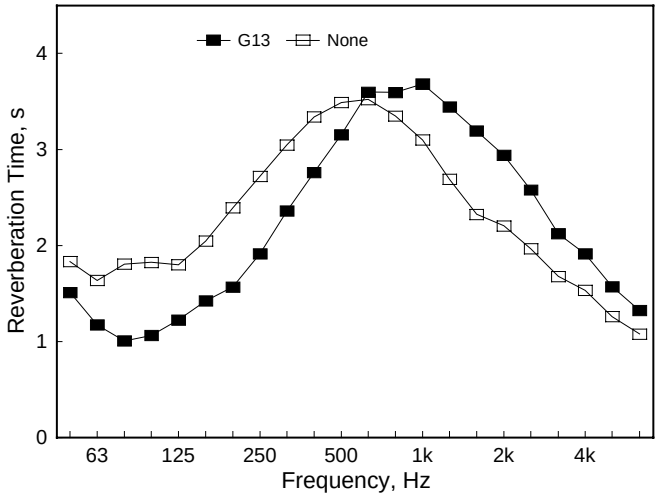

Figure 8-9: Reverberation times under normal test conditions: 100 mm foam lining the plenum and diffusers in the room – G13 and the empty room, no ceiling case.

Table 8-1: Average reverberation times in the RAT room under standard conditions.

	A895	A755B	FGvin	FGTL	A2910	G13	none
50	1.43	1.41	1.20	1.49	1.56	1.51	1.83
63	1.23	1.19	1.00	1.13	1.28	1.17	1.64
80	0.77	0.79	0.61	0.64	0.84	1.01	1.81
100	0.84	0.77	0.48	0.55	0.58	1.06	1.82
125	0.94	0.81	0.51	0.52	0.54	1.22	1.80
160	1.02	0.95	0.52	0.51	0.57	1.42	2.05
200	1.14	1.05	0.68	0.65	0.78	1.57	2.39
250	1.09	1.06	0.60	0.62	0.72	1.91	2.72
315	1.02	1.02	0.68	0.68	0.73	2.36	3.05
400	0.97	1.02	0.67	0.66	0.71	2.76	3.34
500	0.93	0.99	0.73	0.72	0.73	3.15	3.49
630	0.83	0.96	0.77	0.77	0.73	3.60	3.52
800	0.73	0.84	0.74	0.74	0.70	3.59	3.35
1000	0.72	0.78	0.76	0.77	0.73	3.68	3.10
1250	0.70	0.70	0.76	0.78	0.70	3.44	2.69
1600	0.63	0.63	0.69	0.71	0.64	3.19	2.32
2000	0.59	0.59	0.65	0.67	0.62	2.94	2.21
2500	0.57	0.57	0.64	0.64	0.62	2.58	1.97
3150	0.55	0.56	0.61	0.62	0.63	2.12	1.68
4000	0.53	0.54	0.59	0.60	0.65	1.91	1.53
5000	0.50	0.51	0.56	0.55	0.71	1.57	1.26
6300	0.48	0.49	0.53	0.52	0.74	1.32	1.08

Changing the absorptive material in the plenum from the 100 mm of foam to the 300 mm of glass fiber had no significant effect on the room reverberation times under the A755B tiles. The reverberation times were reduced slightly at high frequencies under the more porous FGvin tiles. In both cases, the addition of a carpet and absorbing panels on the walls had a much greater effect on the reverberation times (See Figure 8-10 and Figure 8-11).

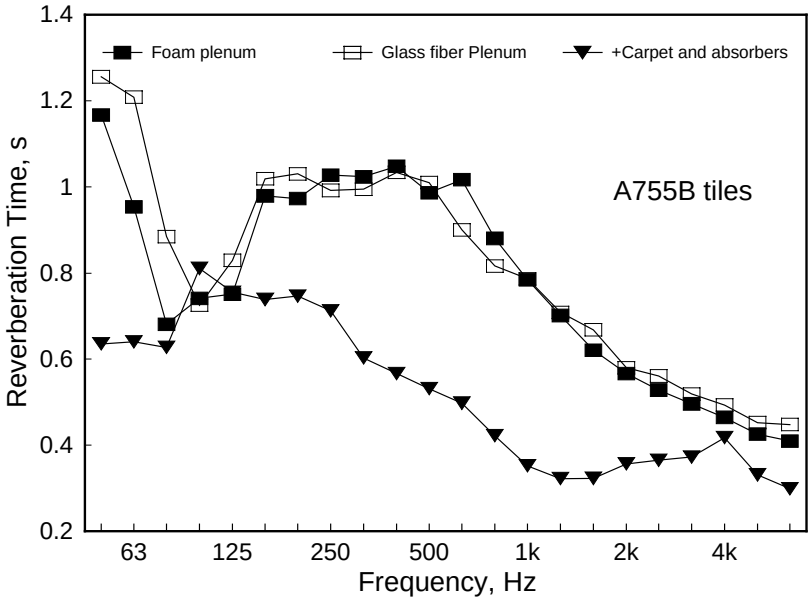

Figure 8-10: Reverberation times for different room and plenum conditions under A755B tiles. The cases where the carpet was added was measured with glass fiber batts in the plenum.

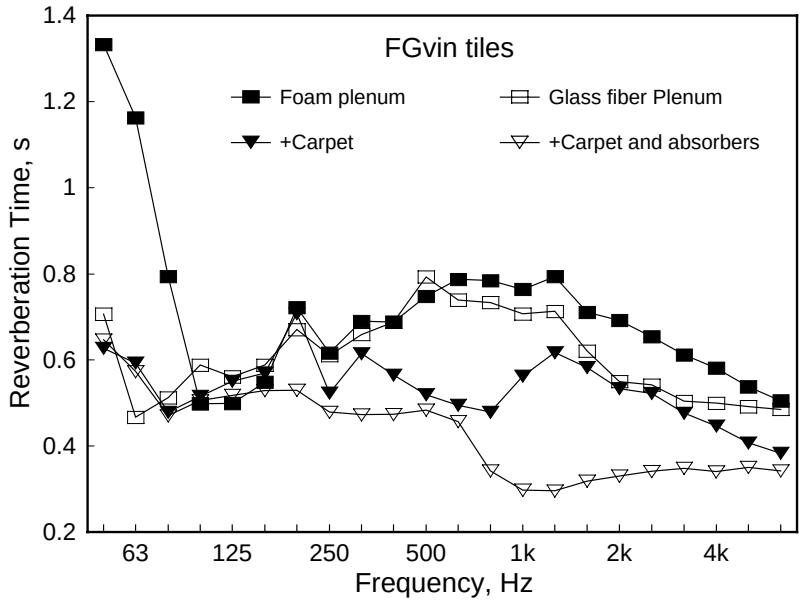

Figure 8-11: Reverberation times for different room and plenum conditions under FGvin tiles. The cases where the carpet and wall absorbers were added were measured with glass fiber batts in the plenum.

9. Ceiling tiles used.

9.1 Physical properties

Five types of ceiling panels were initially selected for this project. The panels measured 625 x 1250 mm and are described in Table 9-1 below. Towards the end of the project, an additional ceiling type (A2910), expected to have much lower sound transmission loss, was added to give more information. The codes in column 1 are used to identify each panel type throughout this report for convenience. Because the A2910 tiles were added later, absorption coefficients and sound transmission loss values were not measured.

Table 9-1: Identification and properties of ceiling panels used in the project

Panel Code	Ceiling panel type	Weight per tile (kg)	Surface mass kg/m^2
A895	16 mm thick Armstrong type 895 Fireguard mineral fiber tiles	3.68	4.70
A755B	16 mm thick Armstrong type 755B Minaboard mineral fiber tiles	1.83	2.35
G13	13 mm vinyl-faced gypsum board	6.8	8.70
FGvin	50 mm thick glass fiber tile with perforated vinyl face	2.4	3.07
FGTL	50 mm thick glass fiber tile with perforated vinyl face and metal foil backing	2.4	3.07
A2910	16 mm thick Armstrong type A2910 random fissure perforated glass fiber tiles	0.69	0.88

9.2 Sound absorption — ASTM C423.

Sound absorption for each ceiling specimen was measured in the 250 m^3 room in M27. These measurements were made with each specimen mounted in an E400 frame with the finished face exposed and with the finished face enclosed in the frame. Measurements were also made with the specimens lying on the laboratory floor with the finished face upwards and downwards. Measurements with the gypsum board were made with only the vinyl face exposed since the coefficients were so small as to be of doubtful value. Table 9-2 and Table 9-3 show the coefficients in each case. To provide a graphical comparison, the coefficients in these tables are plotted in Figure 9-1 to Figure 9-4.

Table 9-2: Sound absorption coefficients with specimens mounted in E400 frame with finished face upwards and downwards.

	Face Upwards					Face Downwards			
Freq.	A755B	A895	FGvin	FGTL	G13	A755B	A895	FGvin	FGTL
80	0.85	0.94	0.99	1.06	0.58	0.89	0.89	0.99	0.88
100	0.31	0.36	0.89	0.62	0.14	0.29	0.31	0.76	0.40
125	0.25	0.28	0.73	0.67	0.12	0.21	0.24	0.76	0.42
160	0.27	0.19	0.93	0.86	-0.00	0.21	0.13	0.81	0.45
200	0.24	0.18	0.88	0.86	-0.02	0.23	0.14	0.79	0.53
250	0.25	0.22	0.94	0.84	-0.00	0.17	0.14	0.85	0.67
315	0.28	0.23	0.99	0.78	0.00	0.16	0.12	0.88	0.72
400	0.33	0.29	0.99	1.01	0.01	0.16	0.14	0.90	0.65
500	0.41	0.35	1.05	1.16	0.01	0.18	0.15	0.98	0.77
630	0.49	0.40	1.14	1.18	0.00	0.17	0.15	1.07	0.79
800	0.53	0.47	1.15	1.18	0.00	0.17	0.14	1.05	0.68
1000	0.58	0.54	1.13	1.16	0.00	0.17	0.14	1.05	0.63
1250	0.61	0.57	1.13	1.15	-0.02	0.17	0.14	1.04	0.60
1600	0.64	0.61	1.13	1.13	-0.02	0.17	0.14	1.02	0.56
2000	0.65	0.64	1.10	1.09	-0.03	0.18	0.13	1.02	0.50
2500	0.67	0.66	1.05	1.04	-0.00	0.19	0.15	0.98	0.43
3150	0.70	0.67	0.99	1.00	0.01	0.21	0.16	1.00	0.37
4000	0.73	0.68	0.94	0.96	-0.00	0.23	0.18	1.01	0.33
5000	0.75	0.69	0.91	0.89	0.01	0.25	0.20	1.01	0.29
6300	0.75	0.71	0.83	0.82	0.00	0.28	0.23	1.01	0.24

Table 9-3: Sound absorption measurements with finished face upwards and downwards in A mounting, flat on laboratory floor.

	Face upwards					Face Downwards			
Freq.	A755B	A895	FGvin	FGTL	G13	A755B	A895	FGvin	FGTL
80	0.05	0.06	0.06	0.15	-0.00	0.04	0.03	0.06	0.32
100	0.02	0.01	0.16	0.11	-0.01	0.03	0.04	0.14	0.34
125	0.05	0.04	0.28	0.15	-0.00	0.06	0.10	0.23	0.49
160	0.09	0.11	0.49	0.37	0.01	0.12	0.13	0.44	0.52
200	0.14	0.14	0.67	0.66	0.02	0.21	0.25	0.61	0.65
250	0.19	0.20	0.87	0.93	0.00	0.35	0.41	0.85	0.94
315	0.28	0.30	1.14	1.11	0.03	0.56	0.61	1.08	1.18
400	0.41	0.42	1.22	1.19	0.05	0.66	0.57	1.16	0.95
500	0.57	0.54	1.19	1.21	0.09	0.56	0.42	1.17	0.98
630	0.71	0.62	1.19	1.20	0.09	0.41	0.33	1.17	0.95
800	0.75	0.65	1.13	1.17	0.10	0.33	0.25	1.15	0.81
1000	0.74	0.65	1.08	1.12	0.08	0.29	0.23	1.10	0.72
1250	0.72	0.67	1.07	1.09	0.07	0.28	0.23	1.08	0.73
1600	0.72	0.71	1.03	1.07	0.06	0.28	0.23	1.05	0.69
2000	0.71	0.72	1.00	1.05	0.06	0.29	0.24	1.03	0.65
2500	0.73	0.73	0.97	1.01	0.05	0.28	0.23	1.02	0.59
3150	0.74	0.71	0.94	0.97	0.05	0.28	0.22	1.00	0.50
4000	0.76	0.74	0.91	0.95	0.03	0.30	0.23	1.00	0.45
5000	0.79	0.74	0.86	0.89	0.04	0.30	0.24	1.03	0.39
6300	0.78	0.74	0.82	0.83	0.03	0.32	0.25	1.03	0.32

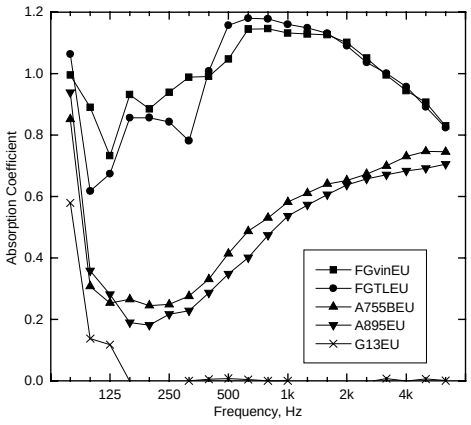

Figure 9-1: Absorption coefficients with specimens in E400 mount with finished surface upwards.

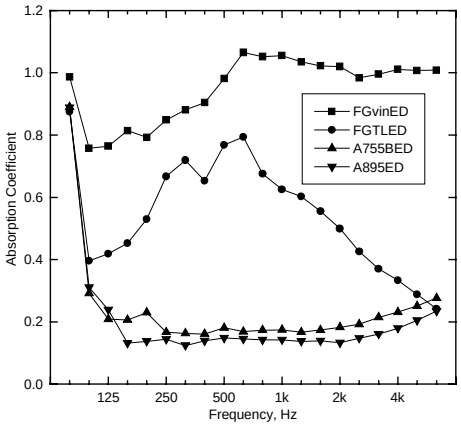

Figure 9-2: Absorption coefficients with specimens in E400 mount with finished surface downwards.

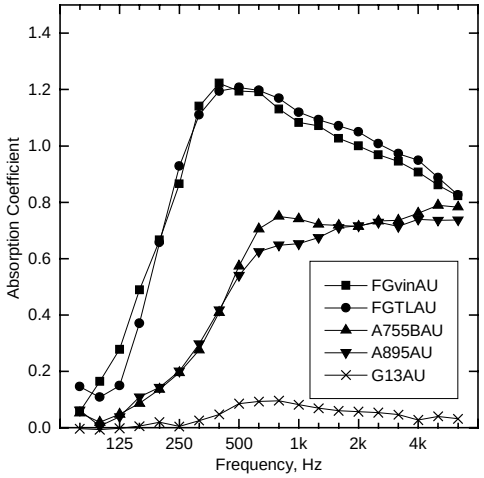

Figure 9-3: Absorption coefficients with specimens flat on laboratory floor with finished surface upwards.

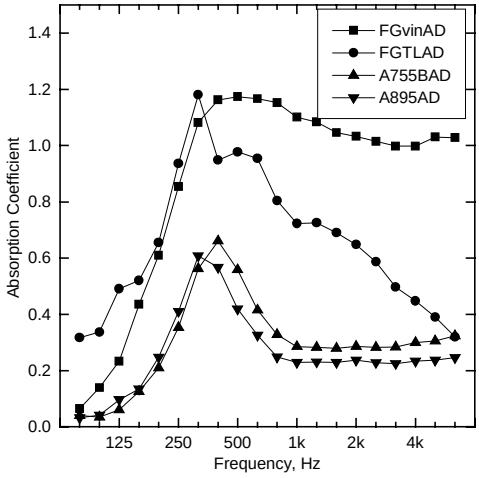

Figure 9-4: Absorption coefficients with specimens flat on laboratory floor with finished surface downwards.

9.3 Sound transmission loss — ASTM E90.

9.3.1 Normal installation.

Sound transmission loss measurements through the ceiling panels were made in accordance with ASTM E90 by installing the panels in a T-bar grid mounted between the

two rooms of the floor facility in M59. The data are listed in Table 9-4 and plotted for comparison in Figure 9-5.

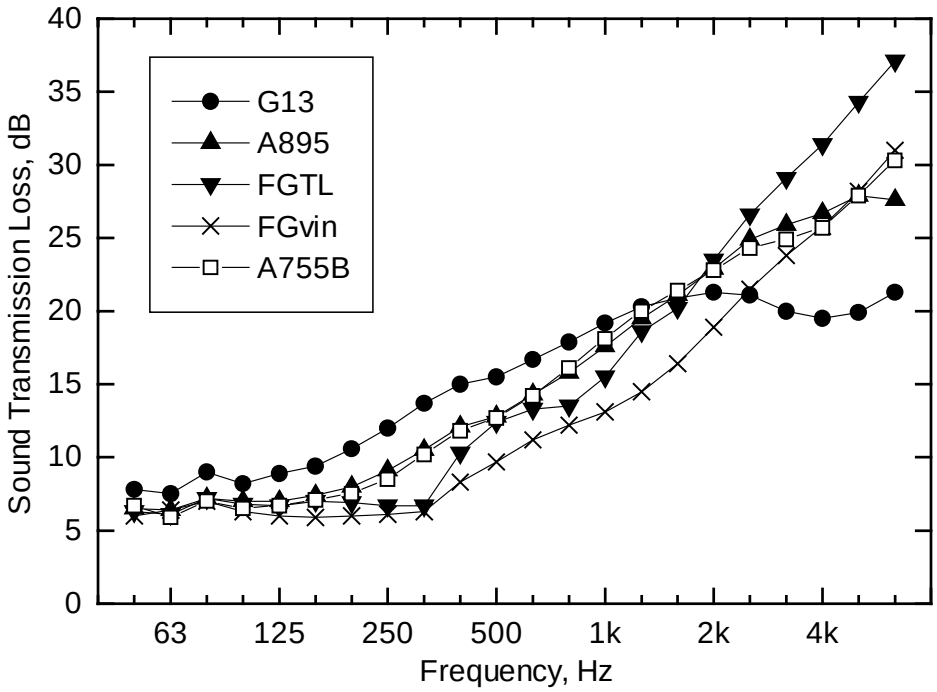

Figure 9-5: Single pass E90 sound transmission loss measurements for ceiling panels

Table 9-4: Airborne sound transmission loss measurements made on the ceiling types according to ASTM E90.

Freq.	G13	G13 taped	A755B	A895	FGvin	FGTL
50	7.8	10.6	6.7	6.5	6.0	6.3
63	7.5	12.5	5.9	6.4	6.4	6.1
80	9.0	14.0	7.0	7.2	7.0	7.2
100	8.2	13.2	6.5	7.0	6.3	6.8
125	8.9	14.1	6.7	7.0	6.0	6.7
160	9.4	16.7	7.1	7.4	5.9	7.0
200	10.6	18.5	7.5	8.0	6.0	6.9
250	12.0	20.6	8.5	9.1	6.1	6.7
315	13.7	23.2	10.2	10.5	6.3	6.7
400	15.0	24.4	11.8	12.1	8.3	10.3
500	15.5	25.2	12.7	12.8	9.7	12.4
630	16.7	26.8	14.2	14.3	11.2	13.3
800	17.9	27.3	16.1	15.8	12.2	13.5
1000	19.2	27.6	18.1	17.6	13.1	15.5
1250	20.3	27.0	20.0	19.5	14.5	18.6
1600	20.9	25.9	21.4	21.1	16.4	20.2
2000	21.3	25.5	22.8	22.9	18.9	23.5
2500	21.1	24.7	24.3	24.9	21.5	26.6
3150	20.0	23.9	24.9	25.9	23.8	29.1
4000	19.5	25.4	25.7	26.7	25.8	31.4
5000	19.9	27.8	27.9	27.9	28.2	34.3
6300	21.3	30.2	30.3	27.6	31.0	37.1
STC	19	26	17	18	14	16

9.3.2 Leakage through gypsum board tiles.

It quickly became evident during the project that a dominant path through the ceiling is leakage between the tiles and the T-bar systems; there was little difference observed in

the sound pressure levels RAT room when ceiling types were changed. To estimate the leakage in a T-bar system, measurements were made in the M59 floor transmission loss suite with gypsum board tiles in a T-bar system with a normal installation and with the gaps between the gypsum board and the T-bar taped. Similar measurements from our old M27 floor transmission loss suite were also available for comparison. These data, shown in Figure 9-6 were used to calculate an approximate value for the leakage through the gypsum board ceiling system as follows.

We measure 2 transmission losses, TL_1 and TL_2, which have corresponding. transmission coefficients

$$\tau_1 = 10^{-TL_1/10} \text{ with leaks, and}$$

$$\tau_2 = 10^{-TL_2/10} \text{ with no leaks, the gypsum board transmission coefficient.}$$

For the transmission through the leaky board we have

$$A_{tot}\tau_1 = \left(A_{tot} - A_{leak}\right)\tau_2 + A_{leak} \times 1$$

where A_{tot} and A_{leak} are the areas of the ceiling and the total area of leaks. The transmission coefficient through the leak is taken as 1. This can be rearranged to calculate the area of the leaks around the tiles. The calculated area as a percentage is shown in Figure 9-7.

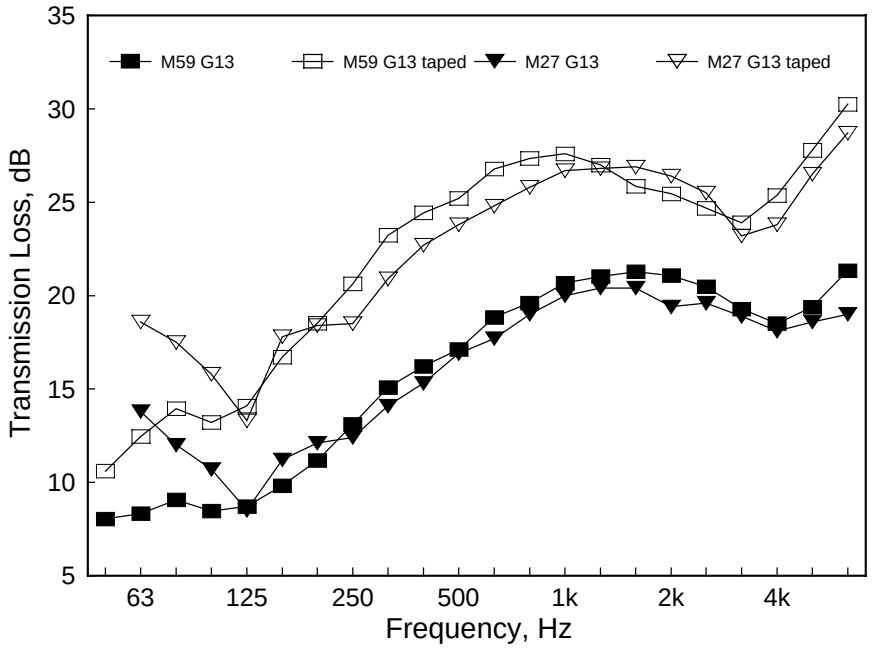

Figure 9-6 Transmission loss through 13 mm gypsum board tiles in a T-bar system in the M59 and M27 test suites. The two results show the effect of taping the joints between the gypsum board and the T-bars.

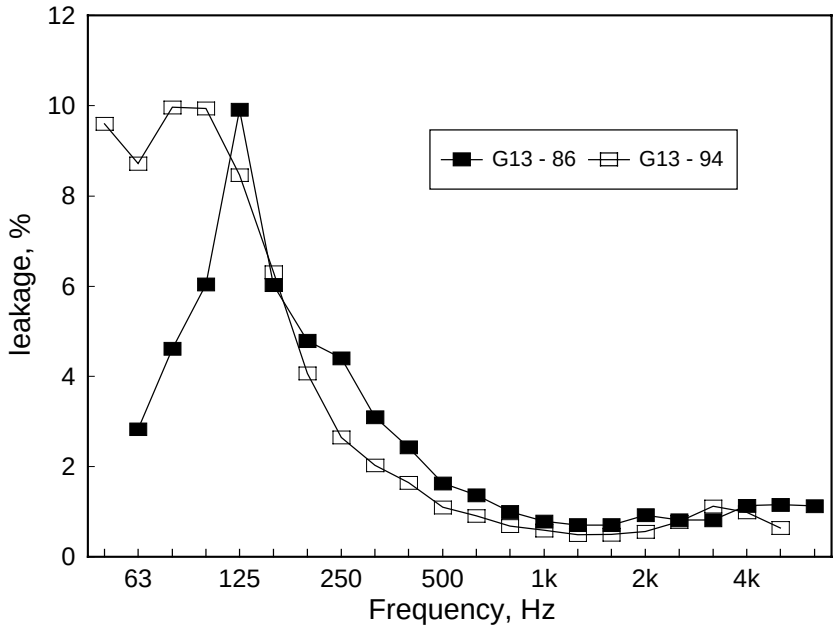

Figure 9-7 Estimated leakage around 13 mm gypsum board tiles in a T-bar system. The G13-86 result is from the M27 facility, the G13-94 result is from the M59 facility.

9.4 Two-pass ceiling sound transmission loss — ASTM E1414.

Each ceiling panel type was tested according to ASTM E1414. To do this, the RAT room was divided into two parts with the dimensions given in Table 5-1. The separating partition extended to the underside of the ceiling plane. Preliminary tests of the partition showed that transmission through it was negligible relative to the path through the plenum and ceiling panels. For these tests the plenum was lined with 100 mm of foam sound absorbing material. Each room contained two loudspeakers driven by separate noise generators and amplifiers. These were used to measure the noise reductions between the rooms and the reverberation times in each room. Eight microphone positions were used in each room.

The test procedure was followed with each room in turn serving as the source room. The calculated normalized ceiling attenuations for each direction of measurement were averaged. The two rooms formed by the dividing partition are called the East RAT and the West RAT room. The West RAT room is the room with the movable wall.

Table 9-5 shows the mean values of normalized ceiling attenuation for each ceiling type. The data are plotted in Figure 9-8. As in all the measurements reported here, the ceiling tiles were simply laid in the T-bar slots. Included in the Table and figure for interest are the data for the case when the joint between the T-bars and the gypsum board ceiling was covered with tape.

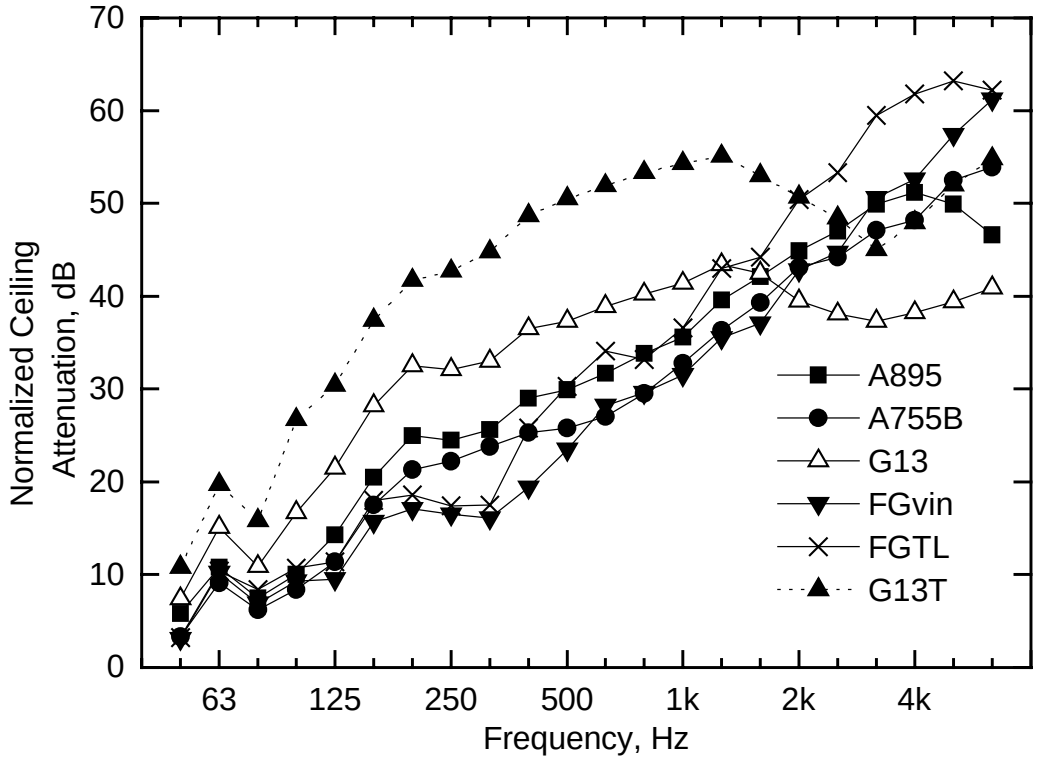

Figure 9-8: Mean normalized ceiling attenuation for the five ceiling boards. The G13T data are for the case where the joints between the G13 tiles and the T-bars were taped over.

Table 9-5: Average normalized ceiling attenuations, dB and Ceiling Attenuation Classes for five ceiling types.

Frequency, Hz	A895	A755B	G13	G13 taped	FGvin	FGTL
50	5.8	3.3	7.4	10.8	3.1	3.2
63	10.8	9.1	15.1	19.7	10.2	10.4
80	7.5	6.2	10.9	15.8	6.9	8.4
100	10.0	8.4	16.7	26.7	9.3	10.7
125	14.3	11.4	21.5	30.4	9.5	11.4
160	20.5	17.5	28.2	37.4	15.7	18.0
200	25.0	21.3	32.5	41.7	17.1	18.6
250	24.5	22.2	32.1	42.7	16.5	17.4
315	25.6	23.8	33.0	44.8	16.1	17.5
400	29.0	25.3	36.5	48.7	19.4	25.8
500	29.9	25.8	37.3	50.5	23.5	30.3
630	31.7	27.0	38.9	51.9	28.2	34.1
800	33.8	29.5	40.2	53.3	29.6	33.2
1000	35.6	32.8	41.4	54.3	31.5	36.6
1250	39.6	36.3	43.4	55.1	35.5	43.0
1600	42.1	39.3	42.5	53.0	37.1	44.2
2000	44.9	43.1	39.5	50.7	42.8	50.4
2500	47.0	44.2	38.1	48.4	44.7	53.3
3150	49.9	47.1	37.3	45.0	50.6	59.5
4000	51.2	48.2	38.2	47.9	52.6	61.8
5000	49.9	52.5	39.4	52.0	57.4	63.2
6300	46.6	53.9	40.9	54.8	61.2	62.2
CAC	34	31	39	49	28	30

9.5 Levels in two adjacent rooms due to source in plenum.

When E1414 measurements were being made in the RAT room, levels from Box A operating in the plenum were measured in the two smaller rooms created by the separating wall. These were done under four types of tiles. Figure 9-9 shows the levels in the East room, the room directly below the simulated source and Figure 9-10 shows the levels in the West room, the adjacent room. For interest, the difference in levels between the two rooms is shown in Figure 9-11. The graphs again make it evident that there is little difference between the ceiling types.

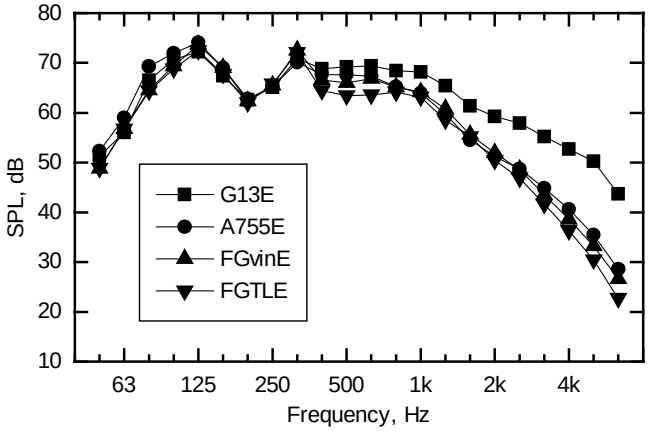

Figure 9-9: SPLs in the East RAT room with the simulated terminal box operating above the ceiling.

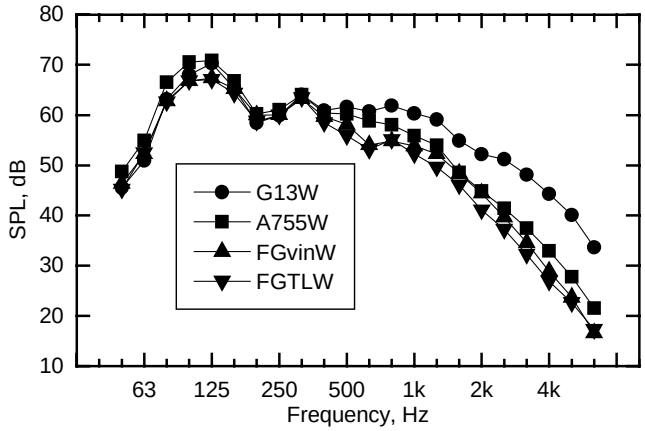

Figure 9-10: SPLs in the West RAT room with the simulated terminal box operating above the ceiling in the East room.

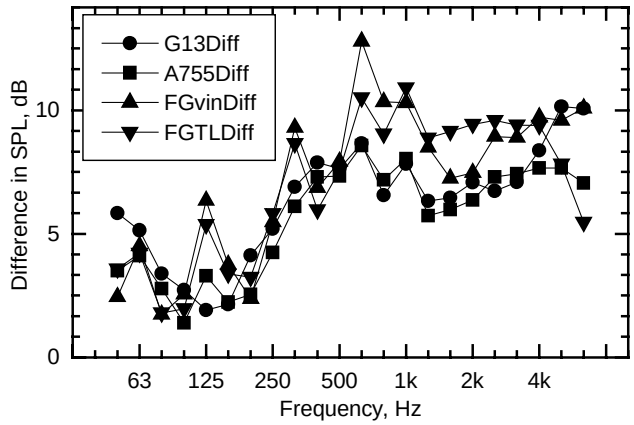

Figure 9-11: Difference in between East and West rooms with the simulated terminal unit operating above the East room ceiling.

10. Sound pressure level versus distance from source.

10.1 Dodecahedral source below the ceiling.

The dodecahedral source and the procedures used for collecting drawaway curves in the RAT room are described in more detail in Section 7.1.1. Examples of octave band drawaway curves for the FGTL tiles are shown in Figure 10-1 to Figure 10-7. Examples for the case of the G13 tiles are shown in Figure 10-8 to Figure 10-14. The dotted straight line in each graph is the regression line for the data within 3.5 metres of the source. These figures are for the upper of the two microphones, 1.6 m above the floor, on the vertical microphone support.

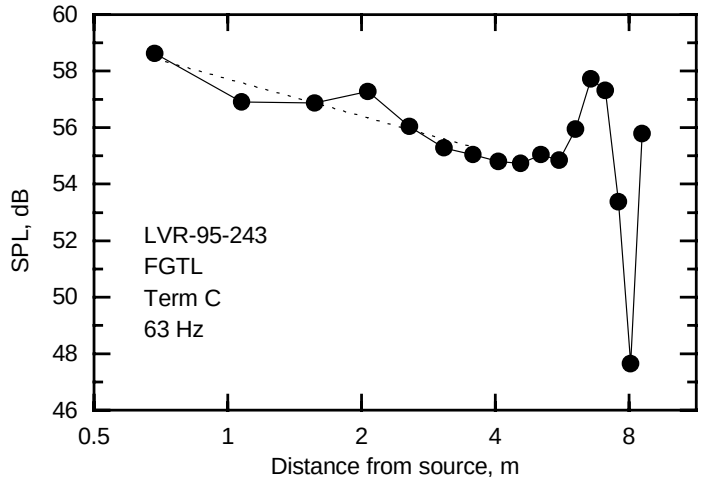

Figure 10-1: Octave Band sound pressure level versus distance from the dodecahedral source for the FGTL tiles at 63 Hz.

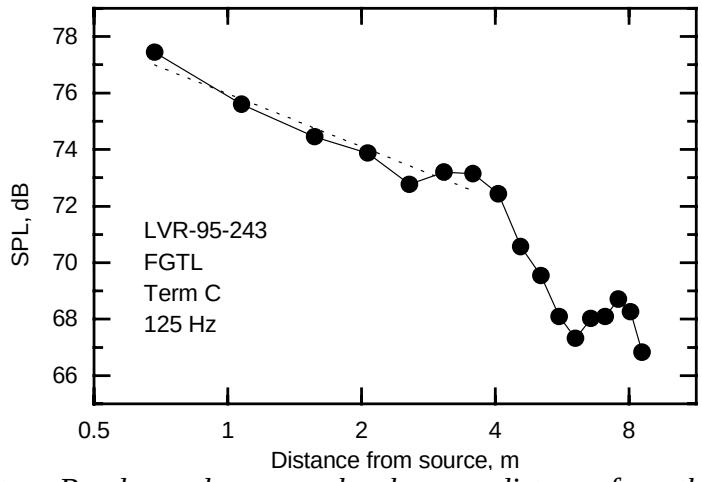

Figure 10-2: Octave Band sound pressure level versus distance from the dodecahedral source for the FGTL tiles at 125 Hz.

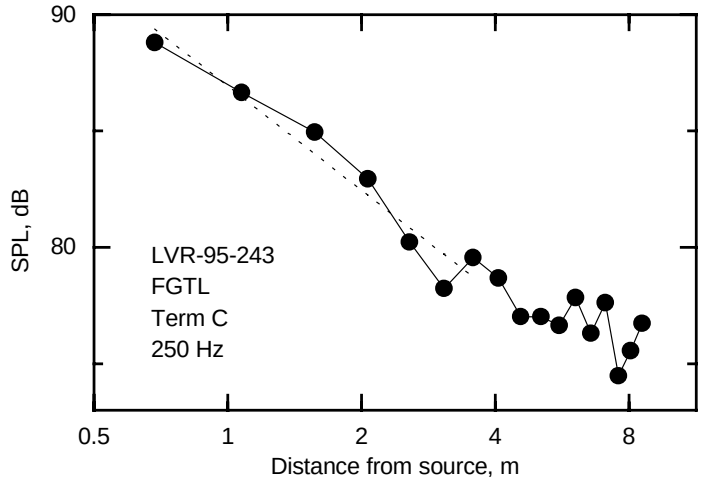

Figure 10-3: Octave Band sound pressure level versus distance from the dodecahedral source for the FGTL tiles at 250 Hz.

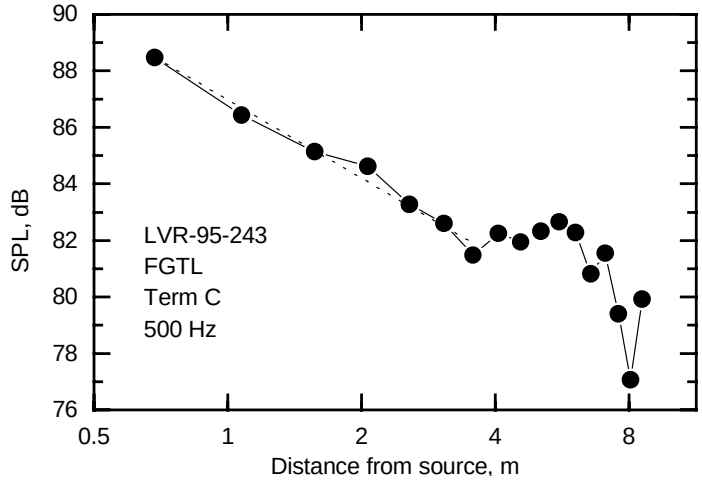

Figure 10-4: Octave Band sound pressure level versus distance from the dodecahedral source for the FGTL tiles at 500 Hz.

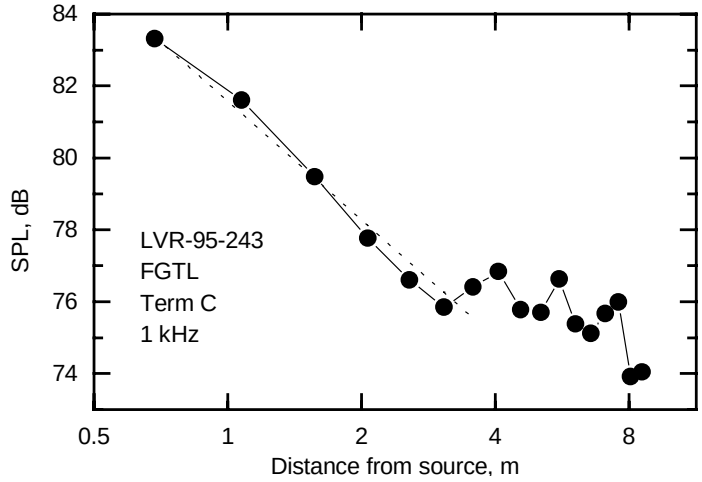

Figure 10-5: Octave Band sound pressure level versus distance from the dodecahedral source for the FGTL tiles at 1000 Hz.

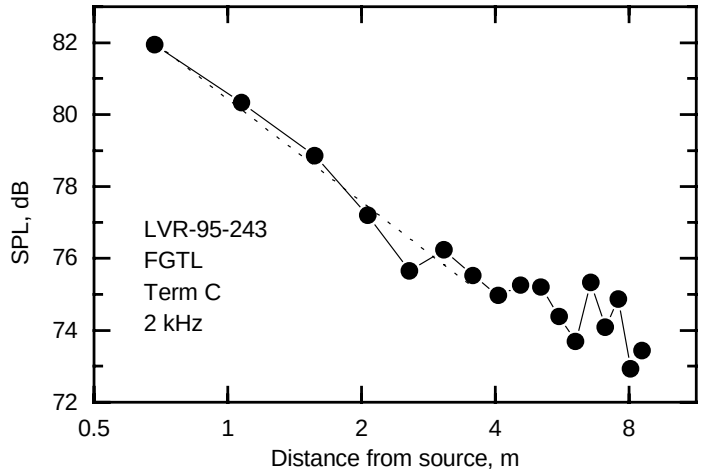

Figure 10-6: Octave Band sound pressure level versus distance from the dodecahedral source for the FGTL tiles at 2000 Hz.

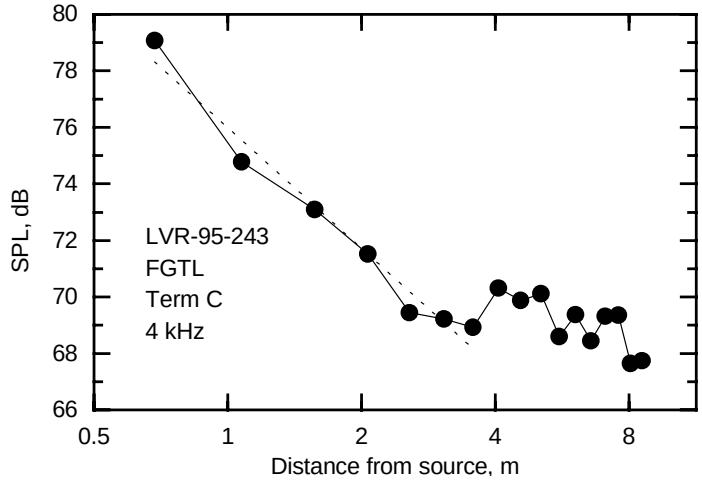

Figure 10-7: Octave Band sound pressure level versus distance from the dodecahedral source for the FGTL tiles at 4000 Hz.

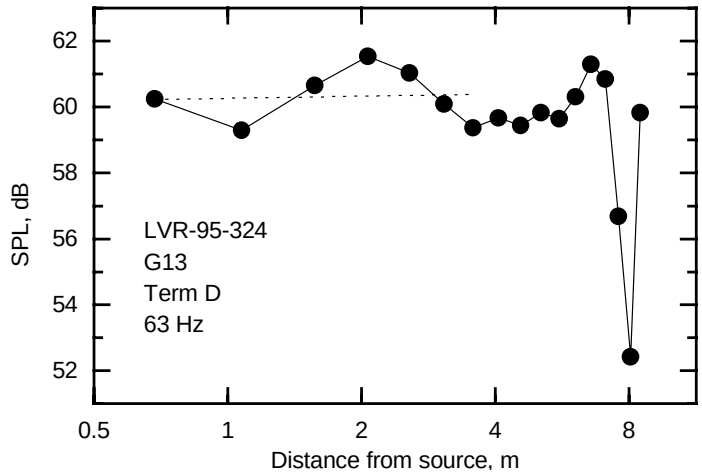

Figure 10-8: Octave Band sound pressure level versus distance from the dodecahedral source for the G13 tiles at 63 Hz.

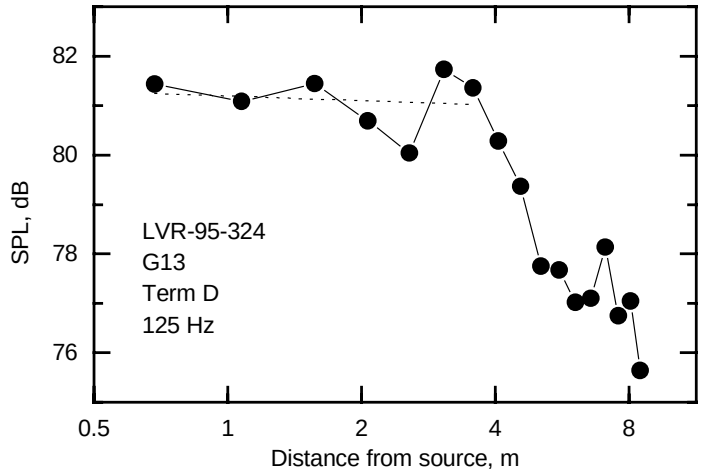

Figure 10-9: Octave Band sound pressure level versus distance from the dodecahedral source for the G13 tiles at 125 Hz.

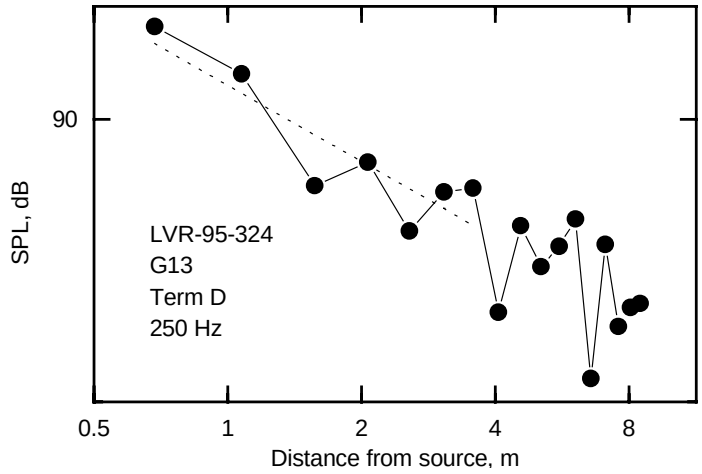

Figure 10-10: Octave Band sound pressure level versus distance from the dodecahedral source for the G13 tiles at 250 Hz.

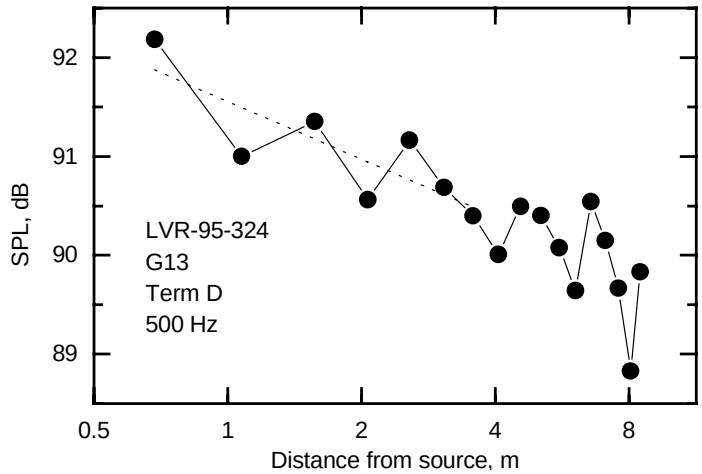

Figure 10-11: Octave Band sound pressure level versus distance from the dodecahedral source for the G13 tiles at 500 Hz.

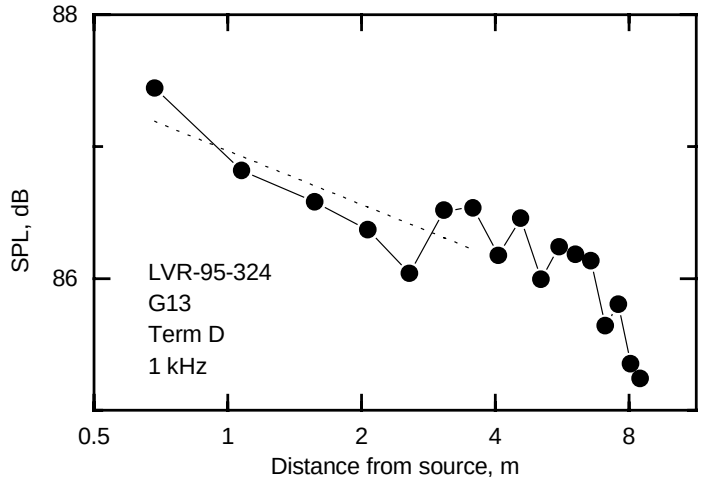

Figure 10-12: Octave Band sound pressure level versus distance from the dodecahedral source for the G13 tiles at 1000 Hz.

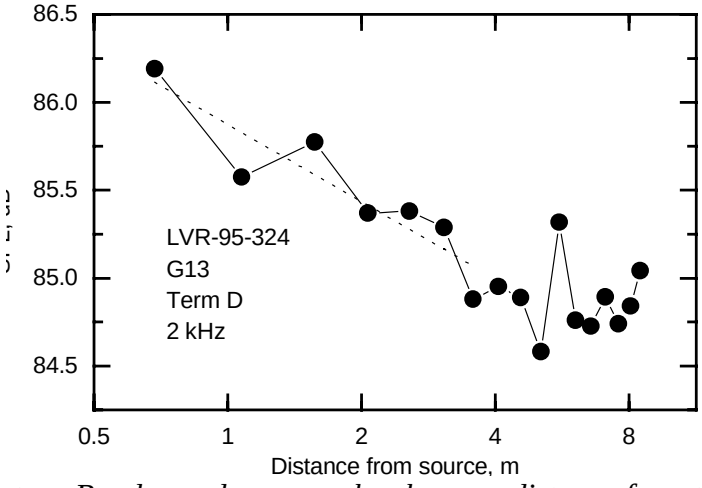

Figure 10-13: Octave Band sound pressure level versus distance from the dodecahedral source for the G13 tiles at 2000 Hz.

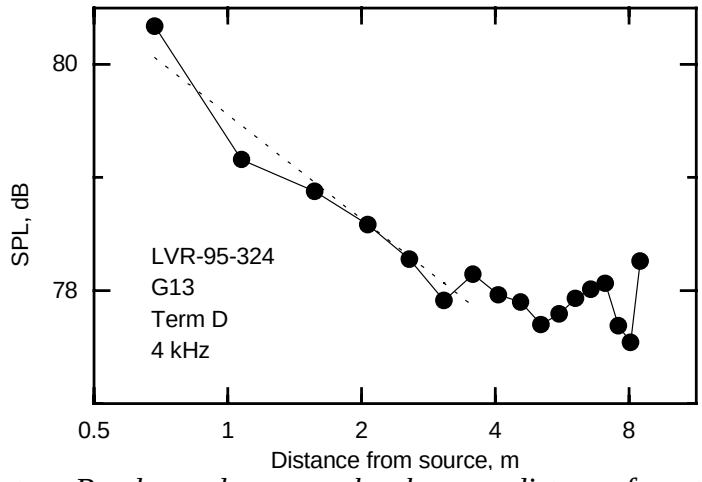

Figure 10-14: Octave Band sound pressure level versus distance from the dodecahedral source for the G13 tiles at 4000 Hz.

For the FGTL tiles, there is no real indication of a uniform reverberant field except perhaps at 1000 and 4000 Hz. At the lower frequencies there are quite strong indications of room resonances which are even more evident when the data are viewed as 1/3 octave bands. Much the same may be said about the curves for the G13 tiles.

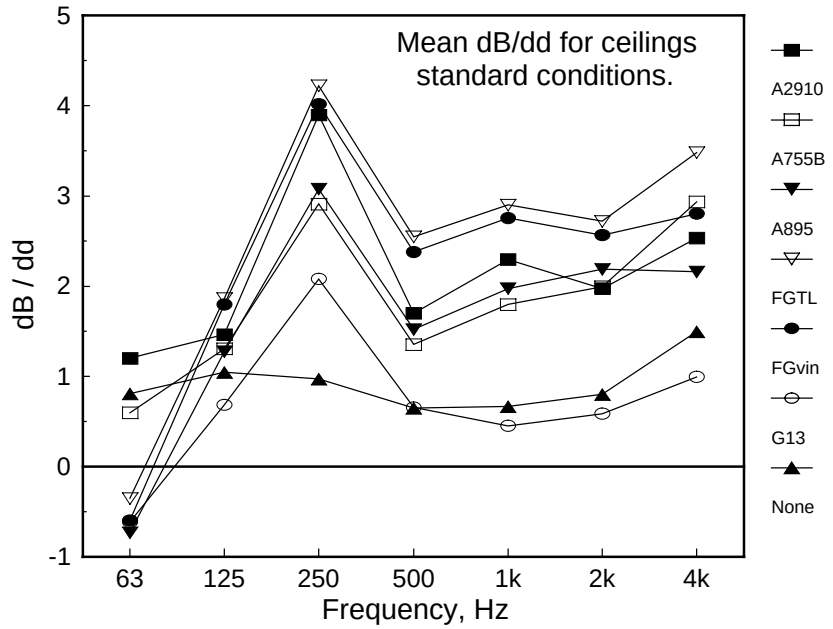

Figure 10-15: Average value of sound attenuation with distance doubling (dB/dd) for the dodecahedral source for the ceiling tiles used in the project.

These drawaway curves were obtained for each tile type each time it was installed beneath one of the terminal units. The mean slope for each tile type is shown in Figure 10-15. The Schultz formula predicts a 10 log *r* dependence or 3 dB/dd. The mean value for all the conventional ceiling tiles from 500 to 4000 Hz is about 2.5 dB/dd. The difference between the types of tiles is quite clear although not very great.

Table 10-1: Mean values of attenuation, dB/distance doubling, for dodecahedral source.

Ceiling Type	Octave Band Frequency, Hz						
	63	125	250	500	1k	2k	4k
A2910	1.2	1.5	3.9	1.7	2.3	2.0	2.5
A755B	0.6	1.3	2.9	1.4	1.8	2.0	2.9
A895	-0.7	1.3	3.1	1.5	2.0	2.2	2.2
FGTL	-0.4	1.9	4.2	2.5	2.9	2.7	3.5
FGvin	-0.6	1.8	4.0	2.4	2.8	2.6	2.8
G13	-0.6	0.7	2.1	0.7	0.5	0.6	1.0
None	0.8	1.0	1.0	0.6	0.7	0.8	1.3

10.1.1 Effects of plenum lining, carpet and absorbers.

It must be remembered that the RAT room was not furnished normally during these experiments. It did have fixed diffusing panels mounted on the walls of the room but the floor was bare and there was no furniture. The bare floor made it easier to move the microphone ladder around and clean the room. To get some information about the effects of a carpet and additional absorption in the room, some measurements were made with a carpeted floor and several absorbing panels added to the room. This was done for two types of ceiling tiles: FGvin and A755B. Aside from reducing reverberation times in the room, the sound levels decreased more rapidly with distance above 500 Hz, in some cases to slightly more than the 3 dB/dd expected from the Schultz formula. The values of dB/dd for some configurations are shown in Figure 10-16 and Figure 10-17.

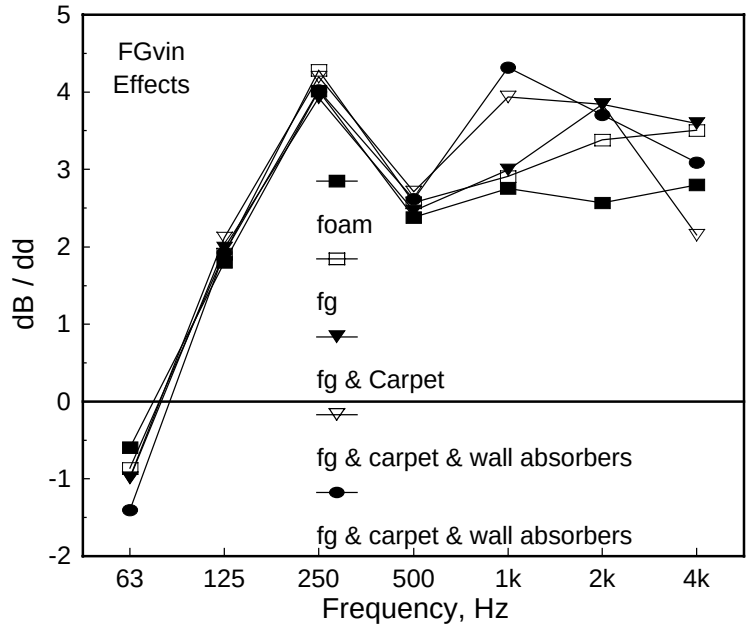

Figure 10-16: Sound attenuation with distance under FGvin tiles for different room conditions. Key: foam – 100 mm foam lining plenum; fg – 300 mm glass fiber lining plenum; carpet – carpet installed on the floor; wall absorbers – sound absorbing panels installed on the room walls.

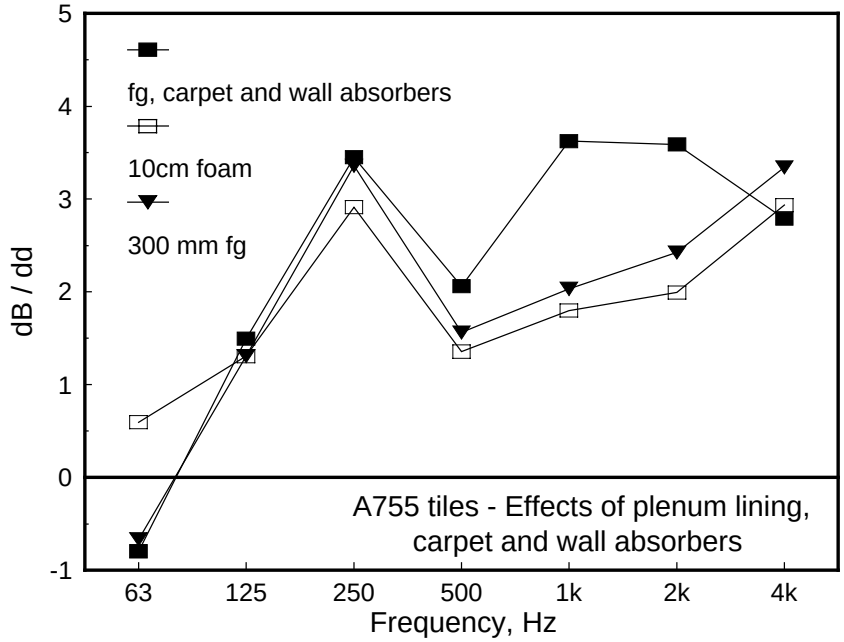

Figure 10-17: Sound attenuation with distance under A755 tiles for different room conditions. Key: foam – 100 mm foam lining plenum; fg – 300 mm glass fiber lining plenum; carpet – carpet installed on the floor; wall absorbers – sound absorbing panels installed on the room walls.

10.2 Acculab Fan source below the ceiling.

Sound levels for the Acculab reference sound source placed on the RAT room floor were measured each time the ceiling tiles were changed or a new VAV terminal was installed. This was done so sound power levels could be calculated using the comparison technique. During the analysis it became apparent that levels from this source also showed quite marked attenuation with distance from the source when absorptive ceiling tiles were installed. In this case the microphone positions were those for the two routine ladder positions described in Section 7.1. There never was any intention to collect drawaway curves as was done for the dodecahedral source. It is still possible, of course, to calculate the distance from the source to the microphone positions. Examples of the variation of sound pressure level with distance from the source are shown in Figure 10-18 to Figure 10-24. The mean values of attenuation with distance are shown in Figure 10-25

A visual comparison of Figure 10-25 with the results for the dodecahedral source in Figure 10-15 shows that the attenuations with distance are not identical. The peak at 250 Hz seen in the dodecahedral results is not there in the results for the Acculab RSS. Instead there is a peak at 1 kHz. This might be explained by the different positions of the sources; one rested on the floor, the other was about 1.5 m above it. This difference in position would lead to different interference effects, some of which can be seen in the results for the dodecahedral source. None were visible for the Acculab RSS, but the sampling array used for the latter source would make it very difficult to see such effects.

This variation of sound pressure level with distance has implications for measurements of sound pressure level and estimation of sound power level in the RAT room when the ceiling is absorptive. Since there is no clearly established reverberant field, the customary relationship between sound pressure level and sound power level is not strictly valid. While these are interesting results, they do not have any major impact on the main part of the research study.

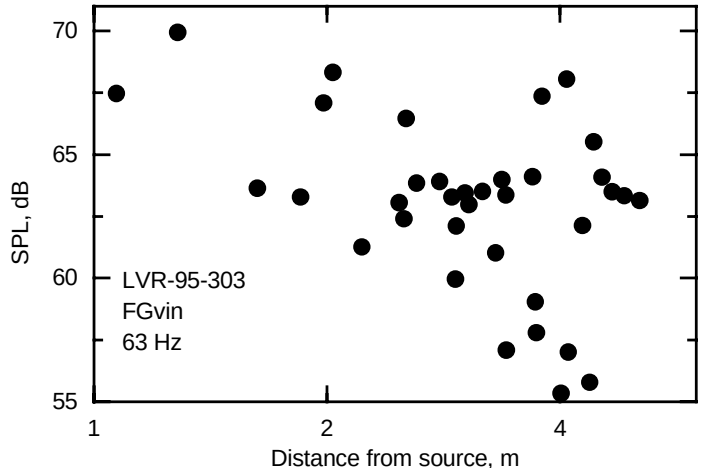

Figure 10-18: Example of measured sound pressure level vs. distance under FGvin tiles at 63 Hz for the Acculab RSS.

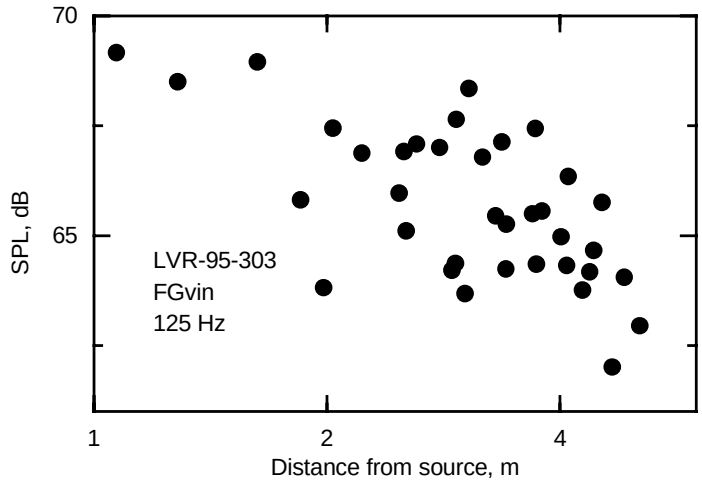

Figure 10-19: Example of measured sound pressure level vs. distance under FGvin tiles at 125 Hz for the Acculab RSS.

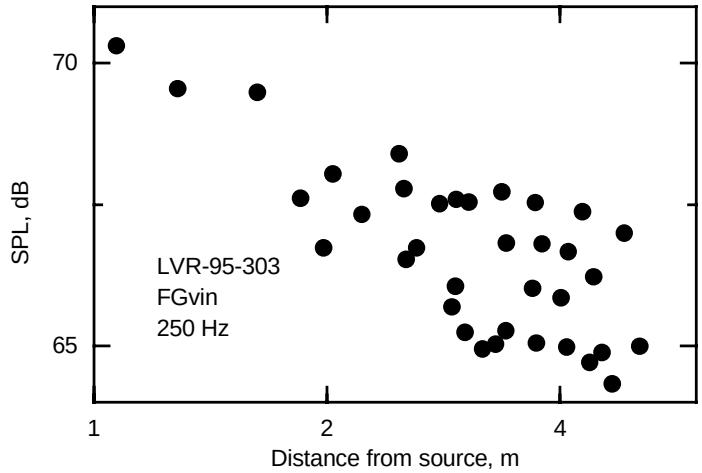

Figure 10-20: Example of measured sound pressure level vs. distance under FGvin tiles at 250 Hz for the Acculab RSS.

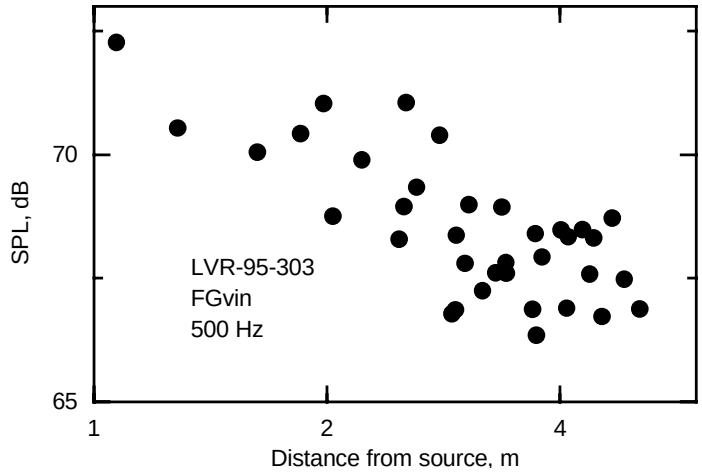

Figure 10-21: Example of measured sound pressure level vs. distance under FGvin tiles at 500 Hz for the Acculab RSS.

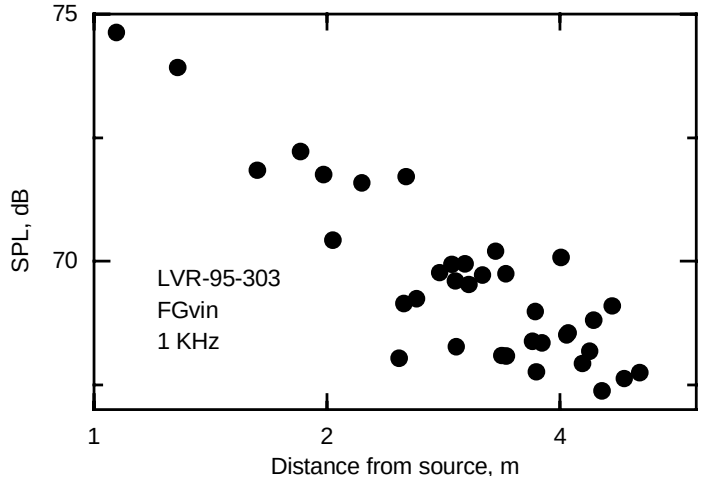

Figure 10-22: Example of measured sound pressure level vs. distance under FGvin tiles at 1000 Hz for the Acculab RSS.

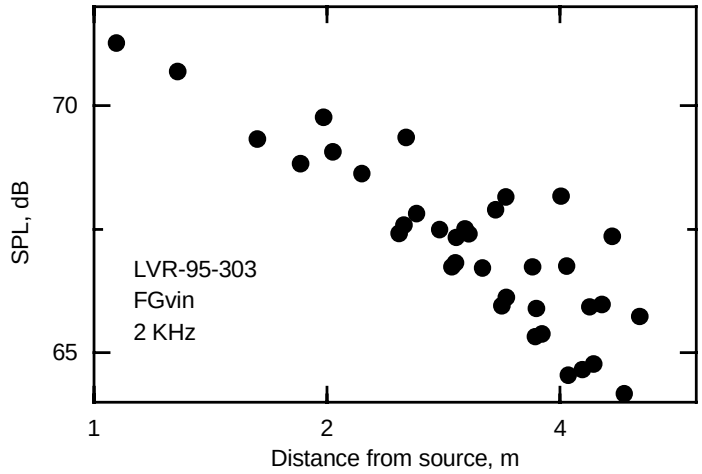

Figure 10-23: Example of measured sound pressure level vs. distance under FGvin tiles at 2000 Hz for the Acculab RSS.

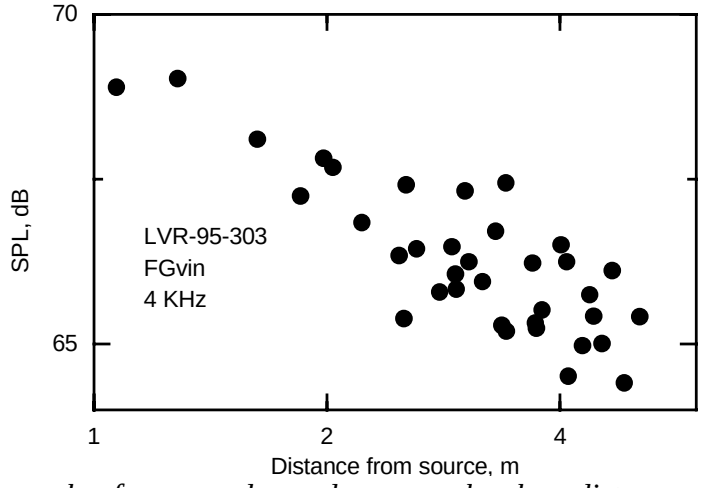

Figure 10-24: Example of measured sound pressure level vs. distance under FGvin tiles at 4000 Hz for the Acculab RSS.

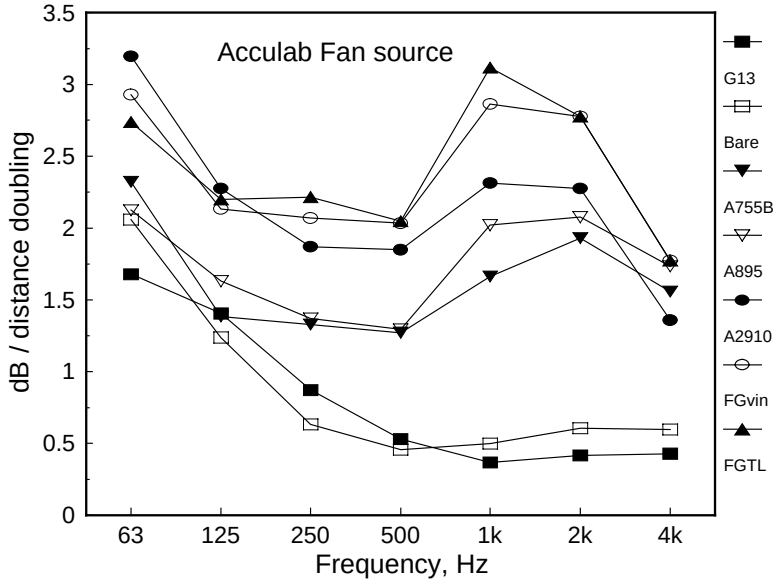

Figure 10-25: Mean values of attenuation with distance for Acculab reference sound source under different tiles.

10.3 Source above the ceiling.

When the source of sound was above the ceiling, the variation in sound pressure level in the room below was not as predicted by the Schultz formula. Instead, over most of the frequency range, the sound field in the room was rather uniform. As examples of this, some plots of sound pressure level as a function of distance from the VAVsim1 source are shown for two ceiling types, G13 and FGvin, in Figure 10-26 and Figure 10-27. As in the previous section, the two standard positions for the microphone ladder were used and distances from the source to the microphones were calculated in the same way.

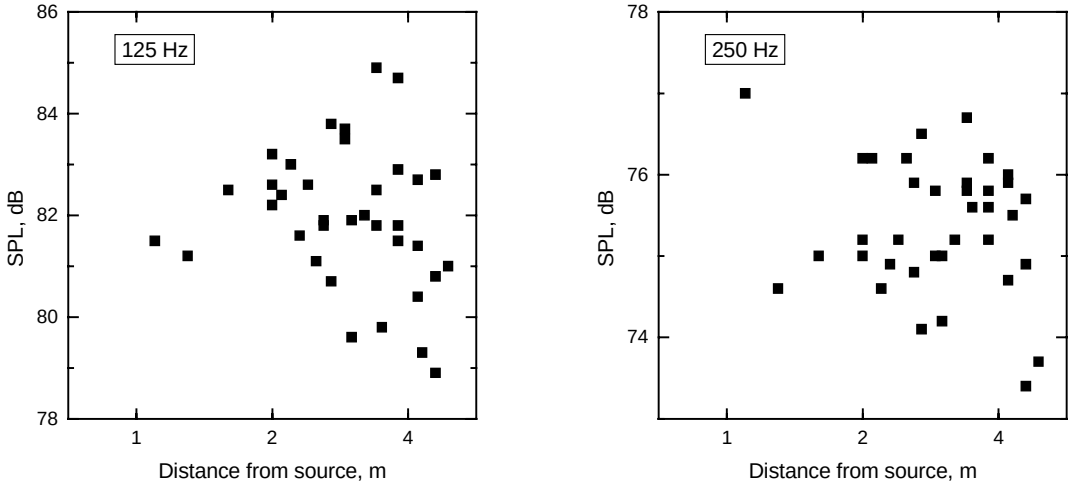

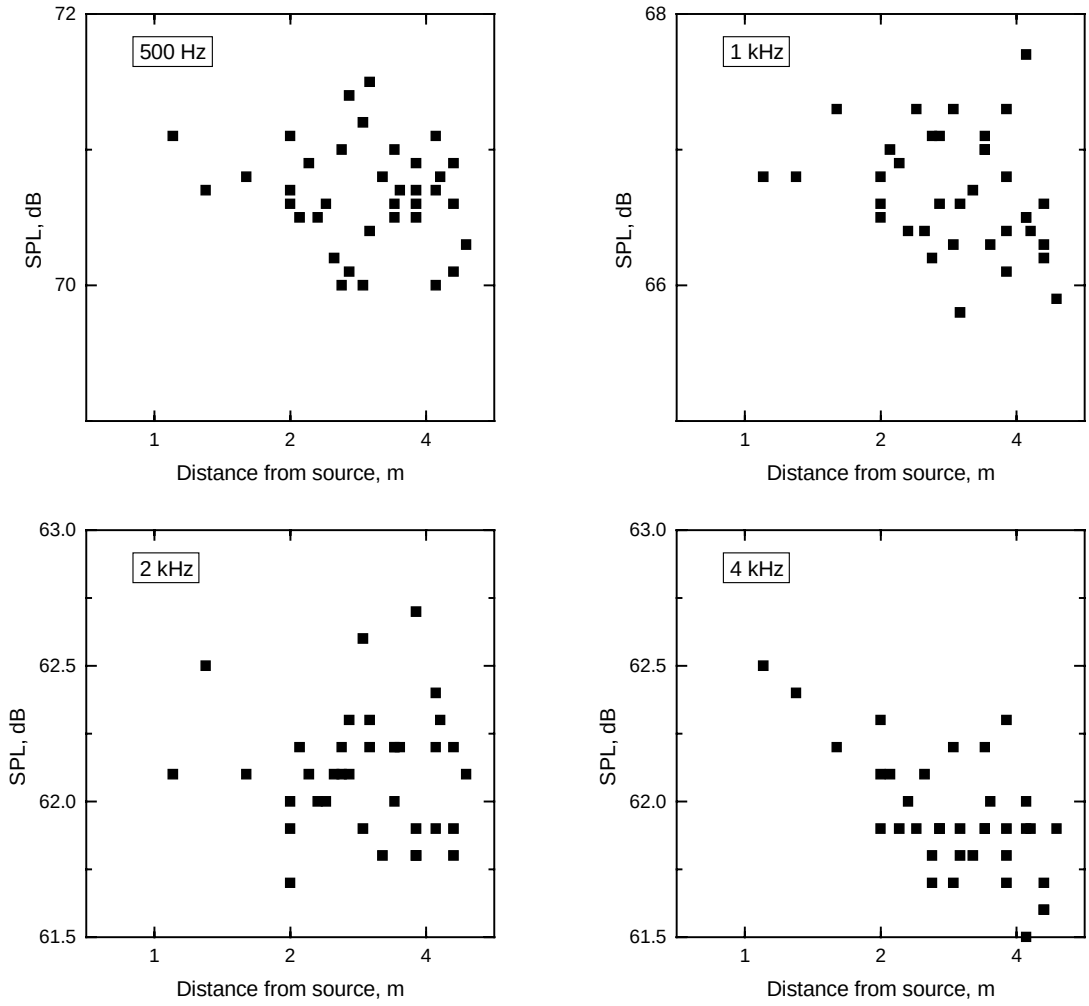

Figure 10-26: Sound pressure level as a function of distance from the VAVsim1 source in the plenum - G13 tiles.

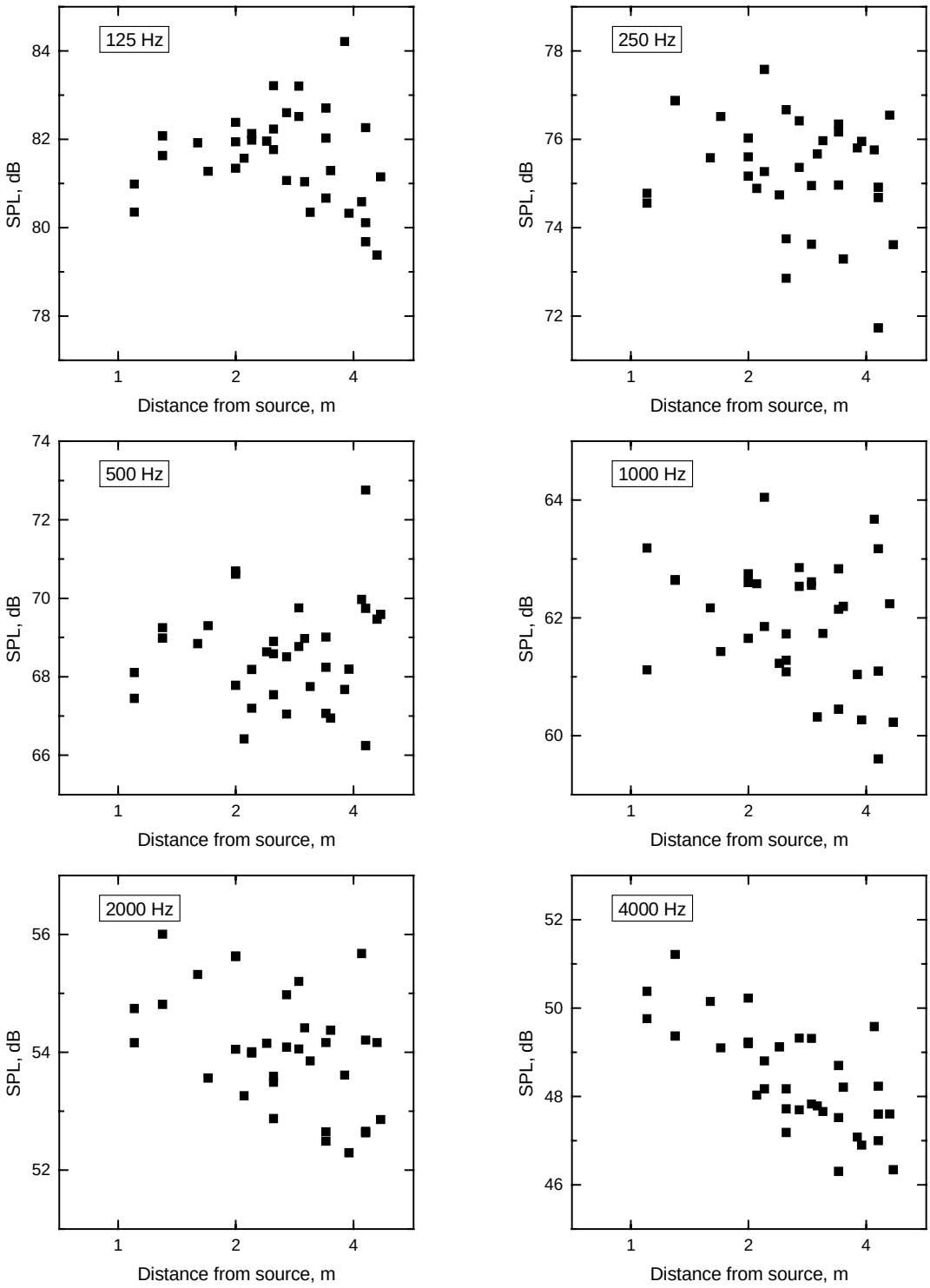

Figure 10-27: Sound pressure level as a function of distance from the VAVsim1 source in the plenum - FGvin tiles.

The mean values of attenuation with distance are shown for all ceilings and for two sources, VAVsim1 and VAVsim2 in Figure 10-28 and Figure 10-29. In the case of VAVsim1, placed centrally in the room, it is only for the FGvin tiles in the 4 kHz band that the attenuation approaches that of the Schultz expression and the values found when the source was below the ceiling. For VAVsim2, positioned near a corner, the attenuations with distance are somewhat larger, but in general not as high as expected from the Schultz formula.

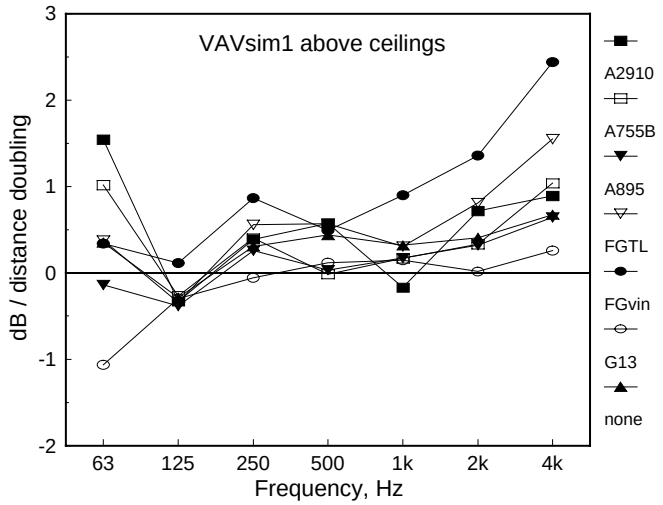

Figure 10-28: Mean attenuation with distance under different ceilings for the VAVsim1 source.

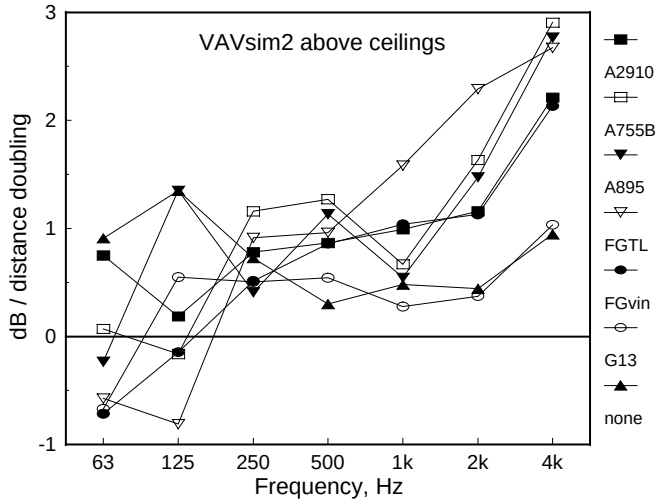

Figure 10-29: Mean attenuation with distance under different ceilings for the VAVsim2 source.

10.3.1 Effects of plenum lining, carpet and wall absorbers.

The addition of a carpet and absorbing wall panels to the room below had negligible effect on the decrease of sound pressure level with distance in the room when the source was above the ceiling. It is probable that a large number of scattering objects such as

desks, bookcases and filing cabinets would have a significant effect on the dB/dd values but this was not investigated. Results for one ceiling tile and the VAVsim1 source are shown in Figure 10-30. Also shown in the figure are the results obtained when the plenum was lined with 300 mm of glass fiber batts.

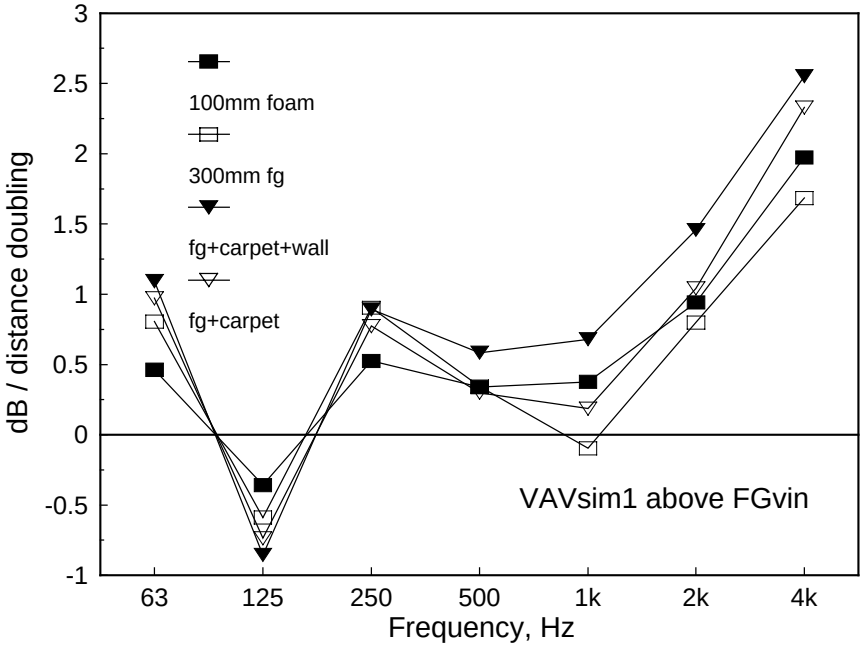

Figure 10-30: Changes in dB/dd in the room caused by changes to the plenum lining and by adding a carpet and absorbing panels on the walls.

10.4 Detailed sound pressure level plots.

In the early stages of the research project, to allow a detailed examination of the sound field, 576 microphone positions were used. This was quickly reduced to 144 and then to 46. Despite the use of an automated collection system, detailed examinations were very time-consuming. For routine measurements a more sparse array of 36 points was used. It was felt that this array would give all the information that was needed to satisfy the aims of the project. Only one set of data was collected with enough microphone positions to allow the creation of contour plots of the sound field in the room.

Figure 10-31 provides contour plots of the sound fields at four frequencies. The source was one of the early incarnations of the VAV simulator and was placed 50 mm above the FGTL ceiling at room coordinates (2.36, 2.85, 3.54). The microphone was placed 1.29 m above the floor. The plenum was not lined with any sound absorbing material and the large duct that was installed later in the project was not present.

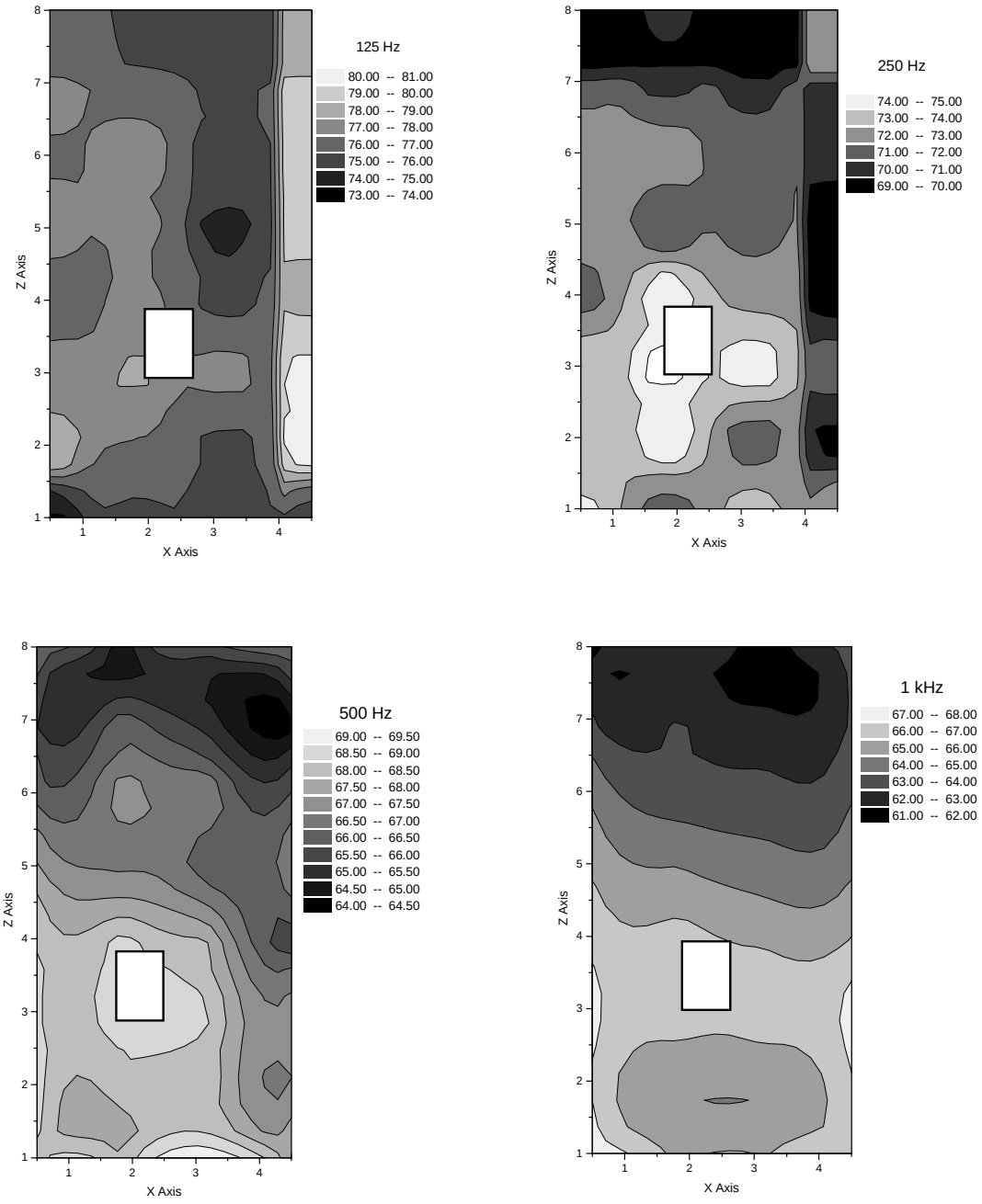

Figure 10-31: 3D contour plots of octave band sound pressure levels in the RAT room beneath ceiling tiles FGTL. Source is Box A in the plenum. The white rectangle shows the source position in the room.

10.5 Attenuation of sound with distance versus reverberation time.

Inspection of Figure 10-15 suggests that the attenuation with distance of sound from a source depends on the ceiling type, or more generally on the amount of sound absorption

in the room. To examine this further, plots of dB/dd versus the reciprocal of the room reverberation time are presented in Figure 10-32 to Figure 10-37.

Data are not presented for the 63 Hz octave band; there was no obvious trend. For 125 and 250 Hz, there is a clear linear dependence of one quantity on the other. At high frequencies, the room reverberation times are mostly about 0.5 s except for the G13 and empty room cases. All that can be said is that longer reverberation times lead to lower values of attenuation with distance from the source. The other point to notice is that it is only when the room reverberation time is around 0.5 seconds that the decay of sound pressure level approaches the value of 3 dB/dd as predicted by Schultz' empirical expression.

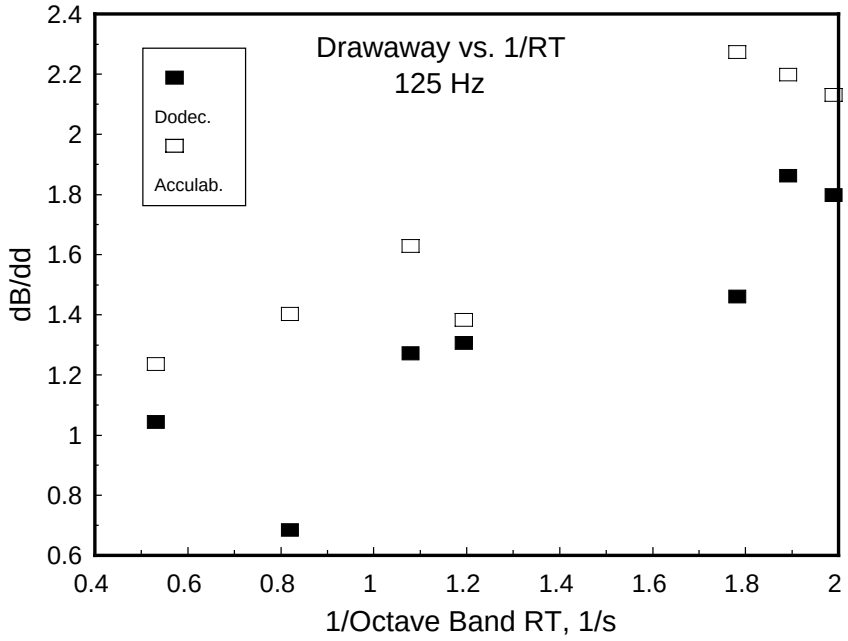

Figure 10-32: Octave band sound attenuation (dB/dd) versus the reciprocal of the room octave band reverberation time for 125 Hz for the dodecahedral and the Acculab RSS.

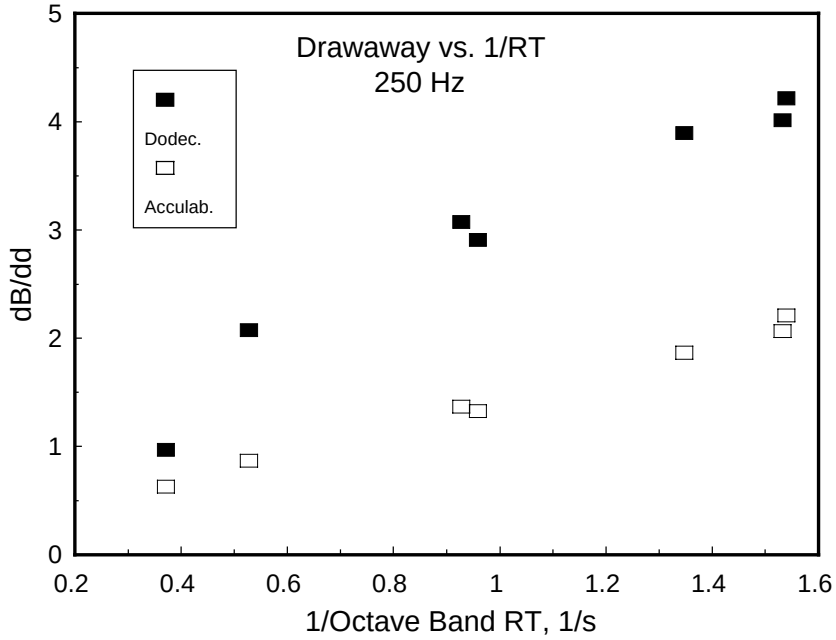

Figure 10-33: Octave band sound attenuation (dB/dd) versus the reciprocal of the room octave band reverberation time for 250 Hz for the dodecahedral and the Acculab RSS.

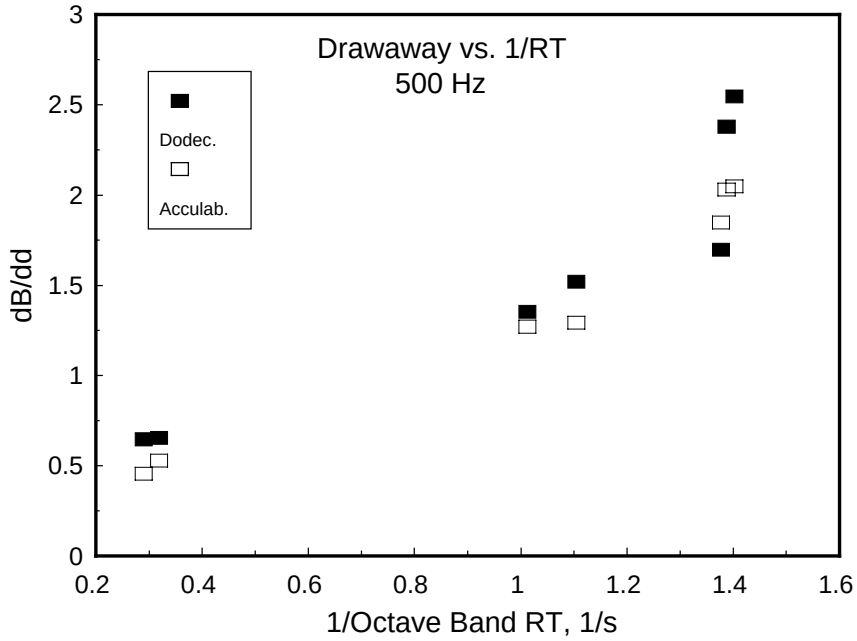

Figure 10-34: Octave band sound attenuation (dB/dd) versus the reciprocal of the room octave band reverberation time for 500 Hz for the dodecahedral and the Acculab RSS.

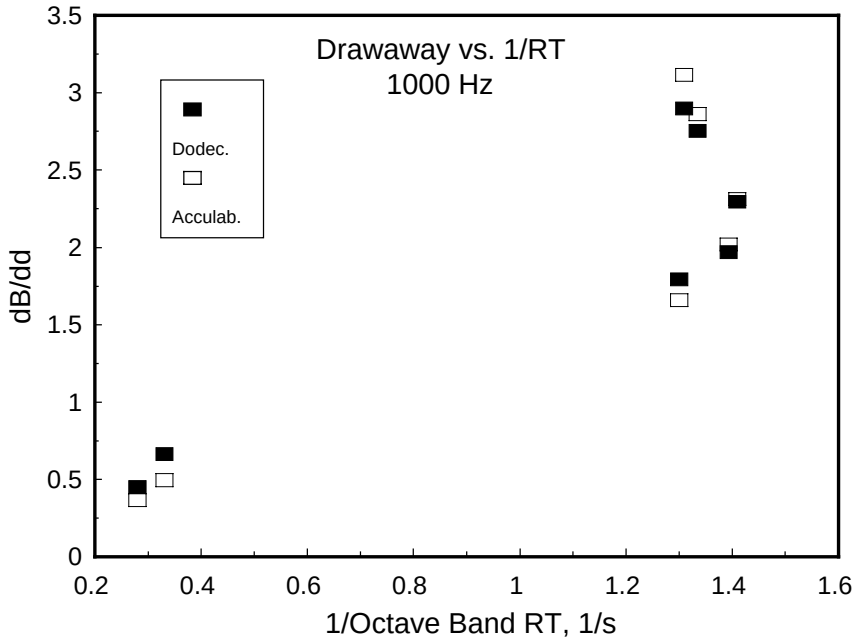

Figure 10-35: Octave band sound attenuation (dB/dd) versus the reciprocal of the room octave band reverberation time for 1000 Hz for the dodecahedral and the Acculab RSS.

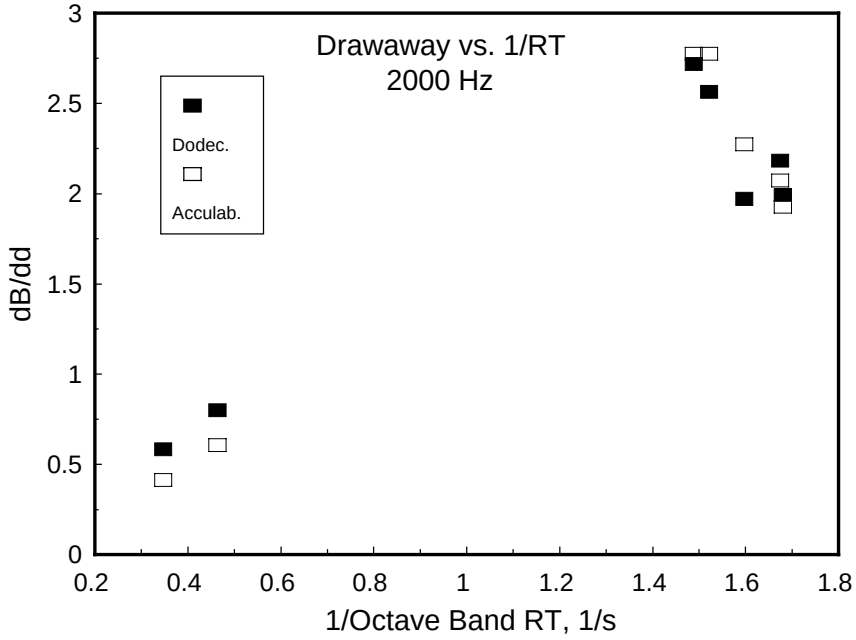

Figure 10-36: Octave band sound attenuation (dB/dd) versus the reciprocal of the room octave band reverberation time for 2000 Hz for the dodecahedral and the Acculab RSS.

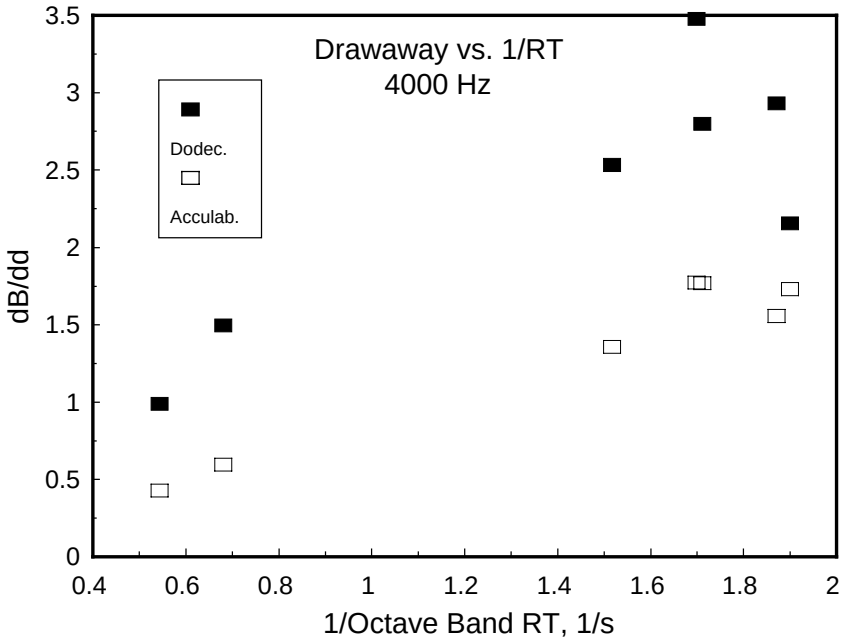

Figure 10-37: Octave band sound attenuation (dB/dd) versus the reciprocal of the room octave band reverberation time for 4000 Hz for the dodecahedral and the Acculab RSS.

10.6 Spatial attenuation versus C423 data.

The tile absorption coefficients calculated from measurements made in the RAT room and those found from C423 measurements (see Section 15), do not show very strong agreement and one might expect that C423 results would not be of much value in predicting the spatial attenuation. To test this hypothesis, the same values of spatial attenuation are plotted against the C423 sound absorption coefficients. To calculate octave band absorption, the three coefficients for the appropriate one-third octave bands were arithmetically averaged.

The graphs show that the C423 coefficients correlate fairly well with the spatial attenuation. In view of the correlation with room reverberation time, it is perhaps hardly surprising. The ceiling tiles are the only significant absorbing elements in the room except for the material in the plenum.

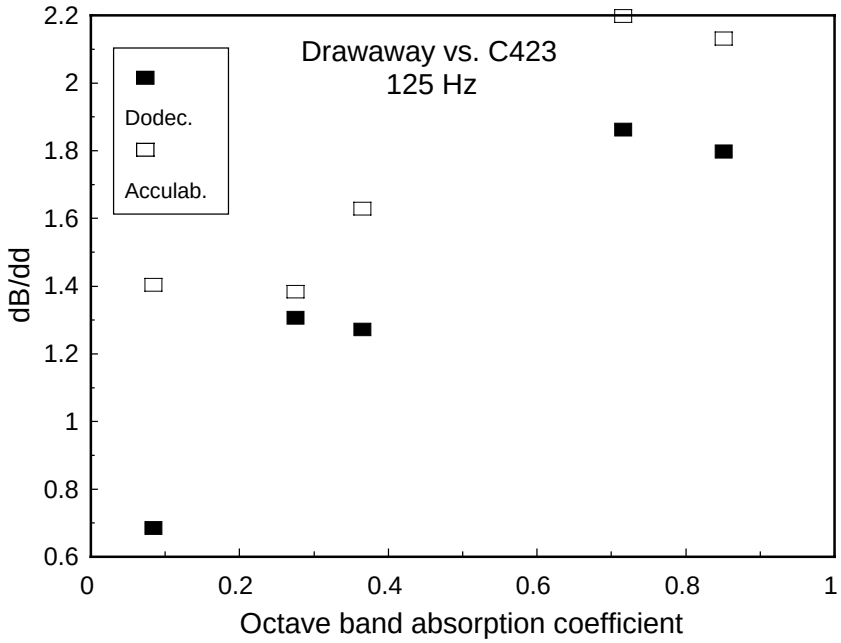

Figure 10-38: Octave band sound attenuation (dB/dd) versus octave band sound absorption coefficient for 125 Hz for the dodecahedral and the Acculab RSS.

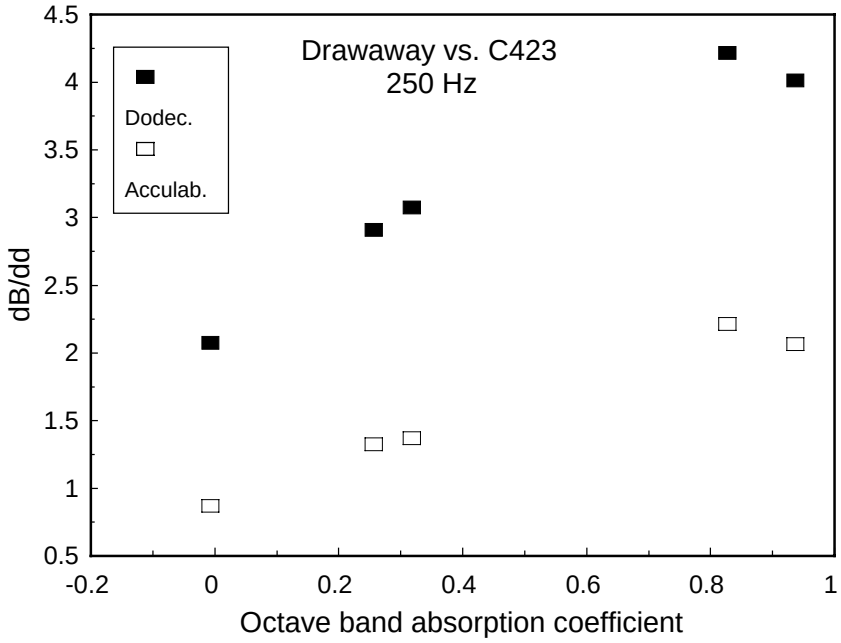

Figure 10-39: Octave band sound attenuation (dB/dd) versus octave band sound absorption coefficient for 250 Hz for the dodecahedral and the Acculab RSS.

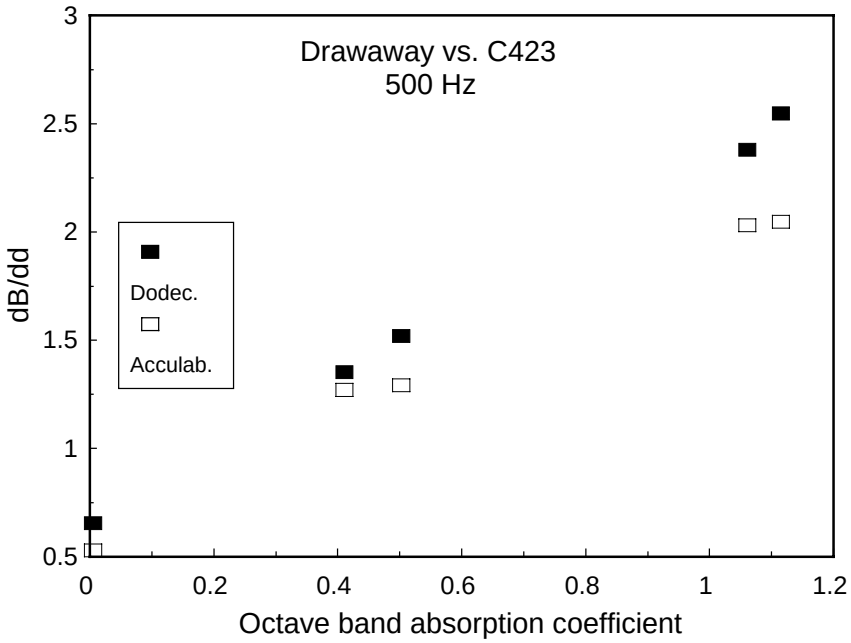

Figure 10-40: Octave band sound attenuation (dB/dd) versus octave band sound absorption coefficient for 500 Hz for the dodecahedral and the Acculab RSS.

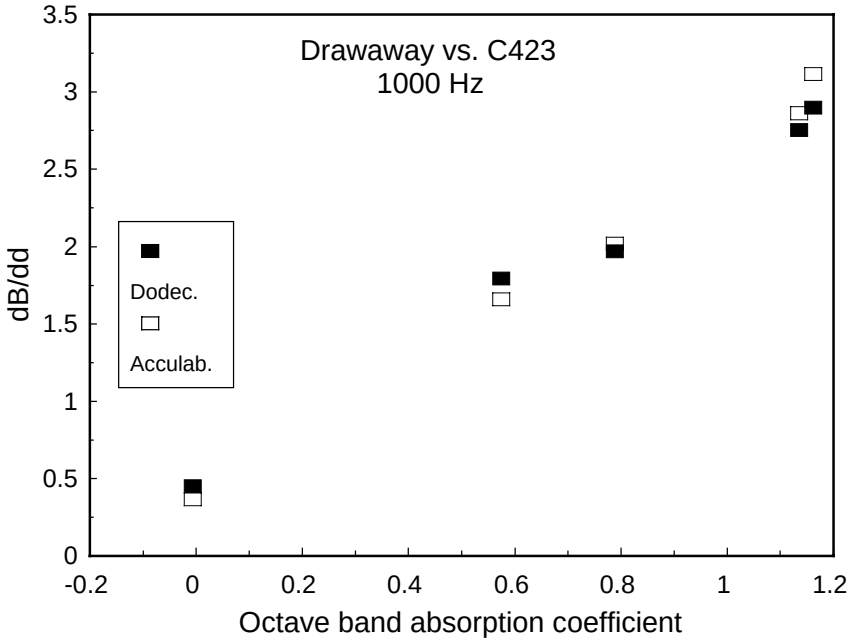

Figure 10-41: Octave band sound attenuation (dB/dd) versus octave band sound absorption coefficient for 1000 Hz for the dodecahedral and the Acculab RSS.

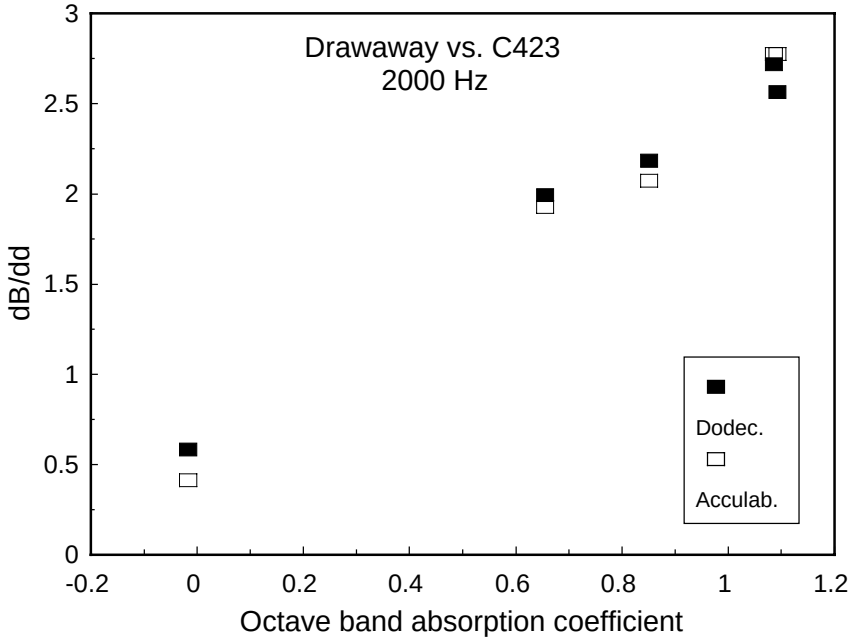

Figure 10-42: Octave band sound attenuation (dB/dd) versus octave band sound absorption coefficient for 2000 Hz for the dodecahedral and the Acculab RSS.

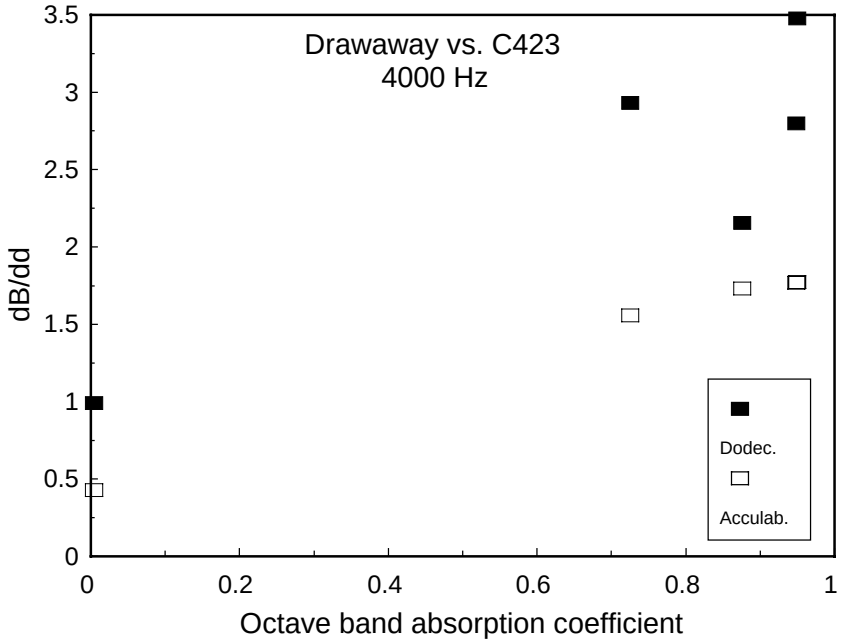

Figure 10-43: Octave band sound attenuation (dB/dd) versus octave band sound absorption coefficient for 4000 Hz for the dodecahedral and the Acculab RSS.

11. Attenuation through ceilings.

11.1 Measured attenuations.

The difference between the sound power level of the source, L_w, and the average sound pressure level, $<L_p>$ in the room is shown for each ceiling tile type in Figure 11-1 to Figure 11-6 . For convenience, the quantity L_w - $<L_p>$ will be referred to as the ceiling attenuation. The general impression gained from an examination of these plots is that there are differences due to the type of source being used but not much difference between ceiling types. These two tentative conclusions are examined more closely in Figure 11-7 and Figure 11-8.

Figure 11-7 shows for each ceiling the value of ceiling attenuation averaged over all the sources used. There are two ceiling types, A2910 and G13, that are clearly quite transparent to sound from sources in the plenum and different from the other four types. An early tentative conclusion in this project was that there was little difference between typical ceiling tiles and hence no need for a test procedure. The addition of the A2910 tile to the project showed that there could be quite significant differences between ceiling types. One can imagine other products that might fall between the A2910 tiles and the others and perhaps the need for a test procedure needs re-examination. On the other hand, from a practical point of view, one does not need a test report to know that the light, porous A2910 tiles are not likely to provide much attenuation of the sound from a VAV unit or anything else.

Figure 11-8 shows for each source the value of ceiling attenuation averaged over all the ceiling types used. This plot shows that there are differences between the sources at and below 250 Hz. The point for Terminal A at 125 Hz is low because of the low value of attenuation measured for this device with the G13 tiles, although this device in general gave lower attenuations than the others at low frequencies. The conclusion to be drawn from this graph is that the presence of the ceiling tiles and the plenum lining changes the emitted sound power of the source from that measured in the empty room. This makes it difficult to predict accurately the sound pressure level in the room below the ceiling using only sound power levels for the device measured in a reverberation room or a hemi-anechoic space.

Table 11-1: Average difference between device sound power and room-average sound pressure level for all combinations of source and ceiling tile. The plenum was lined with 100 mm foam the room below was fitted only with diffusers.

		63	125	250	500	1k	2k	4k			63	125	250	500	1k	2k	4k
A895	Duct	12.5	16.4	17.7	20.0	25.8	31.0	34.8	**FGTL**	Duct	13.3	17.5	17.5	23.4	27.0	32.7	38.6
	Terminal A	9.4	11.3	15.2	19.0	24.7	30.0			Terminal A	9.4	11.6	15.6	19.9	26.3	32.4	
	Terminal B	11.9	15.0	16.7	19.0	24.3	28.3			Terminal B	12.8	17.1	17.5	21.2	26.4	30.8	
	Terminal Cb	17.1	18.4	23.4	21.3	26.2	30.8			Terminal Cb	17.1	19.3	22.7	23.5	26.7	31.3	
	Terminal Ci	14.3	15.6	19.3	20.7	25.5	31.4			Terminal Ci	15.2	17.2	19.7	23.0	26.2	32.0	
	Terminal D	18.6	20.4	19.8	20.6	28.8	32.4			Terminal D	18.8	21.8	19.9	21.5	28.8	32.8	
	VAVsim1	11.5	15.3	16.7	19.4	24.1	32.1	36.7		VAVsim1	11.9	16.2	15.7	21.4	25.1	32.0	38.7
	VAVsim2	10.9	15.6	16.4	20.0	25.9	31.9	35.2		VAVsim2	11.7	15.8	16.2	22.5	25.8	31.8	38.7
	Mean	13.3	16.0	18.1	20.0	25.7	31.0	35.6		Mean	13.8	17.1	18.1	22.1	26.5	32.0	38.7
	SD	3.2	2.6	2.6	0.8	1.5	1.3			SD	3.1	2.9	2.5	1.3	1.1	0.7	
A755B	Duct	11.6	15.2	16.8	18.9	24.6	29.9	32.9	**G13**	Duct	12.5	16.5	17.2	17.5	20.4	21.4	20.1
	Terminal A	8.5	10.5	13.3	17.0	24.3	29.8			Terminal A	11.9	8.4	14.9	19.1	20.9	23.4	25.8
	Terminal B	11.3	14.1	15.4	17.9	23.9	27.8			Terminal B	11.7	14.9	16.1	16.8	19.4	20.3	19.0
	Terminal Cb	16.7	17.6	21.7	20.3	25.2	30.1			Terminal Cb	17.2	18.5	23.8	19.3	21.3	22.1	22.9
	Terminal Ci	15.2	16.1	18.5	19.7	24.5	30.7			Terminal Ci	15.6	16.7	19.5	18.4	20.3	22.4	23.4
	Terminal D	18.0	19.2	18.3	19.2	27.7	31.4			Terminal D	18.3	20.1	19.5	18.7	23.2	23.4	18.8
	VAVsim1	9.9	14.2	14.6	18.1	23.1	30.7	33.9		VAVsim1	11.1	15.5	15.6	17.3	19.1	21.7	21.1
	VAVsim2	10.5	15.1	15.4	18.7	24.5	30.5	33.3		VAVsim2	10.4	15.9	14.9	15.9	18.8	21.1	19.7
	Mean	12.7	15.3	16.7	18.7	24.7	30.1	33.4		Mean	13.6	15.8	17.7	17.9	20.4	22.0	21.3
	SD	3.4	2.6	2.7	1.1	1.4	1.0			SD	3.0	3.4	3.1	1.2	1.4	1.1	2.5
FGvin	Duct	13.4	16.7	17.6	21.9	25.9	28.9	34.4	**A2910**	Duct	11.9	14.9	16.2	18.5	18.1	16.9	18.4
	Terminal A	10.4	10.6	15.6	19.4	24.0	29.4										
	Terminal B	12.9	16.1	17.1	19.5	23.7	27.1										
	Terminal Cb	18.3	19.5	22.4	22.2	25.7	29.2			Terminal Cb	16.4	21.0	15.8	18.9	17.9	18.8	24.3
	Terminal Ci	16.0	17.2	19.6	21.4	24.6	29.5			Terminal Ci	15.1	15.8	16.4	16.5	16.2	18.4	21.0
	Terminal D	19.3	21.4	20.1	20.9	27.3	30.4			Terminal D	17.9	18.7	16.2	16.1	18.1	17.9	15.1
	VAVsim1	12.1	15.7	15.8	20.0	24.3	30.1	35.0		VAVsim1	8.7	13.8	13.8	16.5	16.0	17.6	18.8
	VAVsim2	12.4	16.7	16.0	20.7	25.1	30.3	35.9		VAVsim2	10.8	14.1	14.1	17.3	16.9	18.3	19.0
	Mean	14.3	16.8	18.0	20.8	25.1	29.4	35.1		Mean	13.5	16.4	15.4	17.3	17.2	18.0	19.4
	SD	3.2	3.1	2.4	1.1	1.2	1.0			SD	3.5	2.9	1.1	1.2	0.9	0.7	3.0

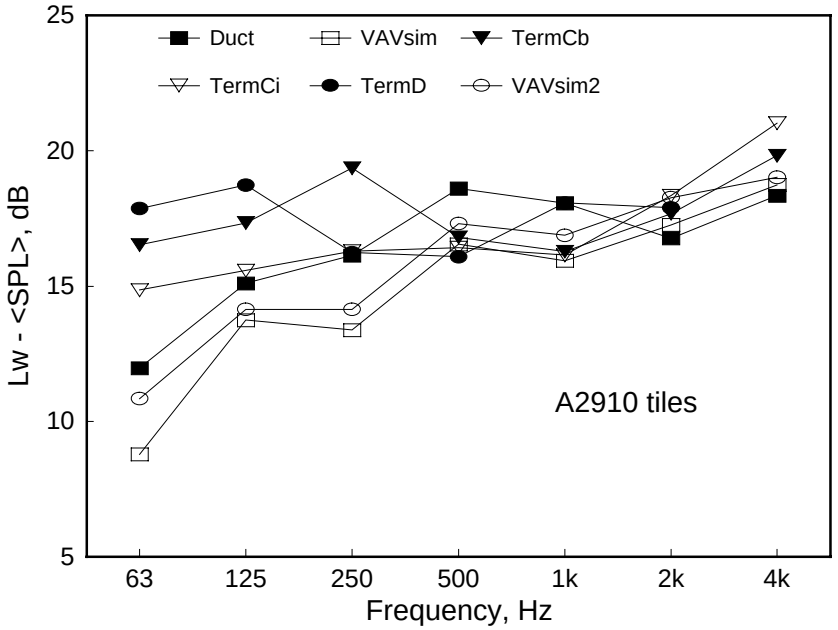

Figure 11-1: Difference between device sound power level and average sound pressure level in the room for each source for A2910 tiles.

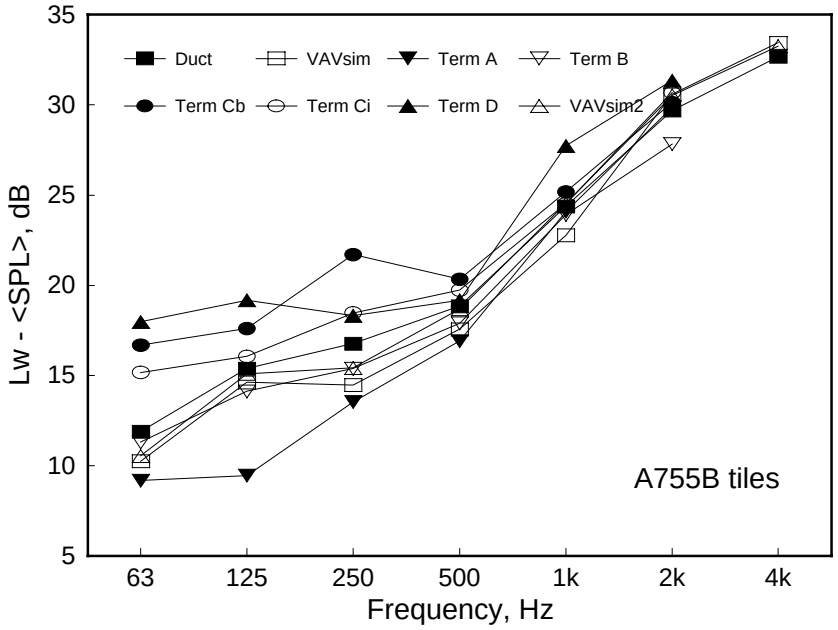

Figure 11-2: Difference between device sound power level and average sound pressure level in the room for each source for A755B tiles.

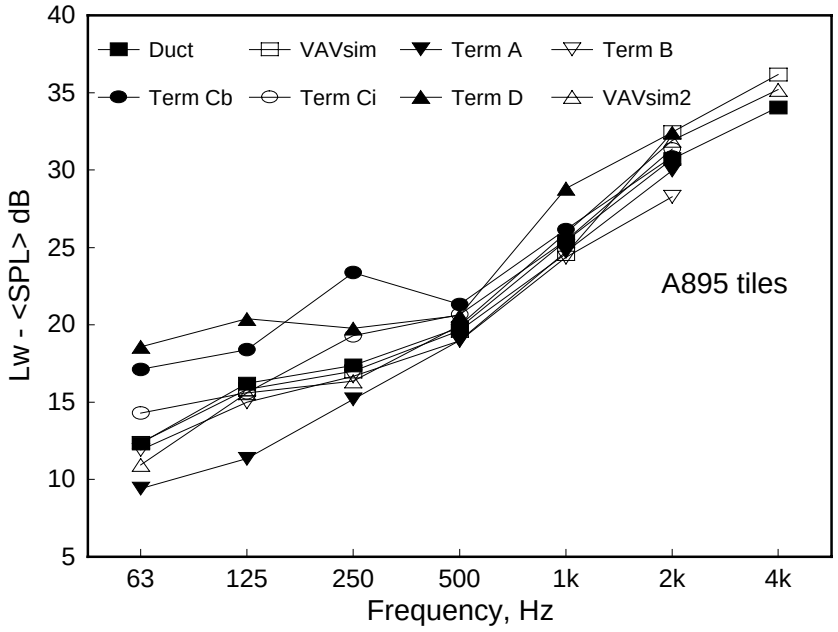

Figure 11-3: Difference between device sound power level and average sound pressure level in the room for each source for A895 tiles.

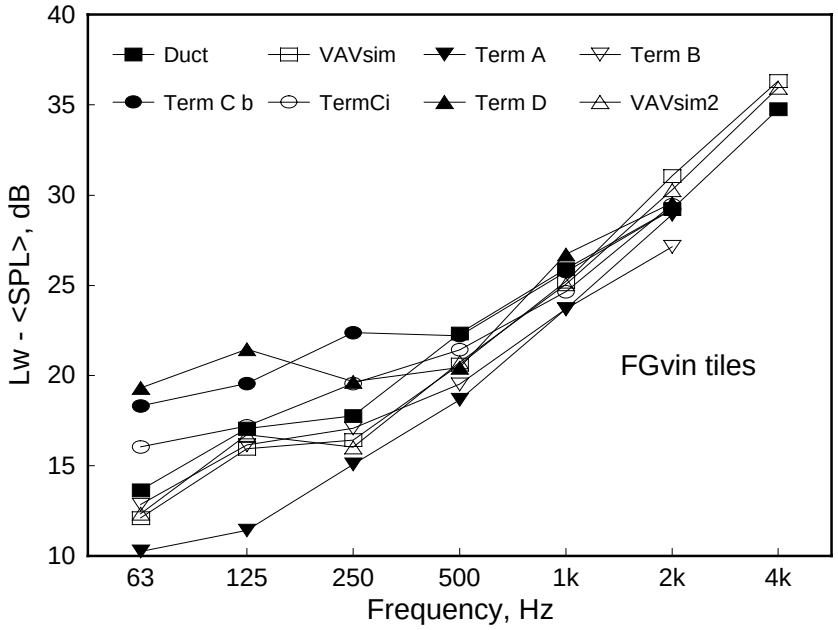

Figure 11-4: Difference between device sound power level and average sound pressure level in the room for each source for FGvin tiles.

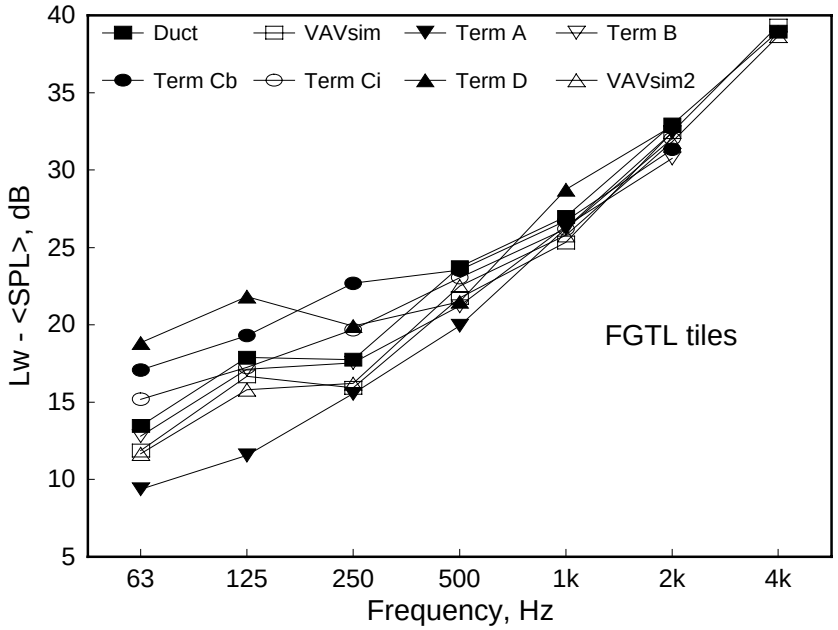

Figure 11-5: Difference between device sound power level and average sound pressure level in the room for each source for FGTL tiles.

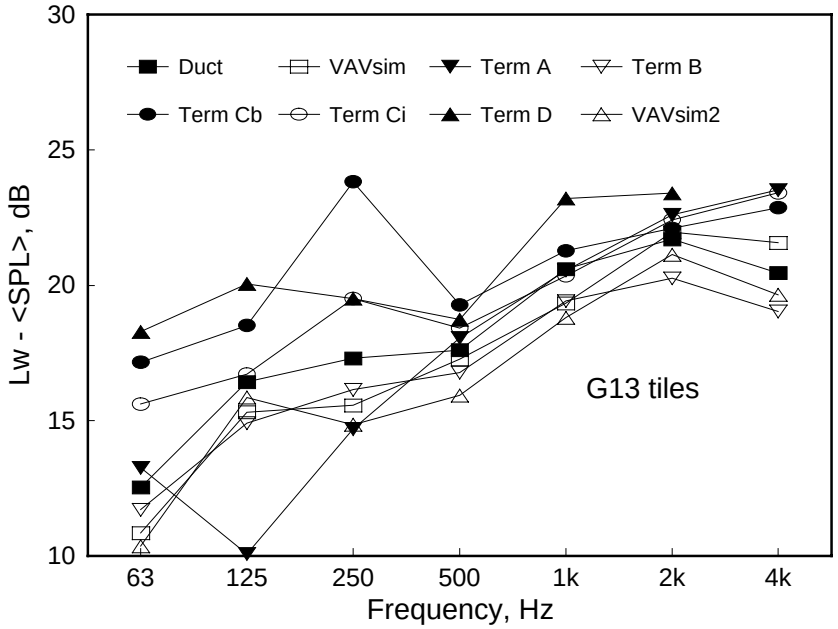

Figure 11-6: Difference between device sound power level and average sound pressure level in the room for each source for G13 tiles.

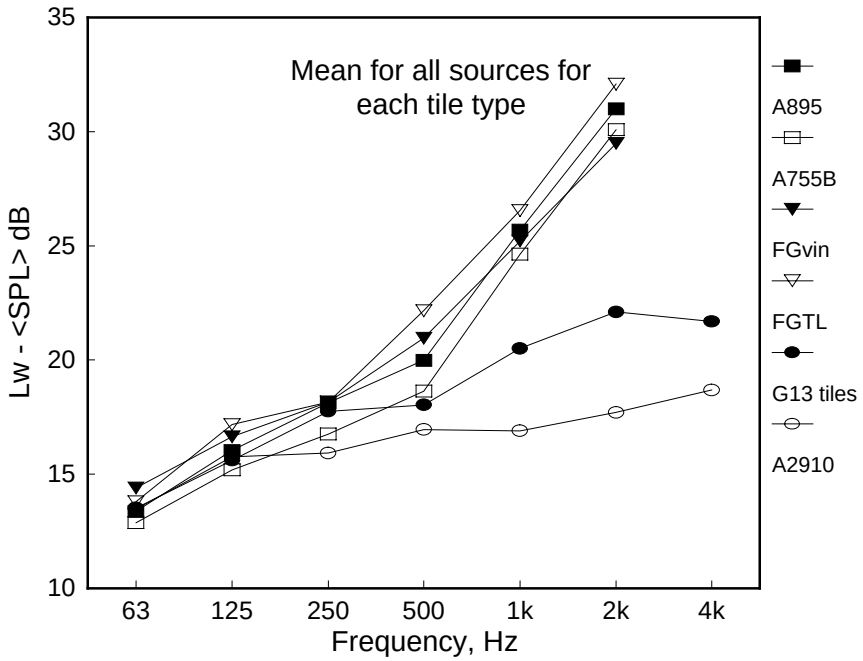

Figure 11-7: Difference between device sound power level and average sound pressure level in the room averaged over all sources for each type of tile.

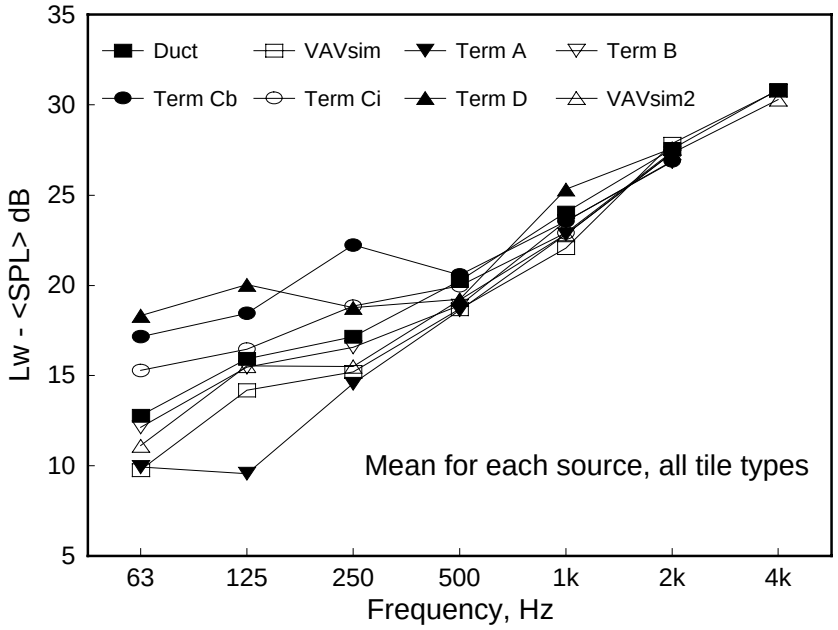

Figure 11-8: Difference between device sound power level and average sound pressure level in the room averaged over all tile types for each source.

11.2 Influence of source area on ceiling attenuation.

In the previous section the measured ceiling attenuations were presented and the point was made that for a given ceiling, the attenuation depended on the source in use, especially at low frequencies. This result means that the uncertainty of predicted sound levels would be too high if only the sound power measured according to ARI 880 [4]

were used together with some insertion loss values for the ceiling. It was thought that the area of the source close to the ceiling might be a factor that could account for some of the variation. This postulate was investigated.

The dimensions and area of the lower face of each terminal unit or simulator are given in Table 11-2. For each tile type and each frequency, plots showing ceiling insertion loss as a function of source area were prepared. (The results for the large duct simulator were excluded from this analysis after a preliminary inspection showed that they just did not fit with the rest of the data.) The set for the A895 tiles is shown in Figure 11-9. From this set alone it is clear that there is a correlation between insertion loss and source area in the lowest three bands and perhaps even some correlation at higher frequencies. The 4 kHz result is not shown; there is no obvious correlation just as in the result for 2 kHz.

Table 11-2: Dimensions and areas of face of terminal units and simulators closest to the ceiling tiles.

Source	width, in	length, in	Area, m^2
Terminal A	15	15.5	0.15
Terminal B	32	58.5	1.21
Terminal C	49	34	1.07
Terminal D	47.6	72	2.21
VAVsim1 and VAVsim2	24	36	0.56

The surprising aspect of this result is that as the area of the source increases, so does the ceiling attenuation. This can be understood qualitatively by postulating two paths through the ceiling tiles. One path for the sound radiated from the upper face and sides of the terminal unit and the second for the sound from the lower face close to the ceiling tiles. The first path comprises the effect of absorption in the plenum and attenuation of the sound energy in the plenum as it passes through the ceiling tiles. While the plenum conditions are far from reverberant, it is reasonable to assume that the associated transmission coefficient is a constant determined by the properties of the plenum and the ceiling tile. Thus the power transmitted along this path will be proportional to

$$\left(A_{tot} - A_{face}\right) v_m^2 \tau_c$$

where

A_{tot} is the total area of the unit
A_{face} is the area of the face nearest the ceiling
v_m is the mean square velocity of the terminal surface
τ_c is the transmission coefficient for this path.

For the second path we postulate that, because of its interaction with the ceiling, the mean square velocity of the lower terminal face decreases as its area increases. The power transmitted along this second path will be proportional to

$$v^2_{face} \alpha_{face} A_{face} \tau_{face}$$

The combination of these two paths gives an effective insertion loss that increases as the area of the terminal unit increases, in general agreement with observations. However, using different simple functions for v^2_{face} does not give an insertion loss that increases linearly with A_{face} as observed. There are too many unknowns in this simplistic model to make it worthwhile to try to produce a better fit with measurement.

The results for each of the other tiles showed similar patterns to those for the A895 tiles. The slope of the regression line for each tile is shown in Figure 11-10. At all frequencies the agreement is quite close. This suggests that it is reasonable to pool all the data and extract a mean slope. This was done by calculating attenuations at each frequency relative to the mean value for each ceiling type. These relative attenuations were then pooled. Figure 11-11 and Figure 11-12 show two examples of the relative attenuation data. Figure 11-13 shows the mean slope for all ceiling types extracted from such data while Figure 11-14 shows the square of the correlation coefficient between the relative attenuations and area. The area effect is only significant in the lowest three octave bands. The values of the slopes and the area where the regression line crosses the relative insertion loss axis for each of these three frequencies are given in Table 11-3.

Table 11-3: Regression of relative insertion loss versus area of lower face of terminal.

Frequency, Hz	63	125	250
Slope, dB/m^2	4.4	4.1	2.5
Area for relative IL = 0	0.82	0.85	0.83

Since the regression lines cross the IL = 0 line at almost the same value, this may be taken as equal to 0.83. With this information, the prediction of the average sound pressure level in the room can be improved using the equation

$$SPL(f) = Power(f) - Attenuation(f) + Slope(f) \times (Area - 0.83).$$

where

SPL(f) is the average sound pressure level in the room, dB,

Power(f) is the power emitted by the terminal unit when tested according to standards, dB

Attenuation(f) is the nominal attenuation of the ceiling tiles, dB,

Slope(f) is the slope of the regression of attenuation on area, dB/m^2 ,

Area is the area of the lower face of the terminal unit, m^2.

The improvement in correlation between the predicted levels and the measured levels when the area term is included is shown in Figure 11-15. Scatter plots showing the improvements are given in Figure 11-16.

The standard error of the estimate in each band using this model is given in Table 11-4.

Table 11-4: Standard error of predicted average room sound pressure level.

Frequency, Hz	63	125	250	500	1k	2k	4k
SE, dB	1.7	1.9	2.2	1.3	1.3	1.2	2.4

The correlation between the area of the lower surface of the source and the insertion loss, discussed in this section can be used to account for the differences within this data set, but this does not provide a physical explanation of what is going on. A theoretical model linking the size and radiation characteristics of sources to the pattern of the sound fields in the plenum and thus to the sound fields in the room below, would require a great deal of work. The value of such an effort is doubtful since there are no immediately obvious practical applications of the information; radiation characteristics are not normally measured and predicting what would happen in a typical plenum would be an extremely complex task. Thus it seems that this empirical model, or perhaps an improved one based on new data, will be the most economical approach to this problem.

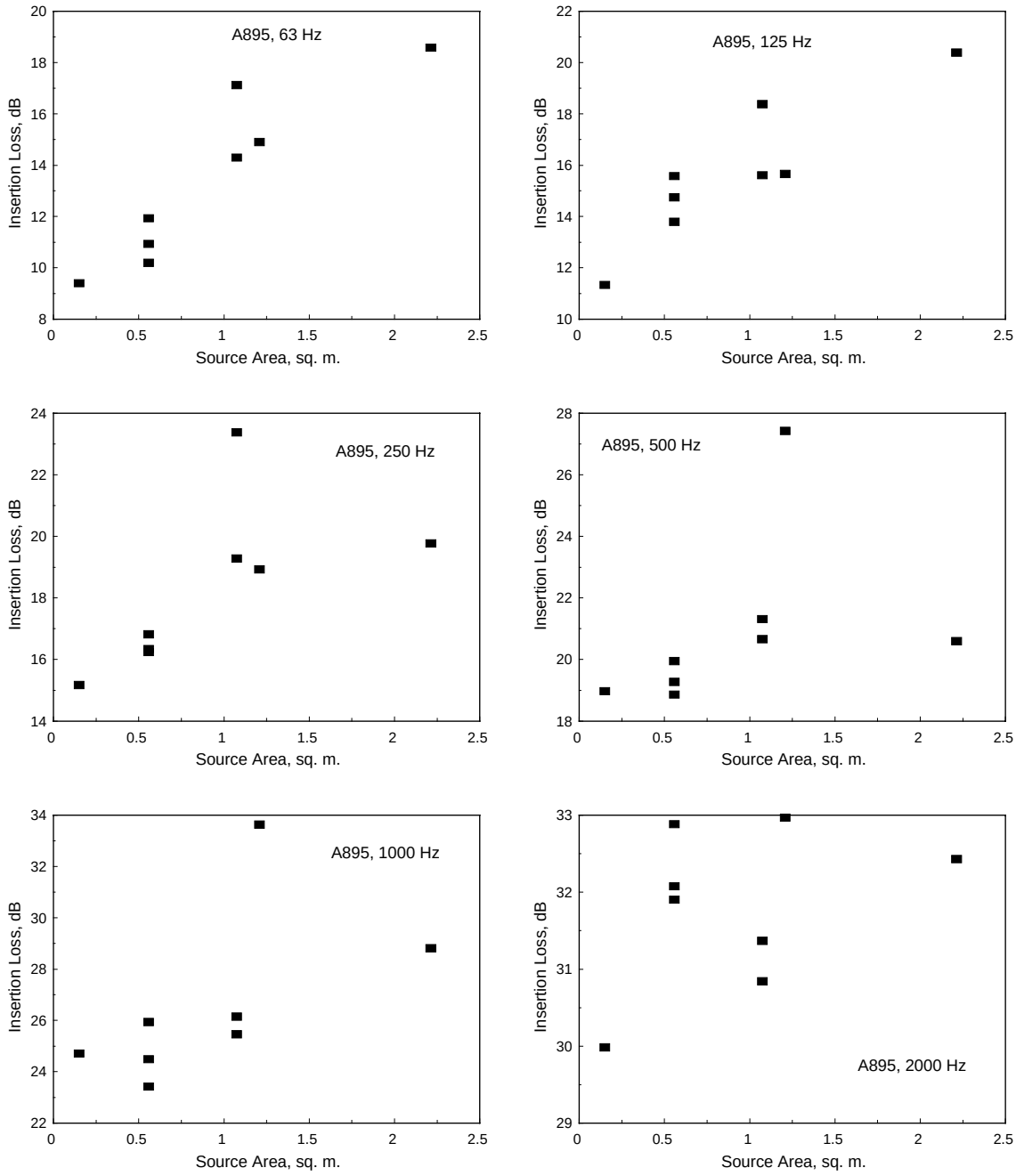

Figure 11-9: Ceiling attenuation vs. source area for A895 tiles.

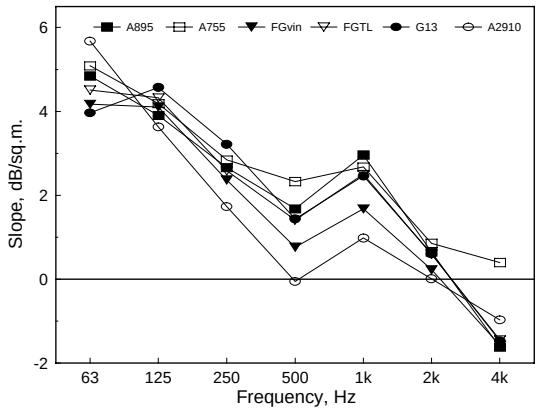

Figure 11-10: Slope of regression lines for ceiling attenuation vs. source area for each tile type

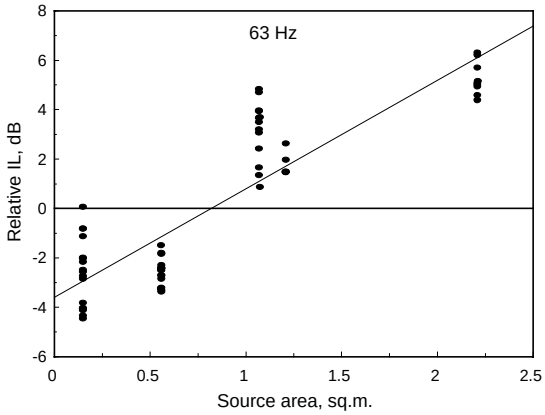

Figure 11-11: Relative insertion loss for all ceiling tile types at 63 Hz versus area of lower face of source.

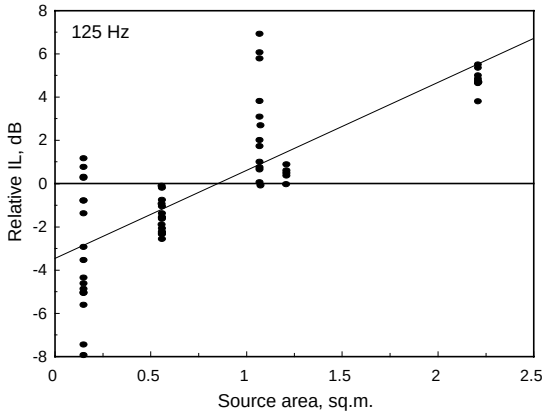

Figure 11-12: Relative insertion loss at 125 Hz vs. area of lower face of source.

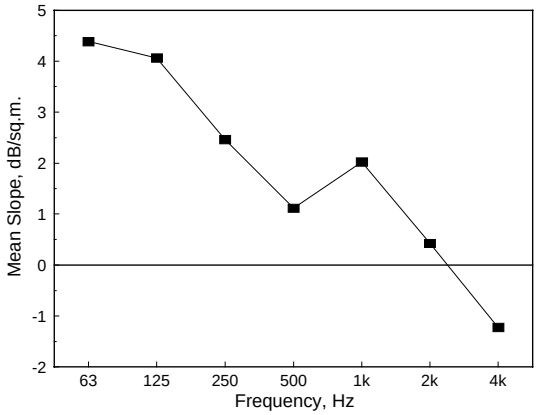

Figure 11-13: Mean slope for regression of relative ceiling attenuation vs. source area.

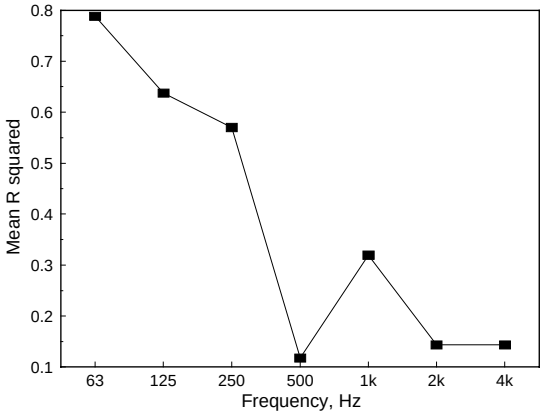

Figure 11-14: Mean of squared correlation coefficient for regression of ceiling attenuation vs. source area.

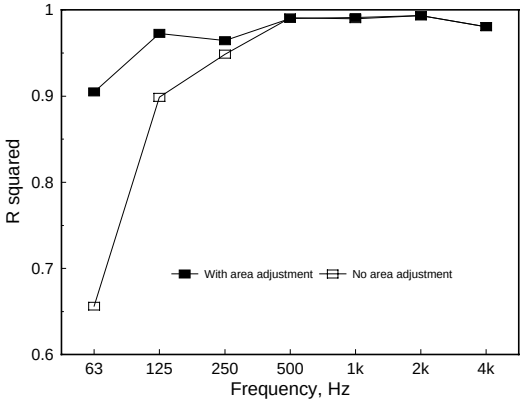

Figure 11-15: Correlation between measured and predicted mean levels in the room with and without area term.

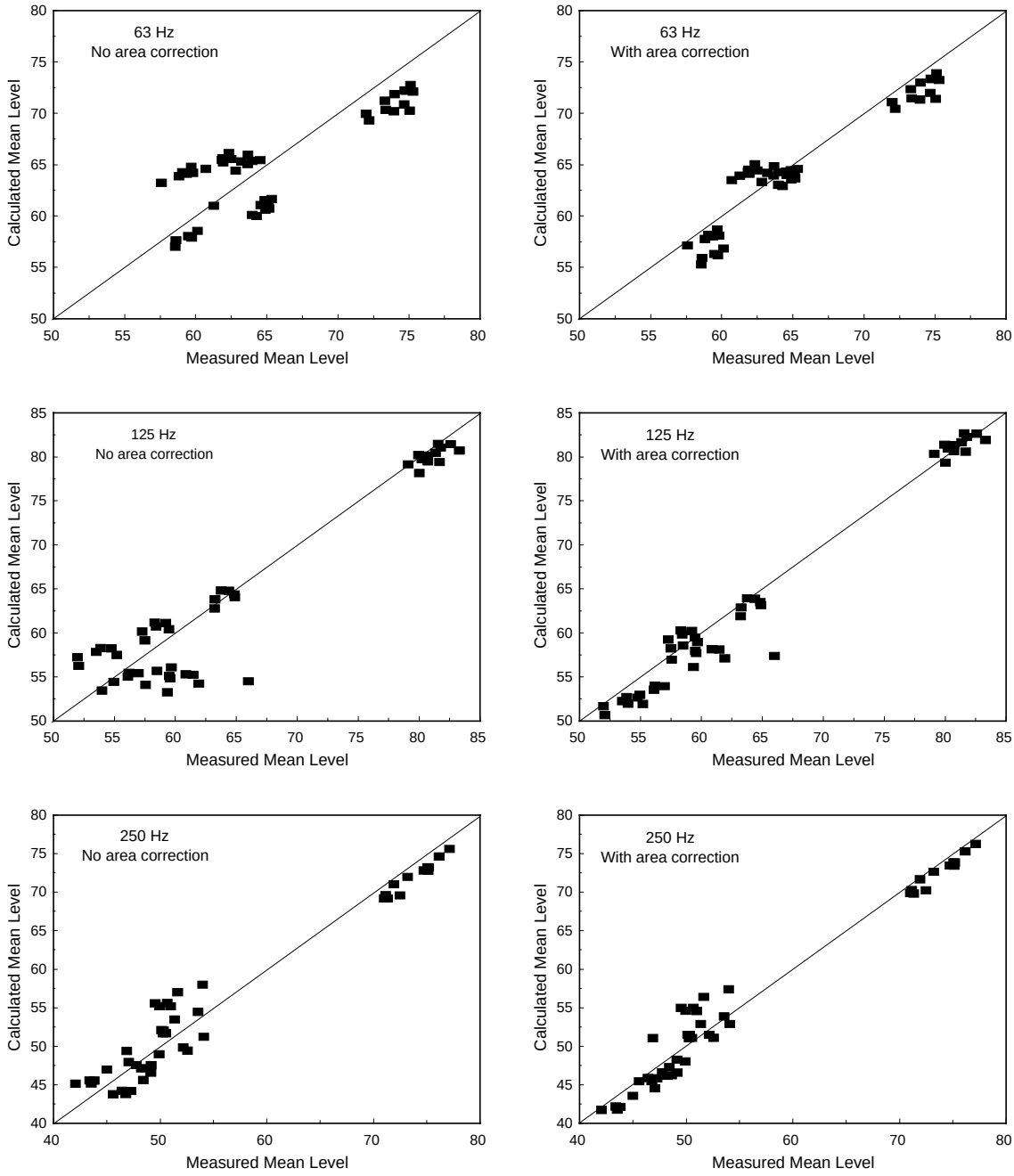

Figure 11-16: Effect of including area term in predictions of average room sound pressure level.

The reasons for the failure of the large duct simulator data to fit into this prediction scheme were not investigated. The duct was terminated at the end remote from the sources by a thick plug of glass fiber. This may have resulted in a strong gradient in sound pressure level from one end of the duct to the other so the radiation was not uniform. Without further measurement, one can only speculate.

11.3 Effect of plenum absorption.

For the A895 ceiling specimen the effect of adding sound absorbing material on the surfaces of the plenum was investigated by adding 100 mm thick foam lining to each plenum surface in turn. As well, for several measurements, the plenum was lined on all four vertical faces with 300 mm of glass fiber instead of the 100 mm of foam that was used in most of the measurements. Figure 11-17 shows for each case the measured levels in the room below with Box A[†] operating in the plenum 50 mm from the upper face of the tiles. There is a relatively steady decrease in level as each face of the plenum is covered. For the step from 3 surfaces to 4 however, the change is much smaller. The data can be compared with that in Figure 4-9. The trend with frequency is quite different.

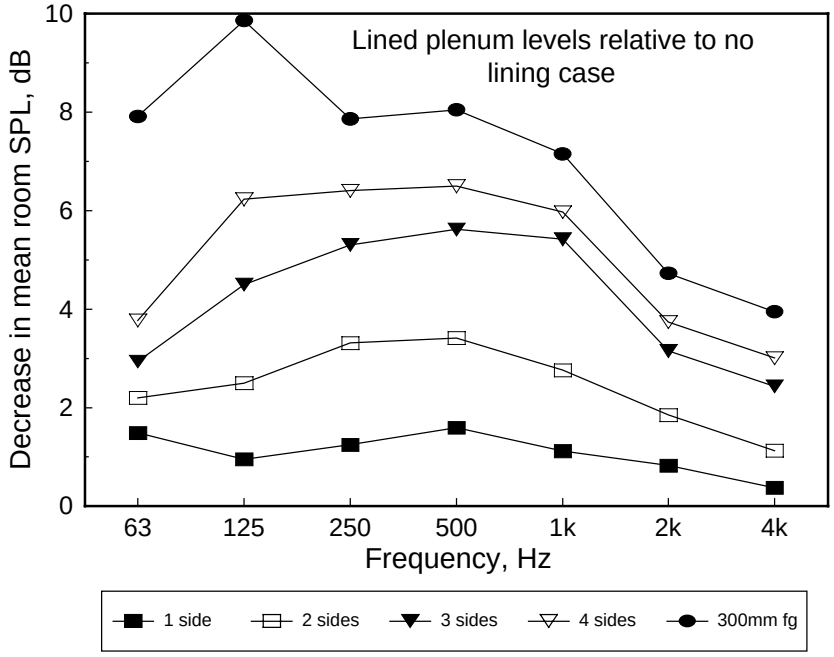

Figure 11-17: Difference in mean room sound pressure levels in RAT room below ceiling of A895 tiles when each face of the plenum was lined successively with 100 mm of sound absorbing foam. Differences are shown relative to the bare plenum case. Also shown are the differences for a 300 mm thick lining of glass fiber batts.

Figure 11-18 shows the effect of using 300 mm glass fiber instead of 100 mm of foam on the levels in the room below the A895 tiles by comparing the device power minus the room sound pressure level for three different sources. The same comparison is made in Figure 11-19 for FGvin tiles. Both sets of data show that changes at and above 250 Hz are small, around 1 dB. In the 63 and 125 Hz bands the change seems to depend on the device. Average values are about 3 dB.

[†] Box A is an earlier incarnation of VAVsim1. The loudspeakers in this box burned out and could not be replaced. With new loudspeakers installed, this became VAVsim1.

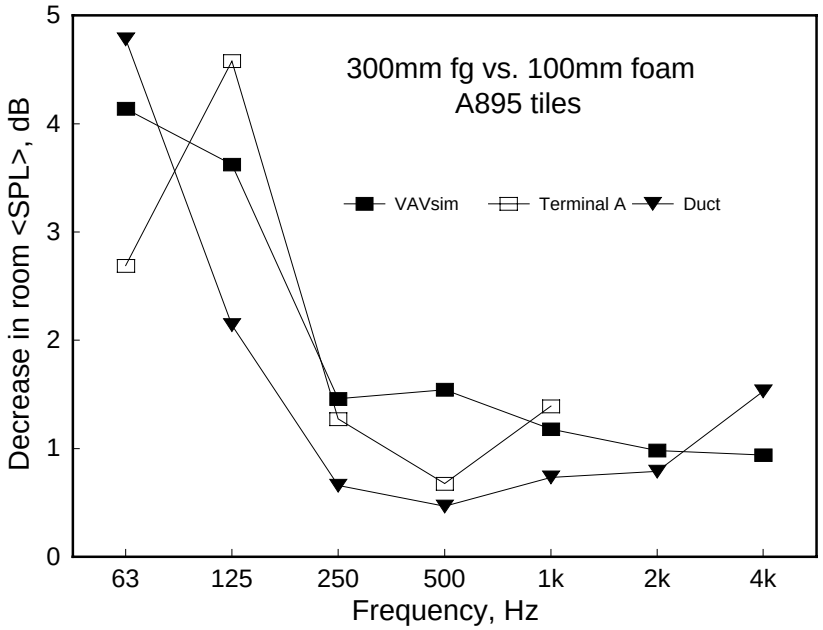

Figure 11-18: Reduction in room sound pressure level caused by use of 300 mm glass fiber on plenum side walls – A895 tiles.

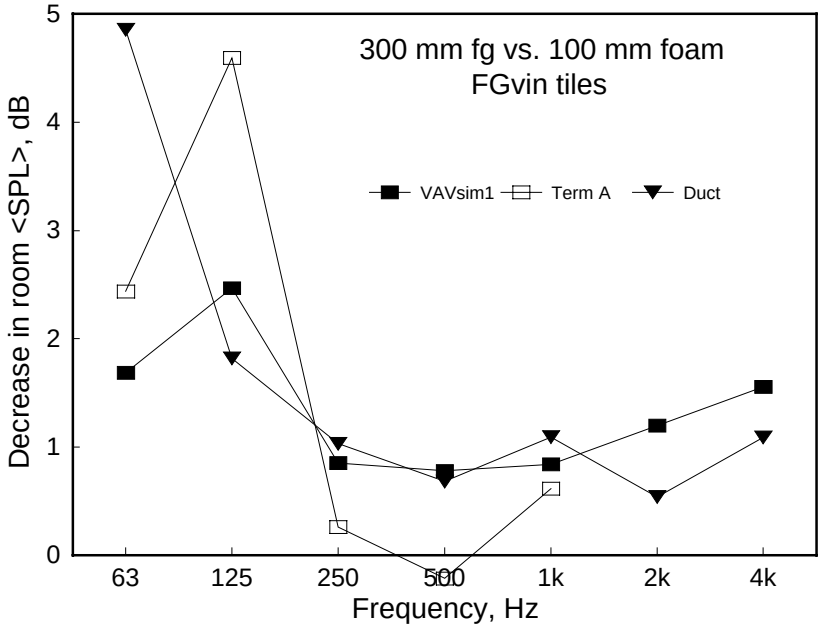

Figure 11-19: Reduction in room sound pressure level caused by use of 300 mm glass fiber on plenum side walls – FGvin tiles

11.4 Effects of carpet and wall absorbers on room sound pressure level.

Most measurements were made with no carpet on the floor of the RAT room and with diffusing panels on the walls. The absence of a carpet made it easier to move the microphone system, equipment and to keep the room clean. It was important, nevertheless to obtain some estimate of the effects that adding a carpet would have on the

sound pressure levels in the room. Measurements to quantify the effect were done when the effect of lining the plenum with 300 mm of glass fiber batts was being investigated. To get some additional data that might help to estimate the effect of office furnishings on the sound pressure levels, twelve of the FGvin tiles were placed at random locations on the walls.

Figure 11-20 shows the reduction in sound pressure level at each stage when the 100 mm foam lining in the plenum was replaced with 300 mm thick glass fiber, carpeting was added to the floor and sound absorbing panels were added to the walls. There is limited information at high frequencies because levels generated by the terminal were too close to background levels in the room. The data in Figure 11-21 for the VAVsim source provide a more complete picture. There one can see that the decrease in level due to the carpet only exceeds 1 dB at and above 2 kHz. The wall absorbers have a more significant effect from 250 Hz upward. In the important low frequency bands, the only change of any real significance is that due to adding the 300 mm glass fiber in the plenum. The combined effects of the 300 mm glass fiber in the plenum, carpeting and wall absorbers can be seen for the FGvin and A755B tiles in Figure 11-22 and Figure 11-23.

All of these results show that the changes in the room and plenum are fairly independent of source type and ceiling type. It can be argued that the RAT room in its standard configuration for testing was significantly more reverberant than a typical office. When the carpet and wall absorbers were added, the room was quite non-reverberant. The data here show that increases in room absorption are not likely to reduce the levels by more than about 3 dB and then only at the higher frequencies. The data collected in the RAT room give conservative estimates of the ceiling attenuations.

Variations in plenum absorption occur in practice. The cases studied here, including the cases with bare side walls, show that these variations can result in quite large variations in the room sound pressure level. It would be extremely difficult to invent a scheme for including the plenum absorption conditions in a prediction model. The practical approach is to accept the RAT room data as typical and use that in modeling.

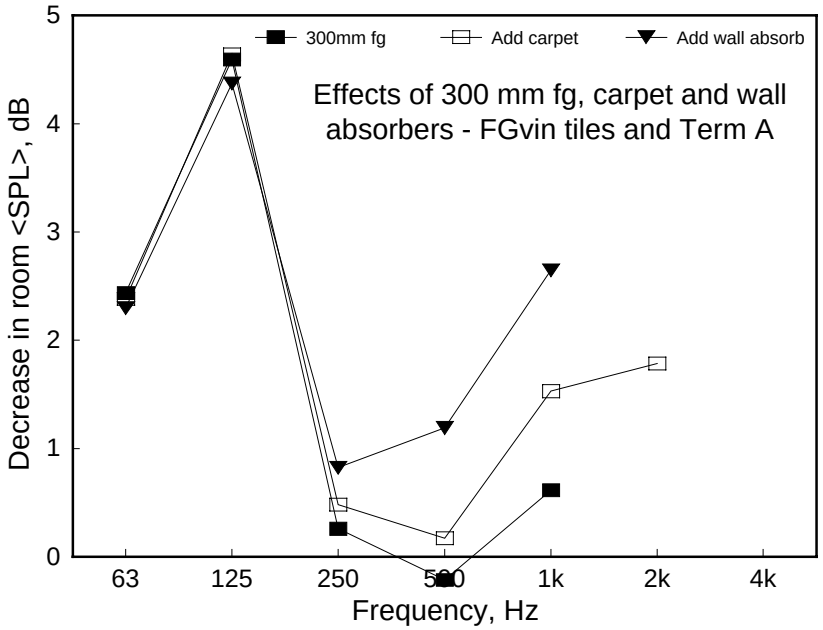

Figure 11-20: Decrease in room sound pressure level caused by replacing the 100 mm foam lining in the plenum with 300 mm thick glass fiber, adding carpeting to the floor and adding sound absorbing panels to the walls in stages – FGvin tiles and Terminal A.

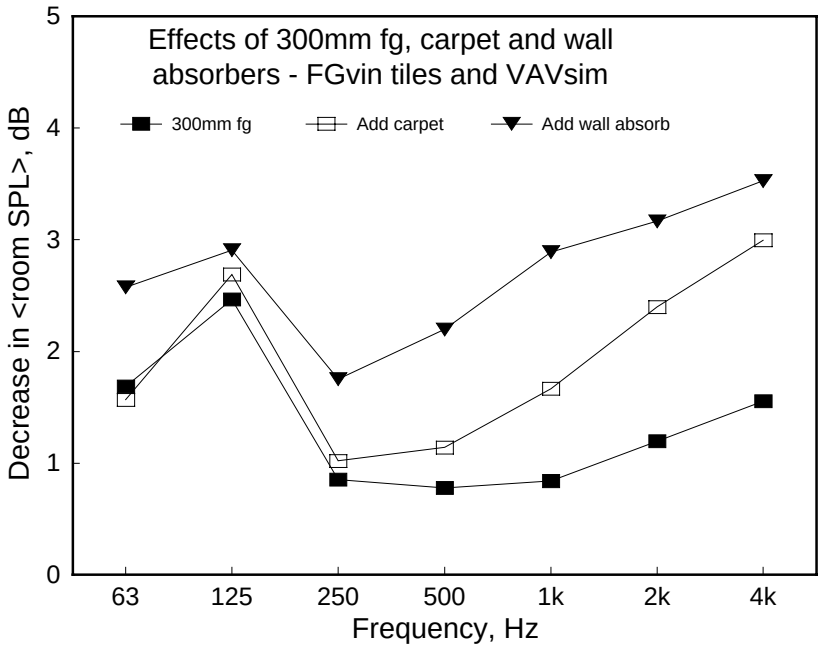

Figure 11-21: Decrease in room sound pressure level caused by replacing the 100 mm foam lining in the plenum with 300 mm thick glass fiber, adding carpeting to the floor and adding sound absorbing panels to the walls in stages – FGvin tiles and VAVsim.

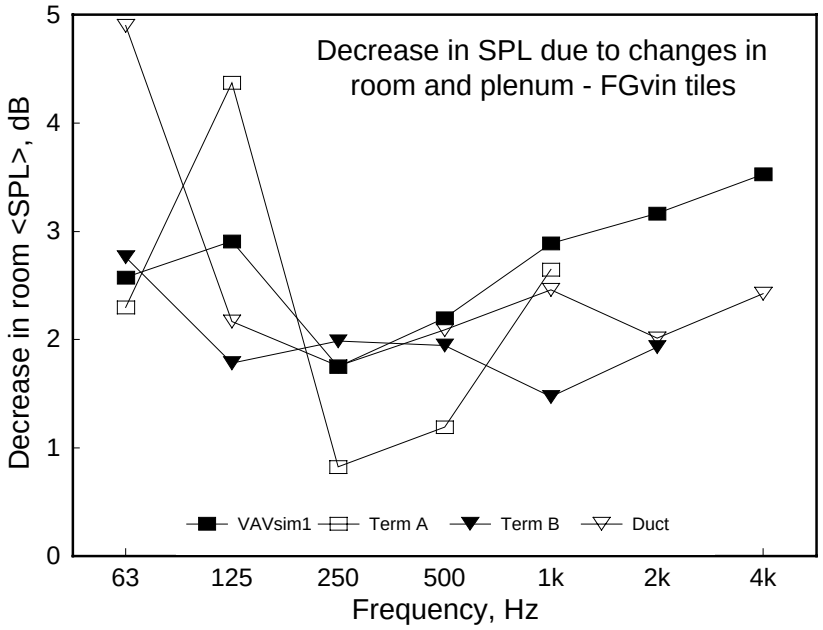

Figure 11-22: Decrease in room sound pressure level caused by replacing the 100 mm foam lining in the plenum with 300 mm thick glass fiber, adding carpeting to the floor and adding sound absorbing panels to the walls – four different sources and FGvin tiles.

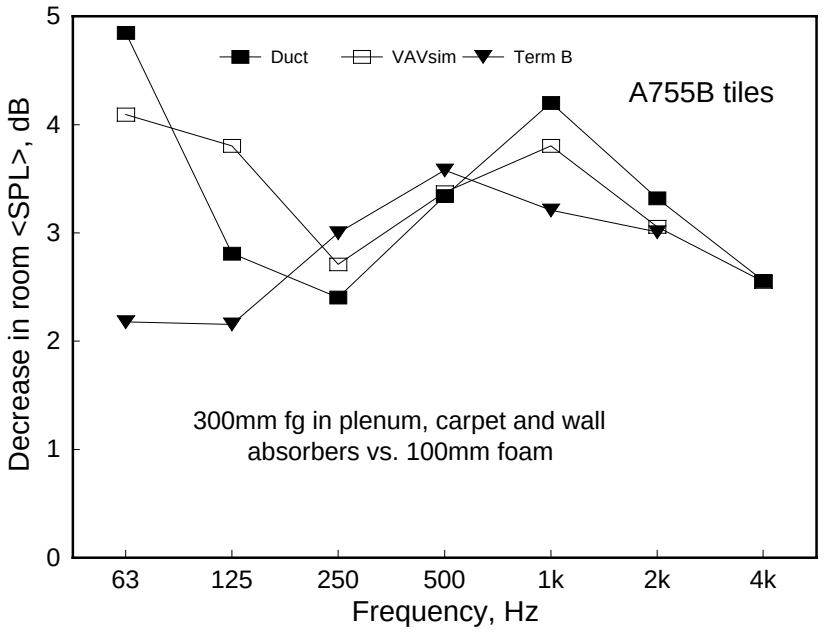

Figure 11-23: Decrease in room sound pressure level caused by replacing the 100 mm foam lining in the plenum with 300 mm thick glass fiber, adding carpeting to the floor and adding sound absorbing panels to the walls – three different sources and A755B tiles

11.5 Effects of slots in ceiling tiles.

Changes in room sound pressure level caused by one and two slots in various positions were measured. Each slot measured 50 x 1200 mm (tiles were cut in half to produce

these slots). When a single slot was used it was positioned directly under Box A. When two slots were used, they were separated by one uncut tile; they were thus two tile widths apart and when the slits were nominally under the source, they were in fact displaced to each side of the source.

As Figure 11-24 to Figure 11-26 show, slits of this size have significant effects only when directly under the source. In the other cases, the distance from the source, the size of the slits and the relatively uniform sound field in the plenum (see Section 14) render their effect negligible. The additional transmission through the slit is negligible relative to other paths through the ceiling/T-bar system.

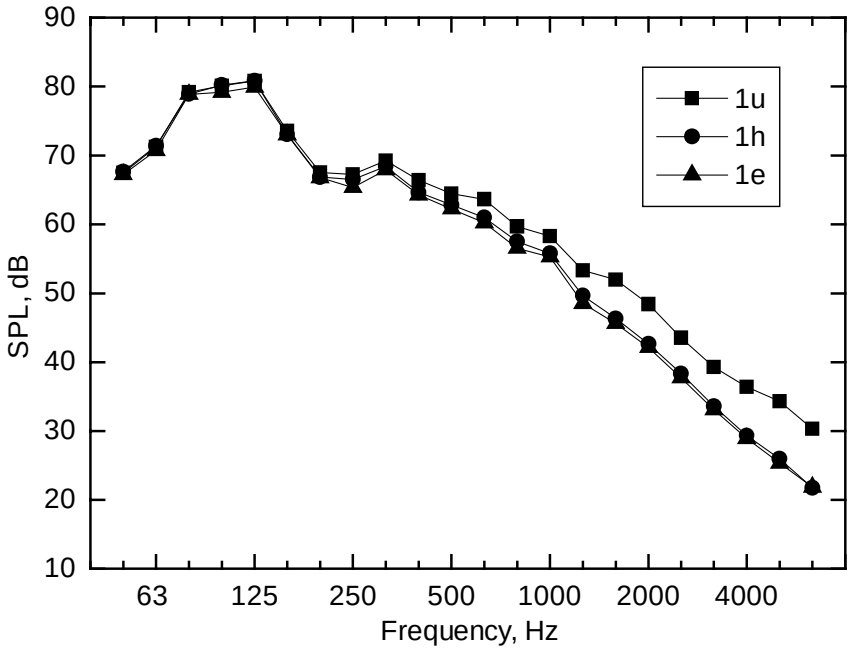

Figure 11-24: Sound pressure levels caused by a single slot in the ceiling. The position of the slot is under(u) the simulated source, halfway along the room(h), and at the end of the room(e).

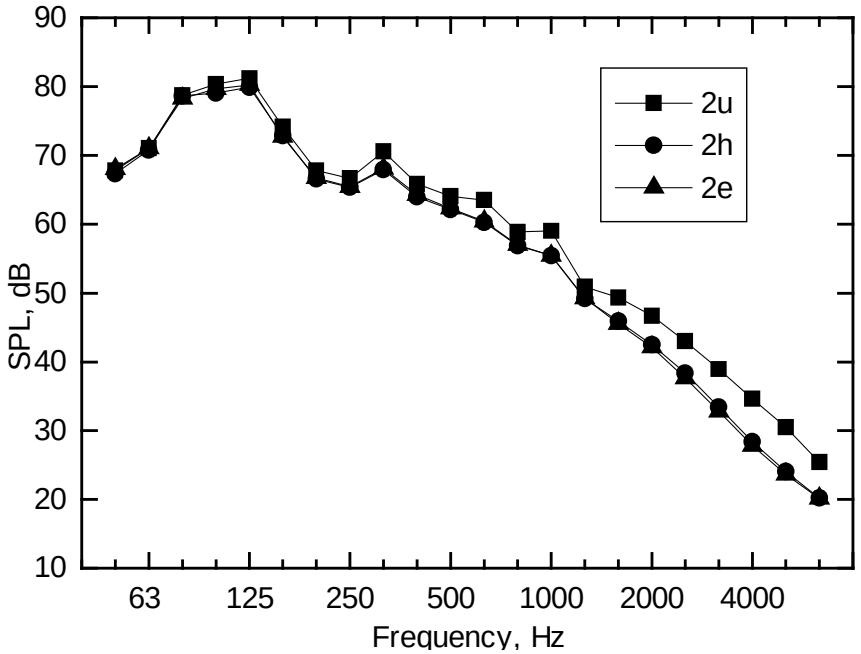

Figure 11-25: Sound pressure levels caused by two slots in the ceiling. The position of the slots is under(u) the simulated source, halfway along the room(h), and at the end of the room(e).

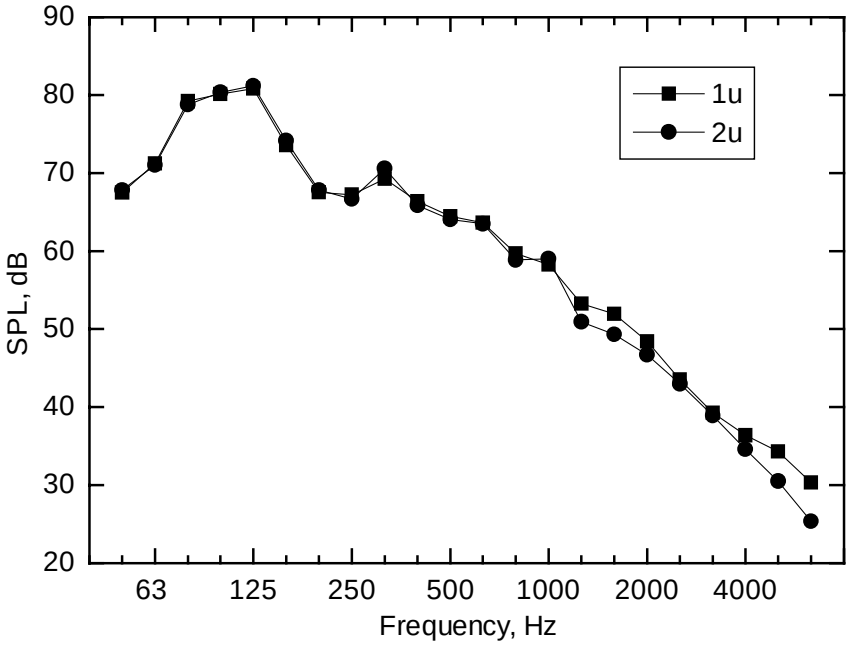

Figure 11-26: Sound pressure levels caused by one and two slots in the ceiling positioned directly under the source, Box A.

11.6 Light fixture with integral ventilation slots.

At the request of the monitoring committee, changes in average room sound pressure level caused by the installation of a light fixture in the ceiling were measured. The light fixture was a Lytecel LYA2GCFSs240-120LE with integral ventilation slots for return air. It measured 610 x 1220 x 134 mm deep. The fixture was mounted in three positions in the ceiling. The x and z coordinates for each position are given in Table 11-5. The general layout of the devices in the plenum and the positions of the light fixture is shown in Figure 11-28 and a picture of the light is shown below in Figure 11-27.

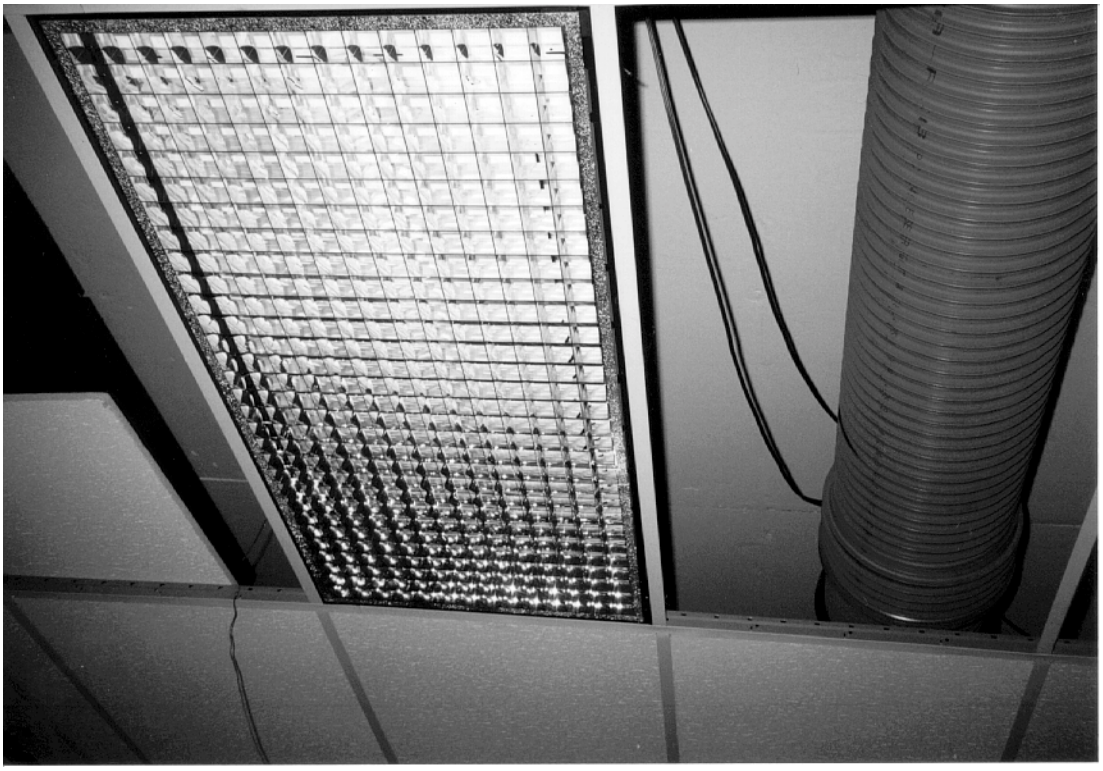

Figure 11-27: View of the light fixture with integrated ventilation slots used in the project.

The sound pressure levels measured for each position of the light fixture are shown for the duct source and VAVsim1 in Figure 11-29 and Figure 11-30. It is plain that the results are similar to those found for the slit experiment. The presence of the light fixture only effects the levels slightly when it is in position 1, closest to the VAVsim1 source when that source is operating. In all other cases, the effect is negligible.

Table 11-5: Coordinates of mid-point of the light fixture surface.

Position	x, m	z, m
1	1.23	6.02
2	2.48	7.22
3	1.23	1.06

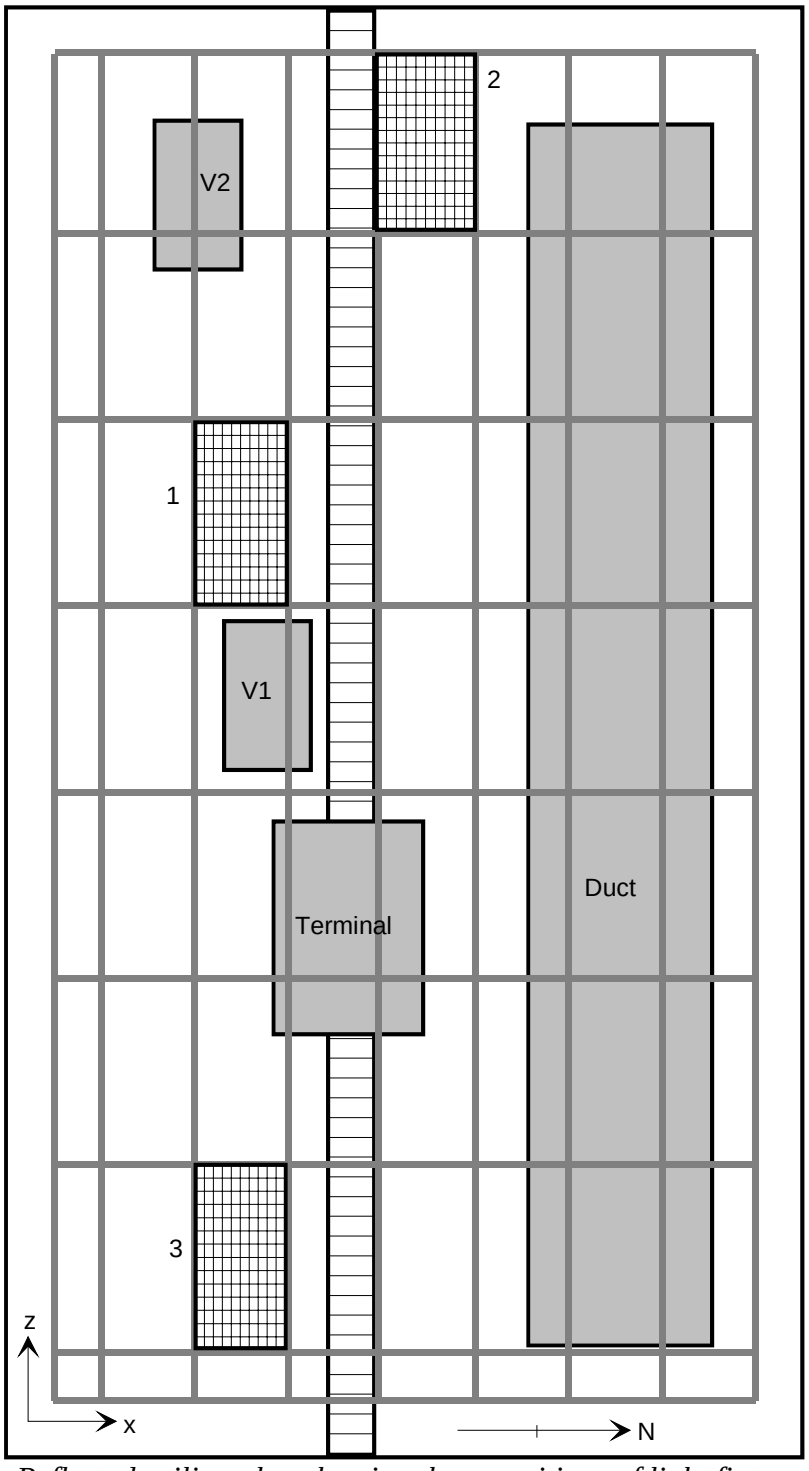

Figure 11-28: Reflected ceiling plan showing three positions of light fixture, ducts, simulators and terminal units.

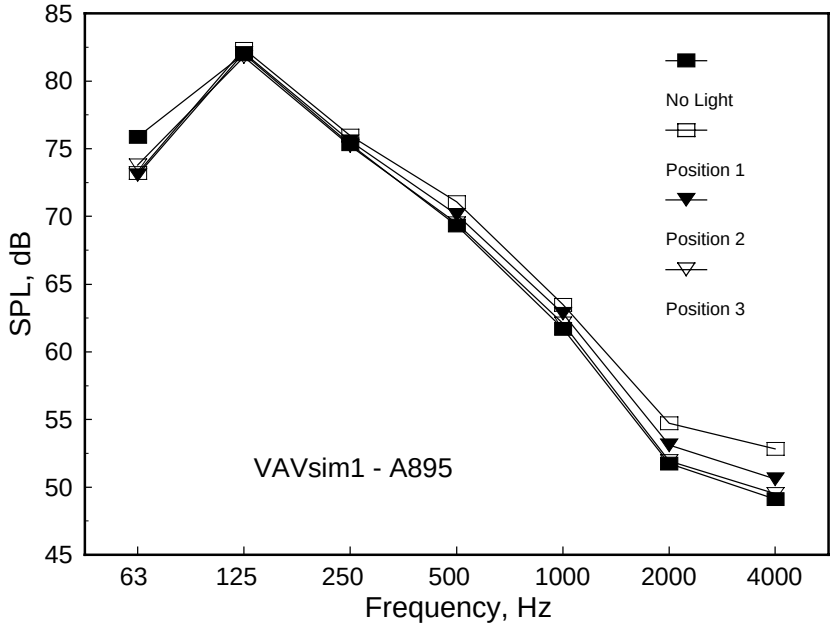

Figure 11-29: Sound pressure levels generated by VAVsim1 under A895 ceiling tiles with and without a light fixture.

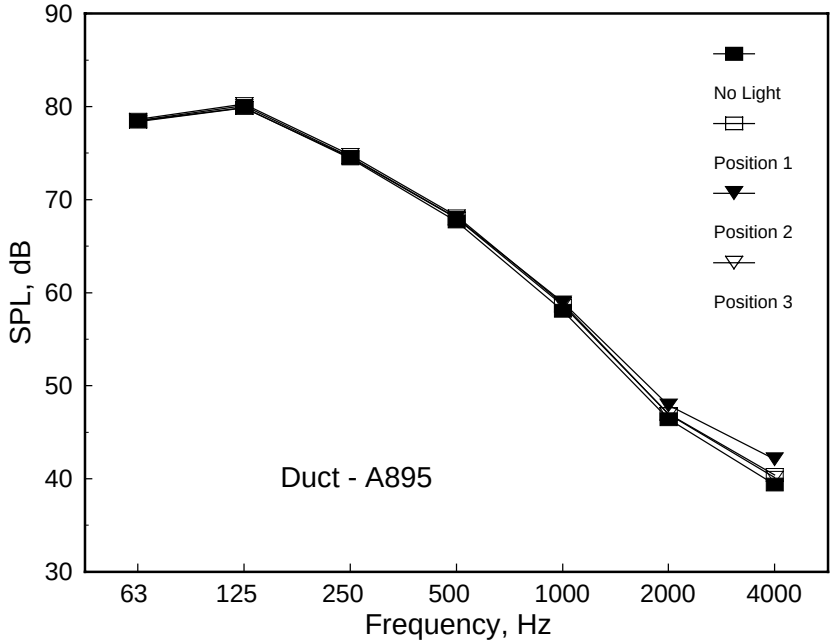

Figure 11-30: Sound pressure levels generated by the duct source under A895 ceiling tiles with and without a light fixture.

11.7 Effect of source height.

At an early stage in the research, the effect of the gap between the simulated VAV source and the A755 ceiling was investigated. The changes in room sound pressure level are

plotted relative to the shortest distance measured (50 mm) in Figure 11-31. The figure shows that, for this case, the changes are rather small. These results are in general agreement with those of Walker [35] shown in Figure 4-7. The influence of the size of the gap between the source and the ceiling is less than that seen in reference [33]. It should be remembered that the situation addressed here is complicated by the presence of sound from the plenum penetrating the major part of the surface area of the ceiling. On the basis of this result, it is reasonable to take the position that the gap between the source and the ceiling tiles is not likely to be a very significant factor. In most practical cases the gap will be around 50 to 100 mm.

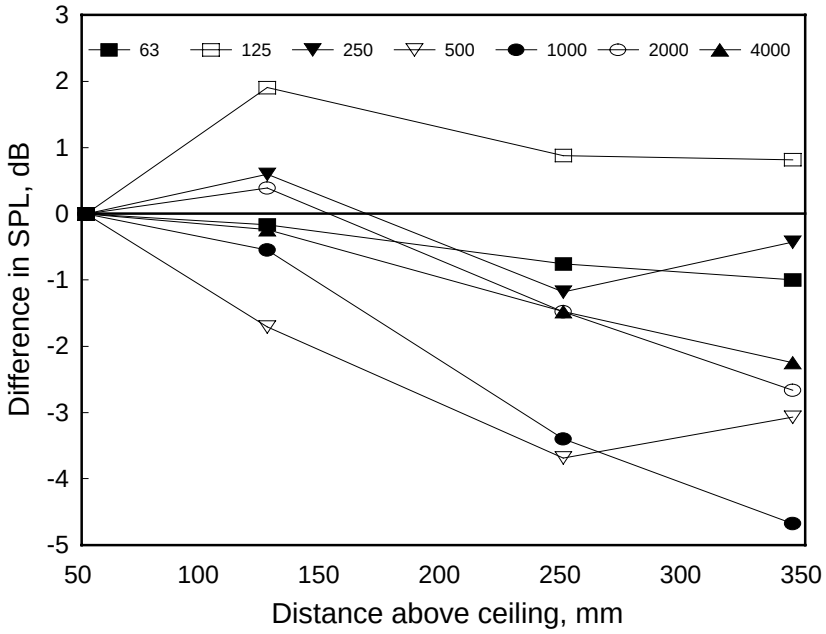

Figure 11-31: Change in mean room sound pressure level caused by raising the source higher, further from the ceiling. A755 tiles.

12. Reverberation Room Ceiling Insertion Loss measurements.

12.1 Test procedure.

Some years ago, a draft ASTM test procedure to measure ceiling insertion loss (CIL) was proposed. Briefly, a metal box measuring 300 x 600 x 900 mm is placed inside a frame that measures 2.44 x 3.05 m by 500 mm high and that is lined on its inner faces with sound absorbing material. The frame is used to support the ceiling panels under test. The metal box simulates an air terminal box and contains two loudspeakers, each driven by a separate noise generator and power amplifier. This same type of simulator was used in the main series of measurements in the RAT room. The upper surface of the metal box is 50 mm from the rear face of the ceiling panels. The sound power from this source placed in four positions inside the frame is measured with and without a ceiling specimen in place in the frame. The difference in sound power between the two measurements gives a spectrum called the ceiling insertion loss (CIL). This procedure is meant to simulate actual installation of air terminal devices and to rank ceiling panels for their effectiveness in preventing the transmission of sound from such devices. The procedure was evaluated during this project.

The frame was constructed from two layers of 16 mm particle board so sound transmission through it was negligible compared to sound transmission through the ceiling tiles under test. Seals were installed at the junction with the floor to eliminate sound leaks there. The picture below shows the frame lined with 300 mm of glass fiber batts and the VAV simulator installed on rubber pads.

12.2 Results with 100 mm foam lining the frame.

The draft test procedure called for an absorptive lining with an NRC greater than 0.9. In the first set of measurements made, the frame was lined with 100 mm thick absorptive

foam that satisfied that criterion. Table 12-1 shows the CIL values measured. They are also plotted in Figure 12-1.

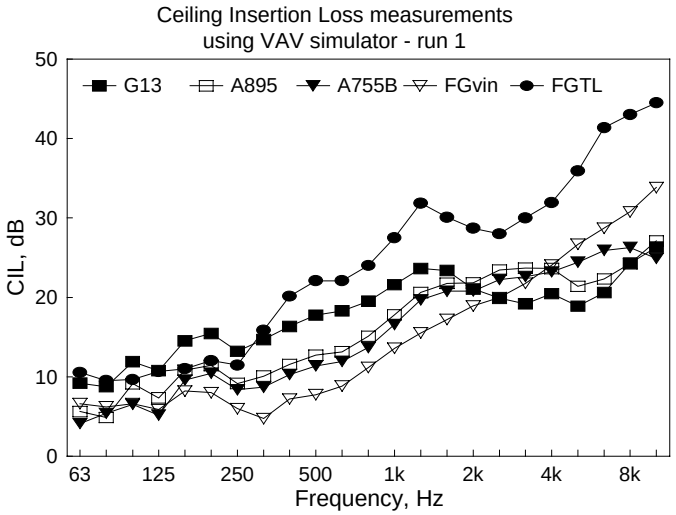

Figure 12-1: First set of CIL measurements for all five ceiling types.

Table 12-1: Mean values of ceiling insertion loss – first set.

Freq.	A895	G13	A755B	FGvin	FGTL
63	5.6	9.2	4.1	6.6	10.5
80	4.9	8.8	5.4	6.2	9.5
100	9.1	11.9	6.5	6.6	9.7
125	7.4	10.8	5.2	5.9	10.7
160	10.9	14.5	9.6	8.2	11.0
200	11.4	15.5	10.4	8.0	12.0
250	9.2	13.2	8.4	6.0	11.5
315	10.1	14.7	8.7	4.7	15.9
400	11.6	16.4	10.3	7.2	20.2
500	12.7	17.8	11.4	7.7	22.1
630	13.2	18.3	11.9	8.8	22.1
800	15.1	19.5	13.7	11.2	24.0
1000	17.8	21.6	16.6	13.6	27.5
1250	20.6	23.6	19.7	15.5	31.9
1600	21.8	23.4	20.8	17.2	30.1
2000	21.8	21.1	20.8	18.9	28.7
2500	23.5	19.9	22.3	20.0	28.0
3150	23.7	19.2	22.6	21.8	30.0
4000	23.7	20.5	23.2	24.1	31.9
5000	21.4	18.9	24.4	26.7	35.9
6300	22.3	20.6	25.9	28.7	41.4
8000	24.2	24.3	26.3	30.8	43.0
10,000	27.1	26.3	24.9	33.9	44.5

12.3 Results with 300 mm glass fiber lining.

As part of the investigation in the RAT room, the effect of lining the vertical plenum surfaces with 300 mm thick glass fiber was examined. There were signficant differences and it was thought worthwhile to re-measure the CIL values with a similar lining in the frame in the hope that the CIL values so obtained might then agree better with measurements in the RAT room. In the second set of measurements, as well as lining the frame with 300 mm thick glass fiber batts, only a single position of the source was used because the space available was so restricted. The data from this second series are shown in Figure 12-2 and in Table 12-2.

Table 12-2: Ceiling insertion loss values for second run with a single loudspeaker position and a 300 mm thick glass fiber lining for the frame.

Freq.	A755B	A895	FGvin	FGTL	G13	G13 taped
50	4.1	3.1	3.7	3.3	4.6	6.4
63	2.5	3.7	3.7	2.8	4.7	7.5
80	7.0	9.1	7.9	8.4	10.7	15.6
100	11.9	13.8	11.0	13.0	15.7	20.9
125	12.7	14.8	11.6	13.9	16.6	20.7
160	14.5	16.1	12.8	14.9	18.5	23.0
200	13.9	15.3	10.8	11.8	17.7	22.7
250	12.9	13.9	9.2	9.6	16.1	19.9
315	14.4	15.2	10.9	11.2	16.1	21.0
400	12.5	13.4	11.5	12.9	13.7	20.0
500	14.8	15.4	13.1	16.2	16.7	23.5
630	15.1	15.3	14.2	16.2	17.0	23.8
800	17.6	17.5	15.8	16.8	19.6	26.1
1000	19.2	19.2	17.2	18.7	21.2	27.6
1250	20.6	20.5	18.2	21.9	20.4	27.1
1600	22.5	23.0	19.7	22.6	21.6	27.4
2000	23.9	24.9	20.9	25.0	21.7	25.7
2500	25.7	27.0	23.3	28.1	21.5	24.5
3150	26.0	28.1	25.2	30.2	22.3	24.9
4000	25.9	27.6	26.6	31.6	21.5	25.5
5000	26.6	26.6	28.4	33.5	20.6	24.6
6300	28.0	27.6	30.9	35.8	21.8	27.2

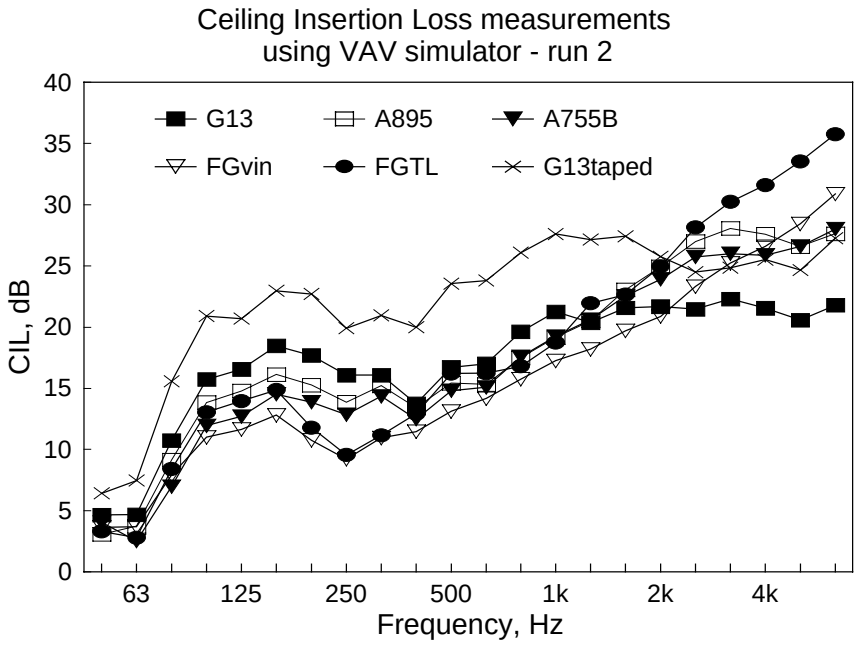

Figure 12-2: Second set of CIL measurements for all five ceiling types and 13 mm gypsum board with joints taped.

12.4 Decay rate vs. Reference source measurements.

During these CIL measurements, in response to a negative comment received during the balloting of the draft standard, the effectiveness of measuring the power insertion loss using a reference sound source was evaluated. Instead of measuring reverberation times and using them with the sound pressure levels to calculate the power from the source directly, levels from the Acculab reference source placed in one position next to the support frame were measured. The difference in level between the unknown source and the reference source can be used to calculate the sound power of the unknown source. CIL values found in this way were found to be extremely close to those found using the direct method.

The three reverberation room CIL values and the power insertion loss obtained in the RAT room are shown in Figure 12-3 through Figure 12-7. These figures show that the absorptive conditions inside the frame and the number of source positions used strongly influence the CIL values measured. What is more important is that none of the CIL measures can be used to accurately predict the sound insulation seen in the RAT room.

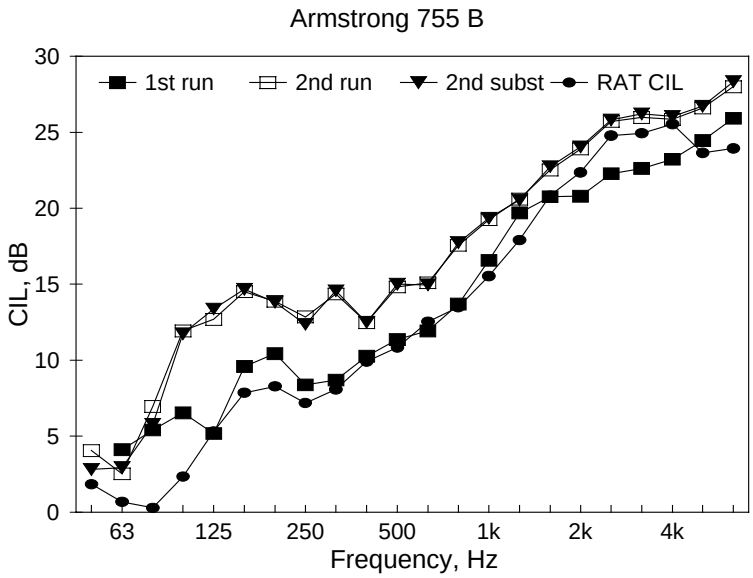

Figure 12-3: Ceiling power insertion loss for A755 mineral fiber tiles using two absorptive linings and two source arrangements. The second set of measurements compares the direct method of measuring power insertion loss with the substitution method.

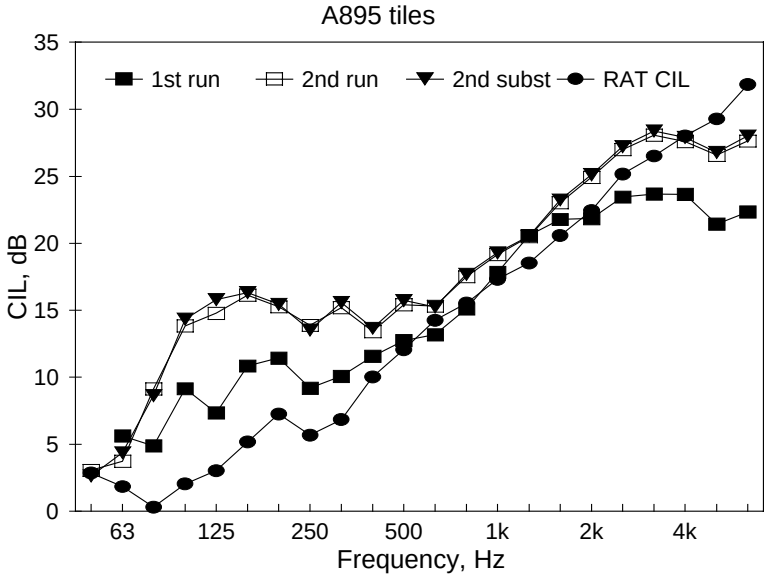

Figure 12-4: Ceiling power insertion loss for A895 mineral fiber tiles using two absorptive linings and two source arrangements. The second set of measurements compares the direct method of measuring power insertion loss with the substitution method.

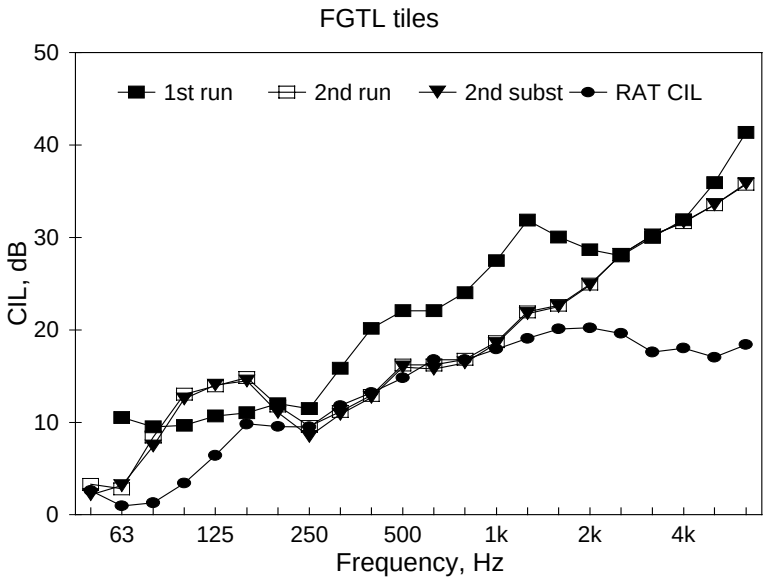

Figure 12-5: Ceiling power insertion loss for vinyl-faced, 50 mm thick glass fiber tiles with TL backing using two absorptive linings and two source arrangements. The second set of measurements compares the direct method of measuring power insertion loss with the substitution method.

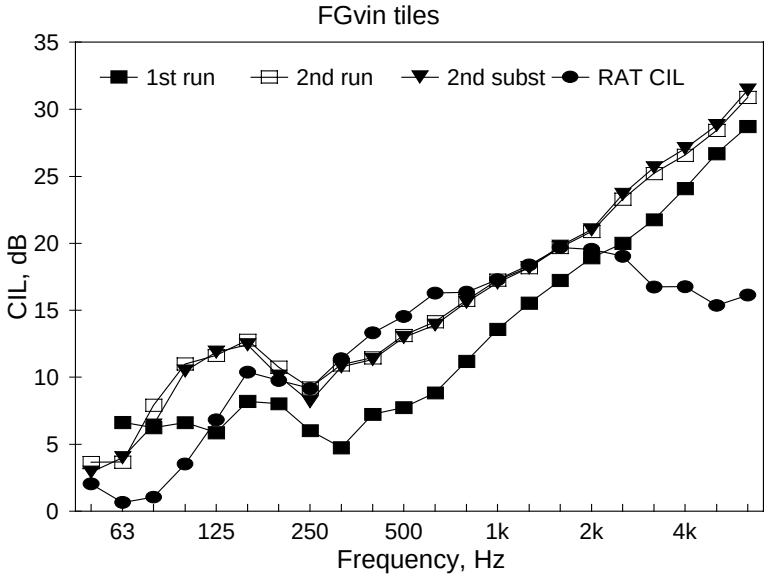

Figure 12-6: Ceiling power insertion loss for vinyl-faced, 50 mm thick glass fiber tiles using two absorptive linings and two source arrangements. The second set of measurements compares the direct method of measuring power insertion loss with the substitution method.

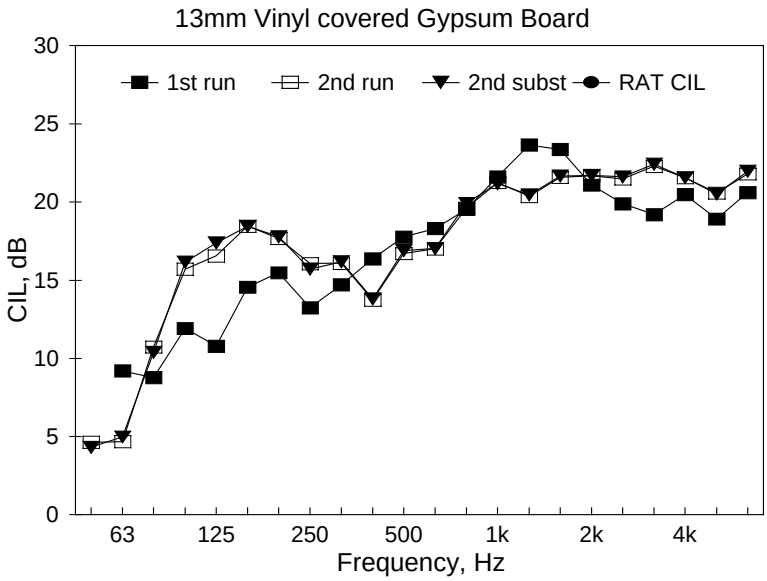

Figure 12-7: Ceiling power insertion loss for 13 mm vinyl-faced gypsum board tiles using two absorptive linings and two source arrangements. The second set of measurements compares the direct method of measuring power insertion loss with the substitution method.

13. Comparison of E90, E1414 and CIL with RAT power insertion loss.

One aim of the project was to find or generate a test procedure that could be used to evaluate ceiling boards as barriers against casing-radiated sound. The two most likely candidates were the E90 procedure (see section 9.3) and the CIL procedure (see Section 12). Differences between E90 results and the ceiling power insertion loss measured in the RAT room, RAT CIL, are shown in Figure 13-1. Differences between RAT CIL and the reverberation room CIL are shown in Figure 13-2 and Figure 13-3. For completeness, the differences for the E1414 test are shown in Figure 13-4. In these figures the actual value of the difference is not too important; it is the range of the data at any one frequency that matters. If the range were reasonably small, then the test procedure could be used to predict levels in a room under a ceiling/plenum system that contains a noisy device; the test procedure would properly rank the ceiling types.

Of the four test methods shown, the second version of the reverberation room CIL test seems most promising with the E90 procedure in second place. The original version of the reverberation room CIL test and the E1414 test are not useful for this situation.

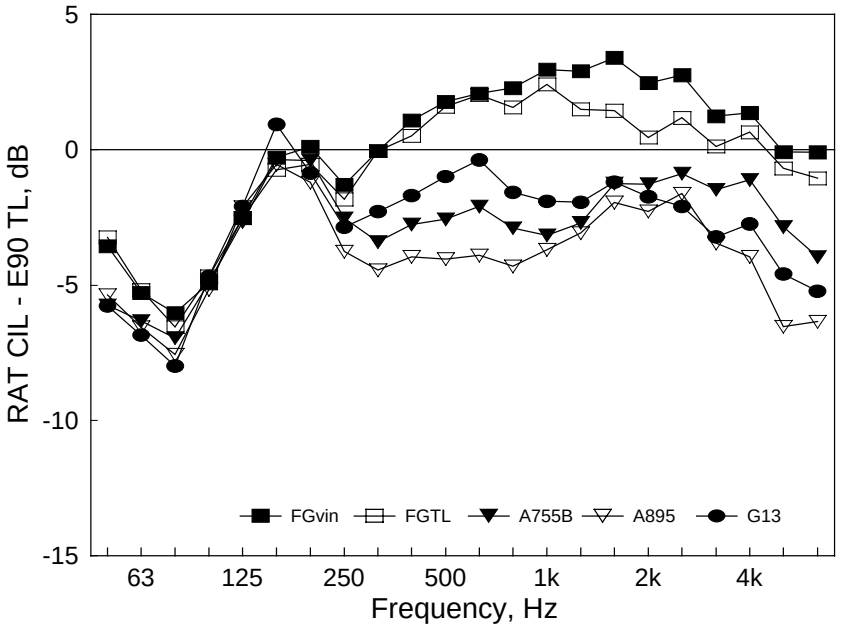

Figure 13-1: Differences between RAT CIL and E90.

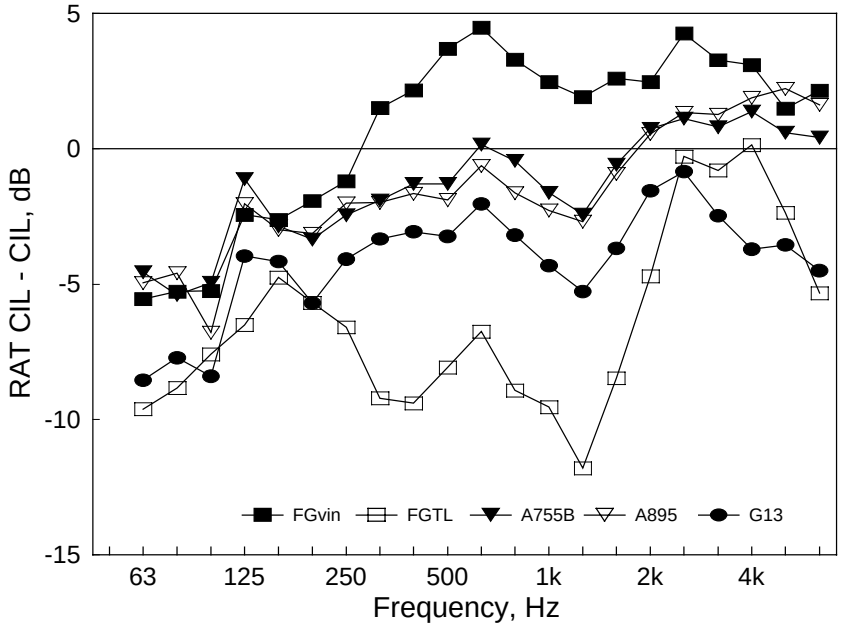

Figure 13-2: Differences between RAT CIL and CIL measured in M59 reverberation room — case 1.

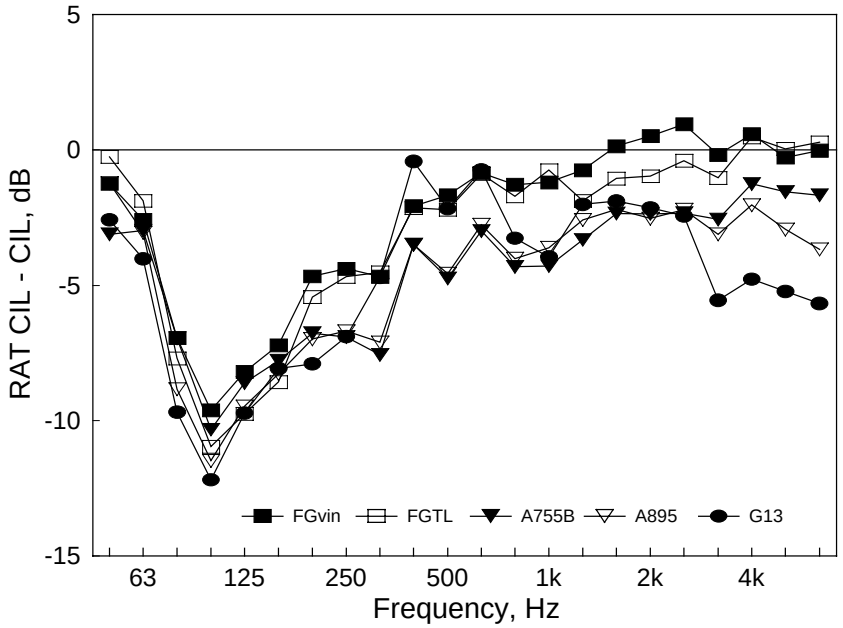

Figure 13-3: Differences between RAT CIL and CIL measured in M59 reverberation room — case 2

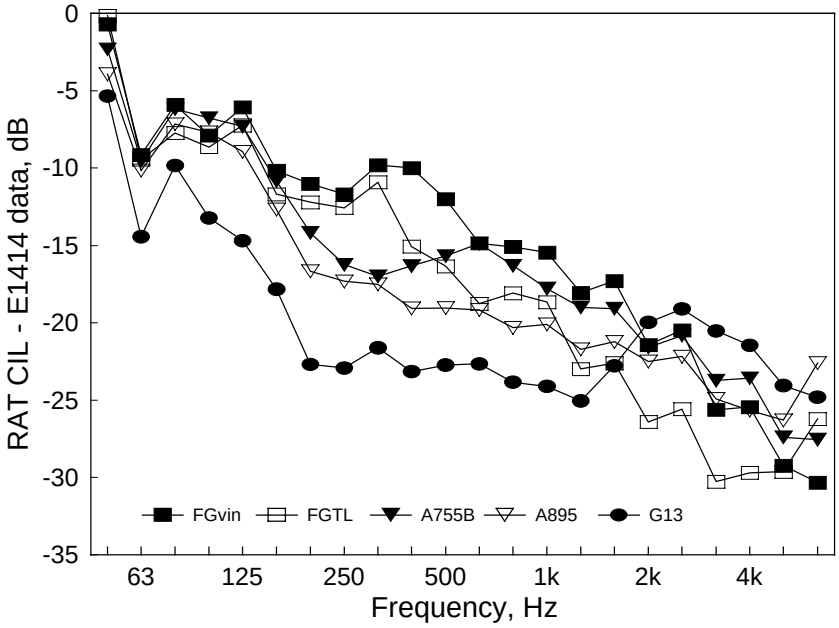

Figure 13-4: Differences between RAT CIL and ceiling attenuation measured according to E1414 — the two room method.

14. Sound in the plenum.

To measure the distribution of sound in the plenum, two holes were cut in two ceiling tiles to allow the insertion of two microphones into the plenum space. The tiles and microphones were then moved along the z-axis of the room. Sound pressure levels from the duct, VAVsim1 and VAVsim2 were measured above three ceiling types: G13, A2910, and A895. The plenum was lined with 100 mm of foam for these measurements. One microphone was moved along a line close to the south wall of the plenum at x =0.615 m. The other was moved along a line at x =2.62 m between the air supply duct and the duct simulator. Each microphone was 375 mm above the rear face of the ceiling tiles. The positions of these microphones relative to the ducts and devices in the plenum are indicated in Figure 14-1. The z positions of the microphones increased by 1.2 m at each step from the initial position of z = 1.1 m.

In general, the two microphone paths gave about the same results. To illustrate the results, only half the data are presented graphically in Figure 14-2 to Figure 14-10. The data for the VAVsim2 source show a steady decrease in level as distance from the source increases. The data for VAVsim1, positioned about the middle of the room, tends to show less dependence on position in the plenum; the field is more uniform. There are decreases in level as the microphone approaches the end walls, and at high frequencies there are steady decreases with distance. The results for the duct show much less variation with position along the z-axis of the room. For all of these measurements, it must be remembered that the microphones were placed in a plenum that was quite cluttered with ducts and other devices, so there would be a certain amount of shielding taking place.

The data for the VAVsim2 source were deemed most suitable for further processing. Figure 14-11 shows the mean value of the slope of the sound pressure level curve for both microphones for each ceiling type tested. As might have been expected, the harder the ceiling, the less attenuation there is with distance from the source.

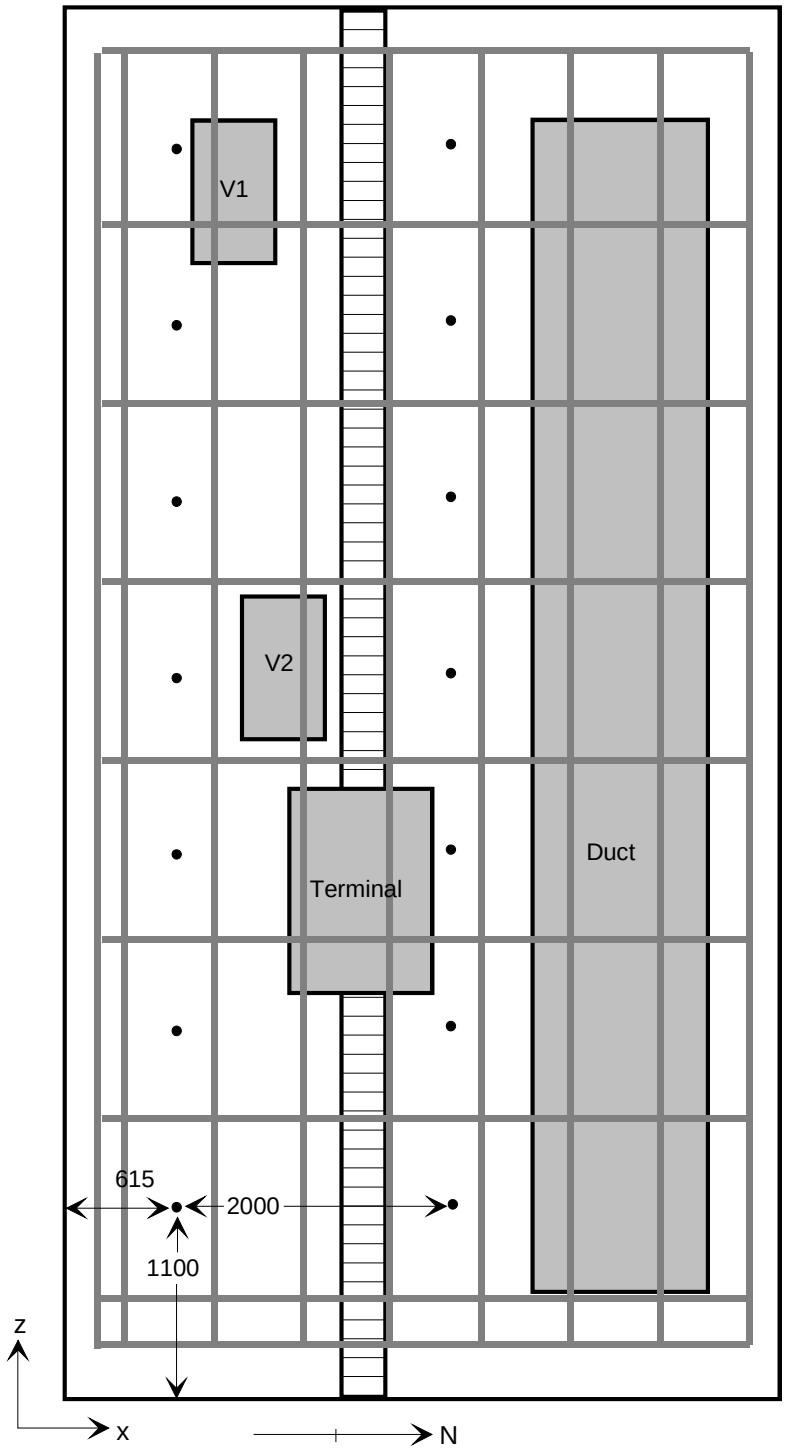

Figure 14-1: Positions of microphones in the plenum (not to scale).

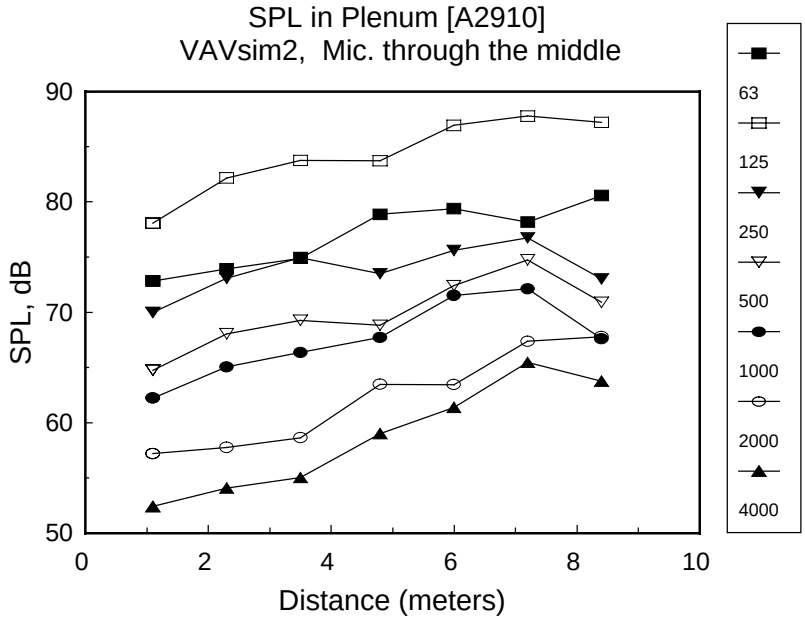

Figure 14-2: Sound pressure levels generated in the plenum above A2910 ceiling tiles by the VAVsim2 source at (2, 2.86, 8.16). Microphone on x =2.62 m plane.

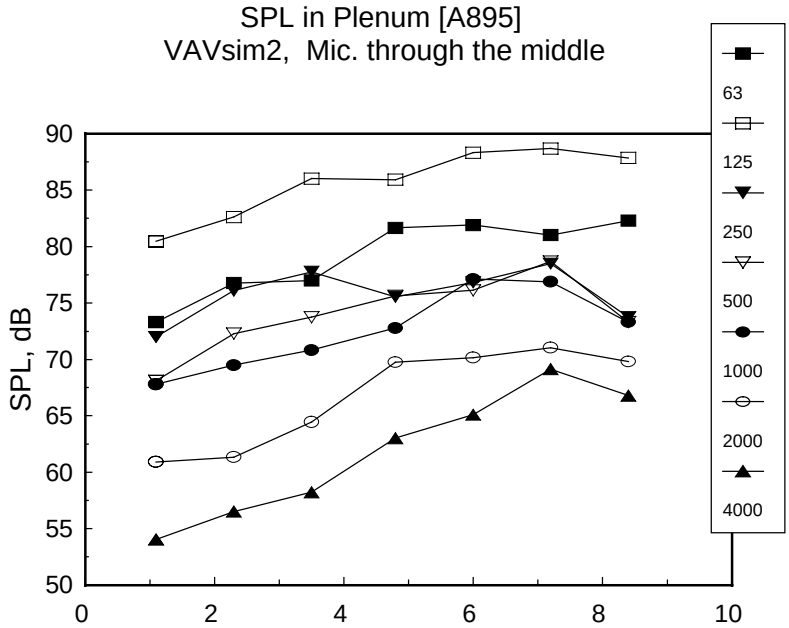

Figure 14-3: Sound pressure levels generated in the plenum above A895 ceiling tiles by the VAVsim2 source at (2, 2.86, 8.16). Microphone on x =2.62 m plane.

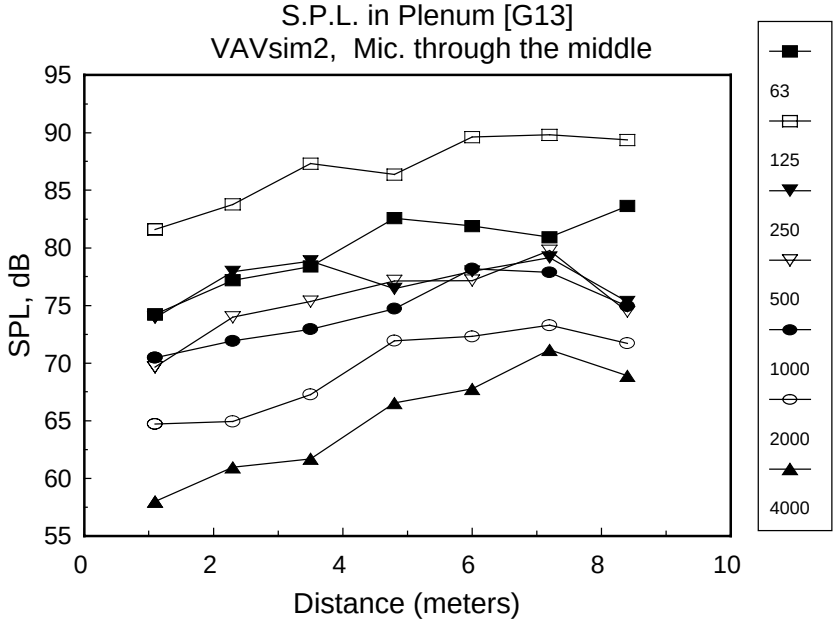

Figure 14-4: Sound pressure levels generated in the plenum above G13 ceiling tiles by the VAVsim2 source at (2, 2.86, 8.16). Microphone on x =2.62 m plane.

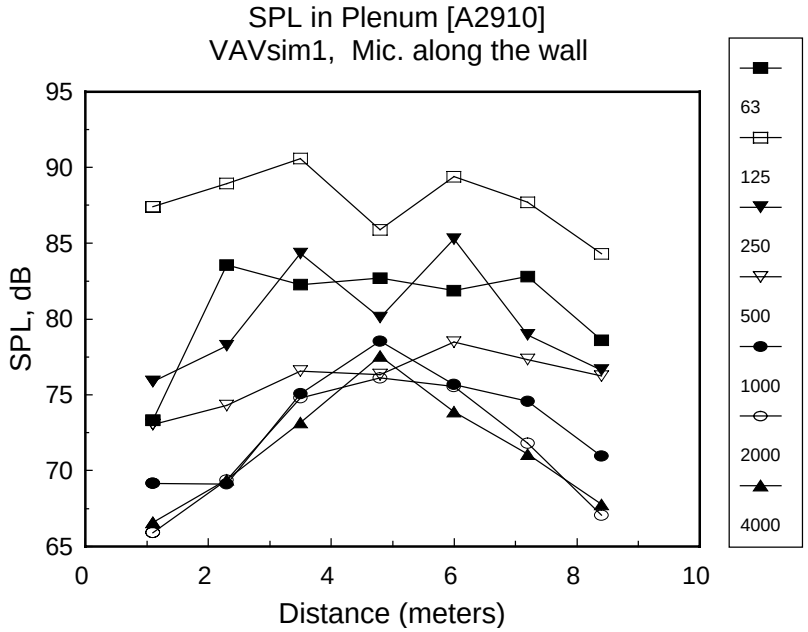

Figure 14-5: Sound pressure levels generated in the plenum above A2910 ceiling tiles by the VAVsim1 source at (1.52, 2.93, 4.73). Microphone on x =0.615 m plane.

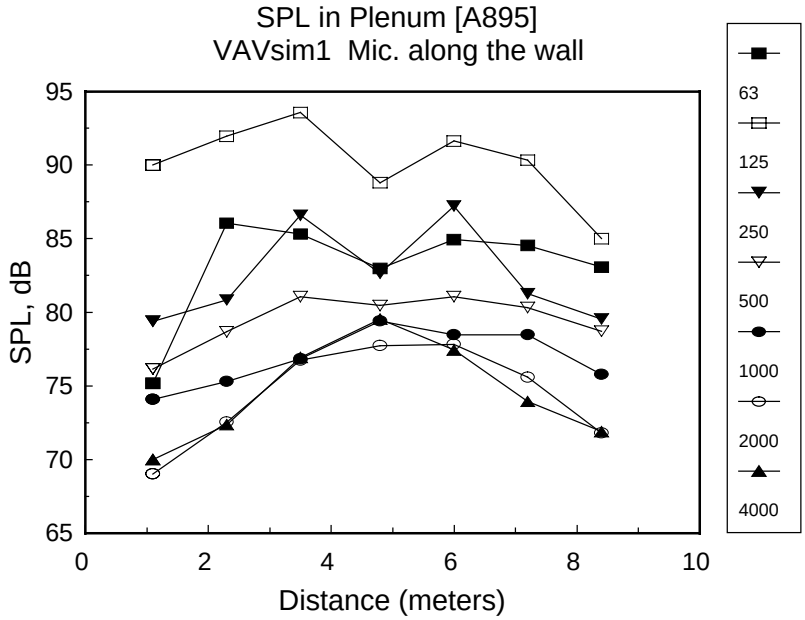

Figure 14-6: Sound pressure levels generated in the plenum above A895 ceiling tiles by the VAVsim1 source at (1.52, 2.93, 4.73). Microphone on x =0.615 m plane.

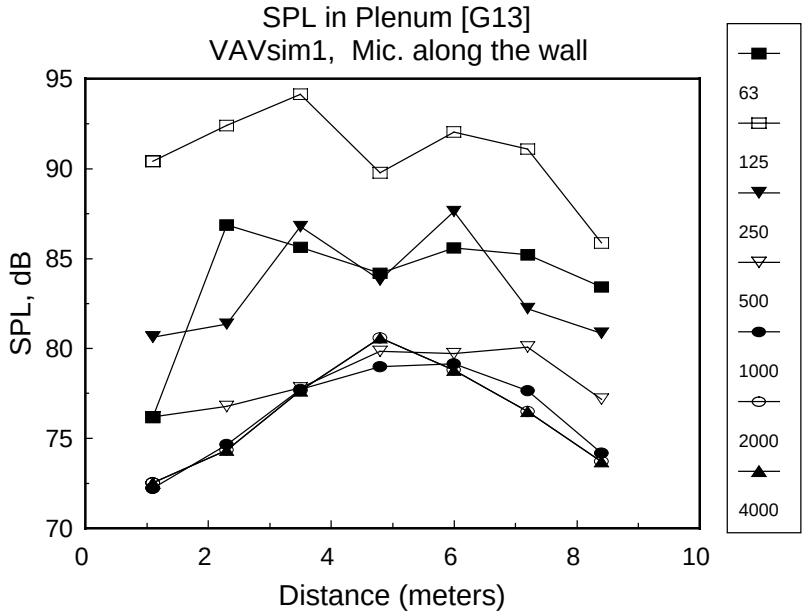

Figure 14-7: Sound pressure levels generated in the plenum above G13 ceiling tiles by the VAVsim1 source at (1.52, 2.93, 4.73). Microphone on x =0.615 m plane.

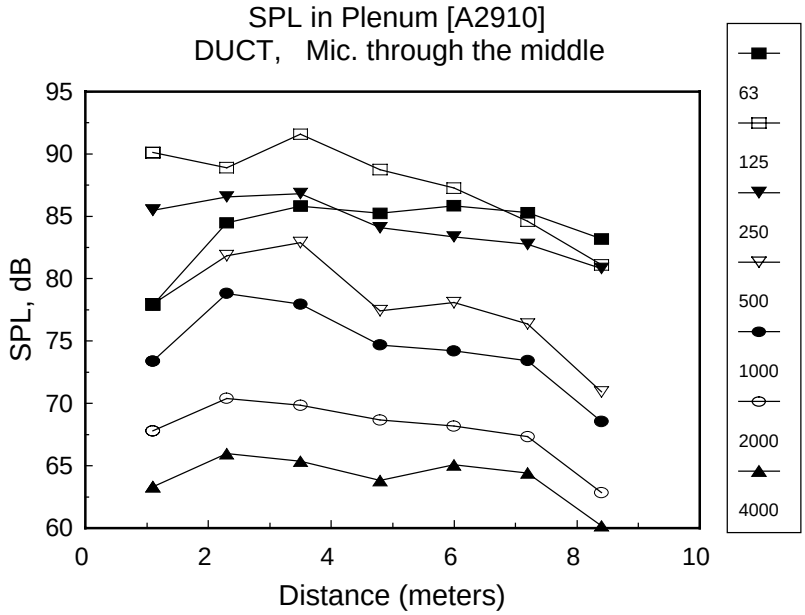

Figure 14-8: Sound pressure levels generated in the plenum above A2910 ceiling tiles by the DUCT source. Microphone on x =2.62 m plane.

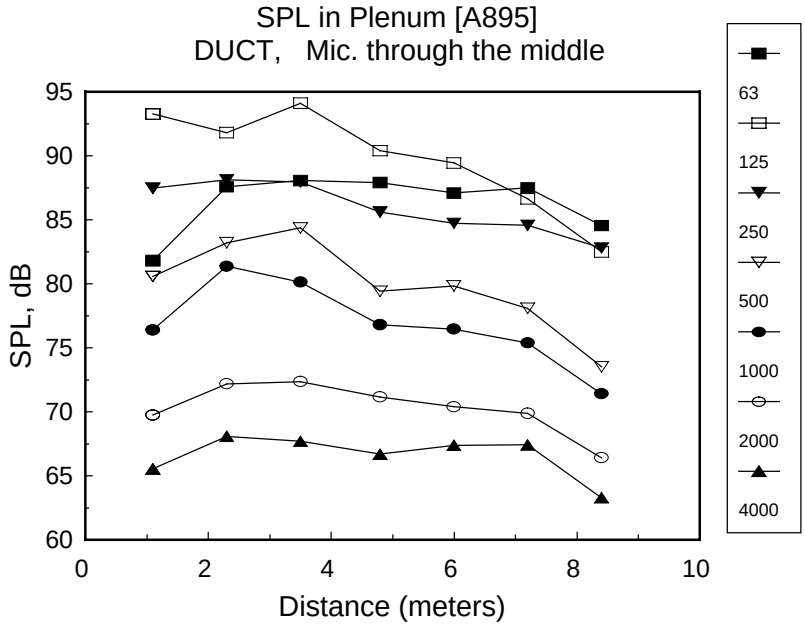

Figure 14-9: Sound pressure levels generated in the plenum above A895 ceiling tiles by the DUCT source. Microphone on x =2.62 m plane.

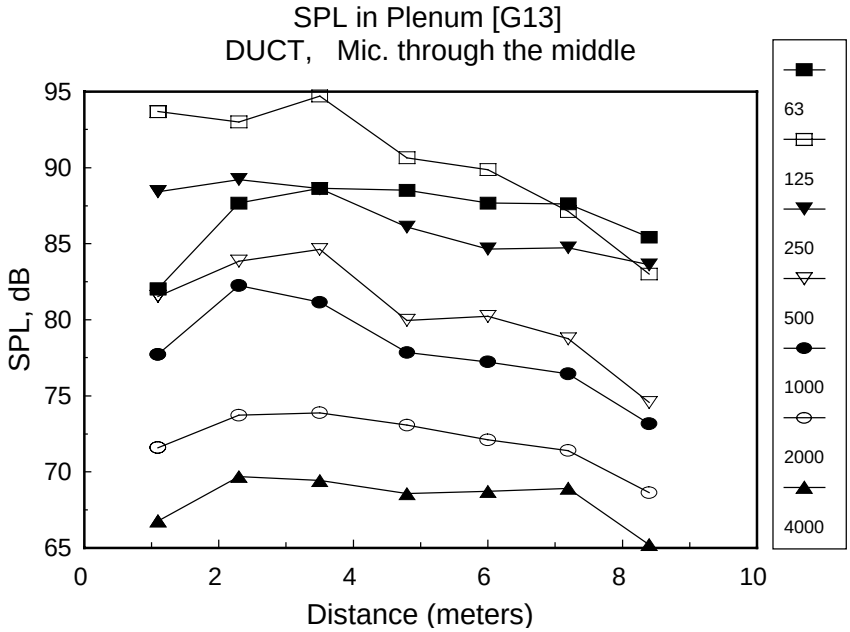

Figure 14-10: Sound pressure levels generated in the plenum above G13 ceiling tiles by the DUCT source. Microphone on x =2.62 m plane.

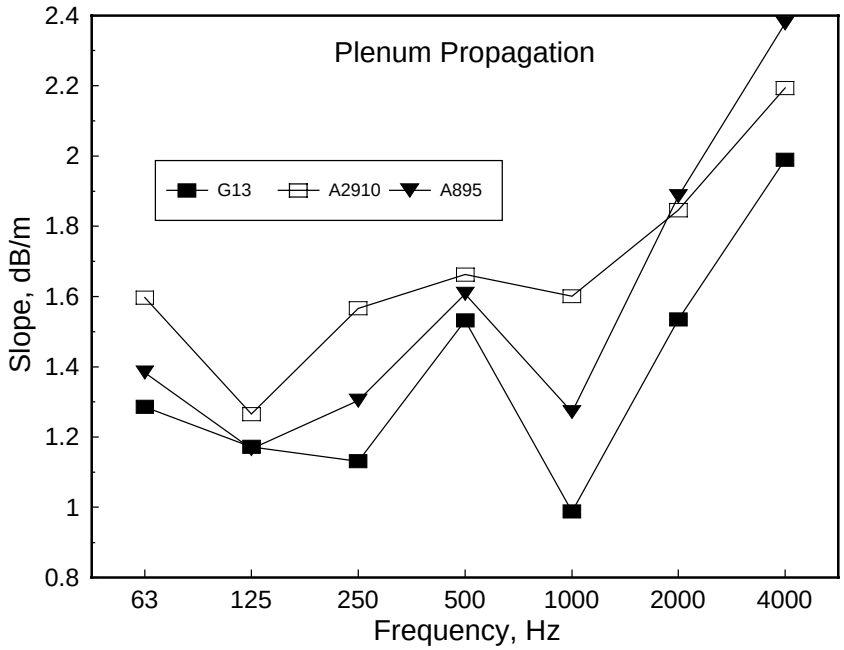

Figure 14-11: Mean values of sound attenuation in the plenum for the VAVsim2 source.

15. Absorption: C423 vs. RAT room measurements.

Measuring reverberation times in the RAT room with and without ceiling tiles allows the calculation of the sound absorption due to the tiles. The values so calculated can then be compared to those found in standard C423 tests using and E400 mounting. The comparison is not strictly fair because the duct and other devices in the plenum, although mostly of hard materials, will absorb sound, especially at low frequencies where panel absorption will be significant. Additionally, the depth of the plenum cavity is not 400 mm.

A second problem is deciding what volume of the room to use when the ceiling is installed. If the tiles are sufficiently transparent to sound, the volume of the plenum should be included. Since this problem is not part of the main project and included only for interest, this question was not resolved. Instead, calculations were made using only the volume of the room below the ceiling and the total volume including the space in the plenum. The absorption coefficients calculated are shown in Figure 15-1 to Figure 15-5. Data for the A2910 tiles are not included because they were added late in the project and not measured in the M27 reverberation room.

Figure 15-1 shows that the G13 ceiling lowers the room absorption at high frequencies by covering up the devices in the plenum but provides increased low frequency absorption due to panel and cavity effects.

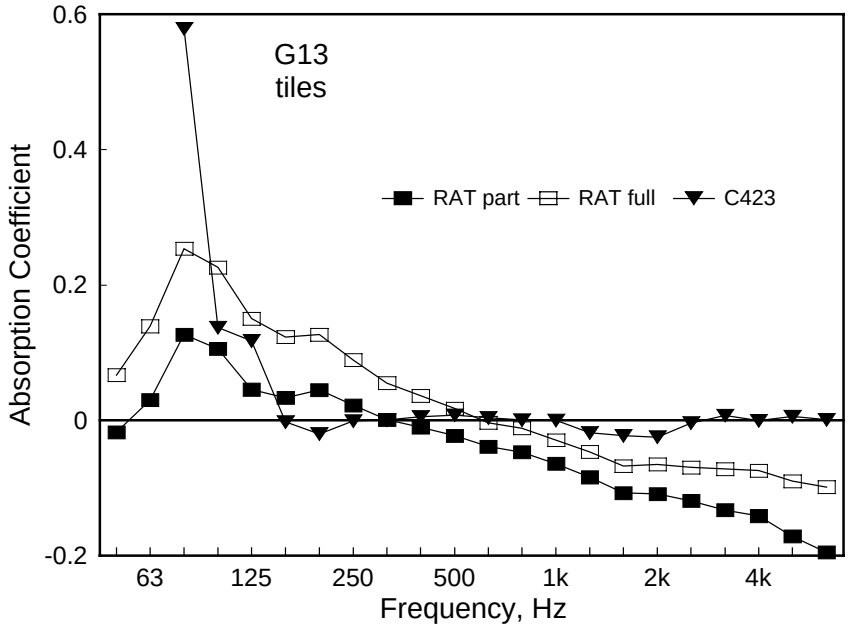

Figure 15-1: Absorption coefficients for G13 tiles in RAT room and from C423.

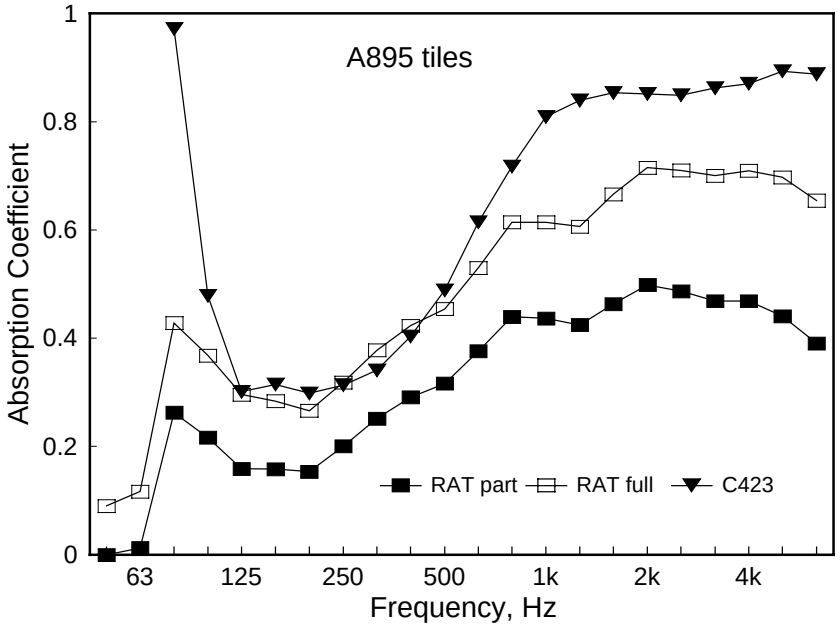

Figure 15-2: Absorption coefficients for A895 tiles in RAT room and from C423.

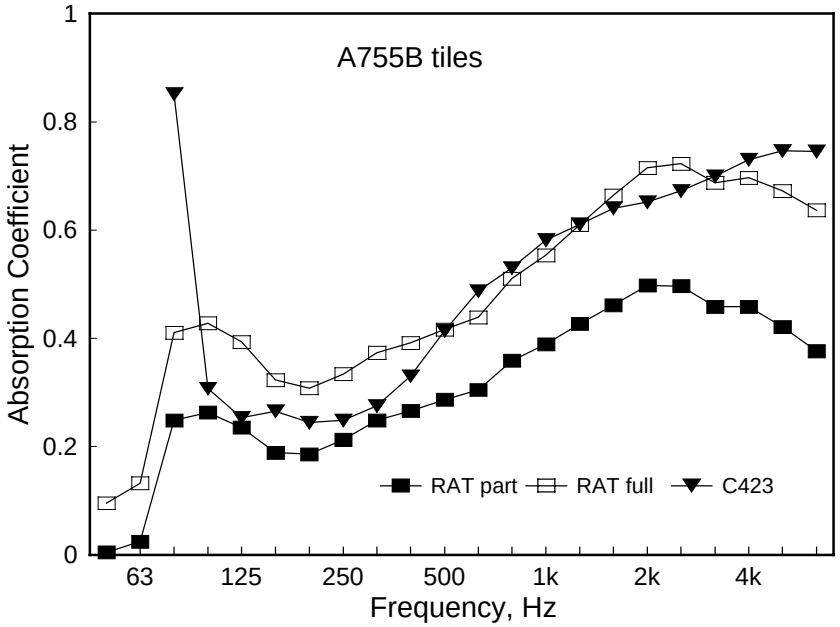

Figure 15-3: Absorption coefficients for A755B tiles in RAT room and from C423.

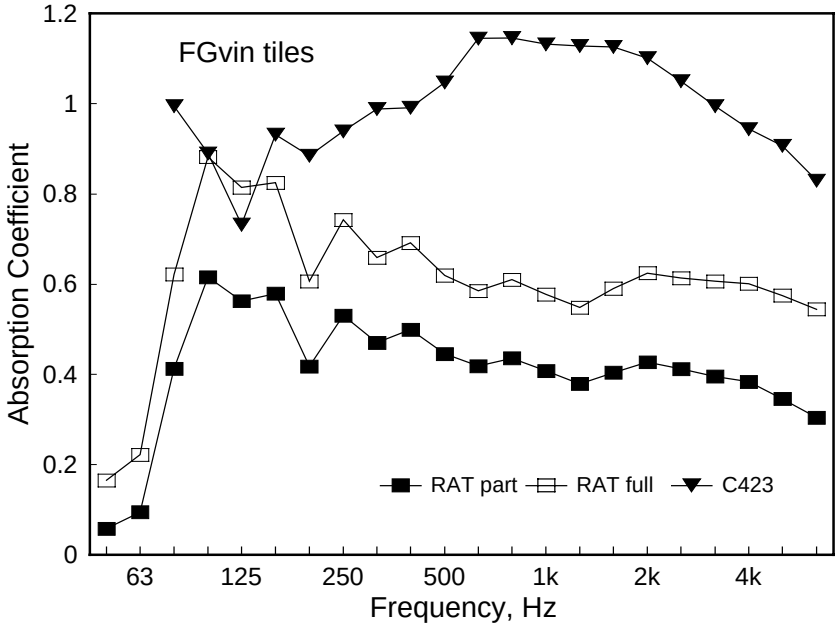

Figure 15-4: Absorption coefficients for FGvin tiles in RAT room and from C423.

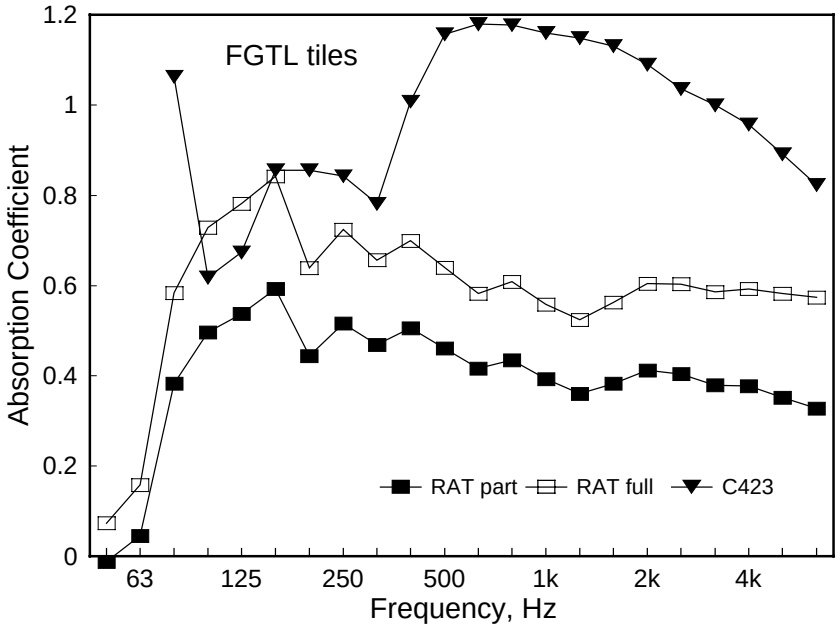

Figure 15-5: Absorption coefficients for FGTL tiles in RAT room and from C423.

16. Comparison of results from NRCC and Anemostat.

A unit nominally identical to Terminal B was tested by Shen, Milsom and Wilke in the Anemostat facility. The ceiling in that case was USG Auratone installed 8 ft 6 in above the floor. The plenum depth was 36 in, the room measured 15 x 20 ft and the floor was carpeted. The test conditions were nominally the same as those used at NRCC: 1.5" inlet SP and 0.35" discharge SP. The report describing the measurements at Anemostat gives only the mean room sound pressure levels. The data in the report for a terminal unit the same as that tested at NRC are shown in Figure 16-1. The agreement between the laboratories is good and the lack of a difference between tile types is quite evident.

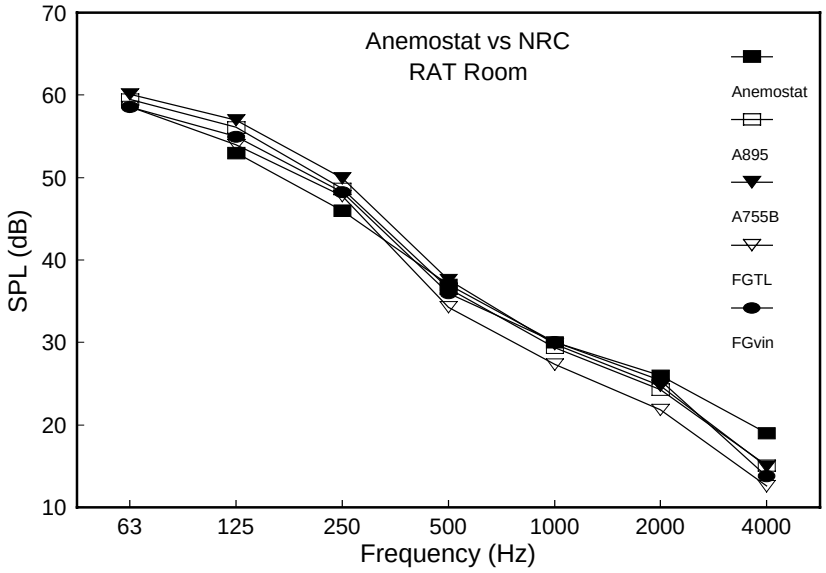

Figure 16-1: Sound pressure levels measured in Anemostat facility and NRC facility for Terminal B, a constant volume unit.

17. Future work.

A prediction of room sound pressure level can be made using the information that has been presented in this report. While efforts were made to vary as many parameters as possible, the information that has been collected has only led to an empirical approach to prediction which is necessarily limited in scope. The extension of the prediction schemes to be outlined here to very large spaces is somewhat problematic. There are some other unresolved issues with different levels of importance. To help focus on these and discuss possible future work, Table 17-1 summarizes what is known and what is unknown about sound from air terminal devices based on this research project.

Examination of this table reveals that there are several factors that might influence the average sound pressure level in the room or the decrease in sound pressure level with distance from the source. These factors are now discussed together with possible strategies for future research.

17.1 Effect of plenum depth and ceiling height

These two factors were not varied in the current project. As suggested in Table 17-1, if the primary source of noise is the lower face of the terminal unit, plenum depth is not likely to be a very significant factor. The effect of ceiling height is unknown but if most ceilings are around 2.4 m, then in practice this may not be a very significant variable either.

These two factors could be investigated in a room whose height can be varied and with a suspended ceiling that can be elevated to different positions. Alternatively, since orientation of the room does not affect the acoustics, ceilings could be installed as vertical planes in front of a movable wall with a VAV simulator directly behind. The movable wall could then be set in different positions, in effect changing the depth of the plenum. The 'height' of the room below the rotated ceiling could be changed by moving the ceiling and adjusting the movable wall. The disadvantage of these approaches is that the room volume below remains fixed.

17.2 Effect of room size

VAV devices can be installed in rooms ranging in size from offices for one or two people to large open plan offices. The range of room sizes covered in the present work was not great enough to allow prediction of the effect of room size. This is perhaps the most important factor that was not fully investigated.

There are two possible approaches to determining the effects of room size on the sound fields below the ceiling. One is to install one or more devices in the plenum in several different rooms. This approach, while it would give data firmly linked to actual installations, is fraught with logistical difficulties. Installing and then removing real VAV units and connecting an air supply would entail a great deal of disruption in an office and would not likely be acceptable to the owners or occupants. A VAV simulator

might be accepted, but one still has to deal with the many variations that would be encountered in different offices. Ceiling types, ceiling penetrations, and plenum conditions would all vary from one office to another. It would not be feasible to separate the effects of these variables from the room size effect.

An approach using scale modeling offers more control over the experimental variables since all the parameters of the model are selected by the researcher. In modeling work it is often difficult to create an accurate scale model of some materials and the critical material in this work would be the ceiling tiles. For this problem, however, it is not really necessary to create an accurate model of the ceiling tiles since it is the differences between simulations that are of interest. Scale model results could be related to the full-scale work done here.

Table 17-2 below shows scaled dimensions of T-bars, ceiling tiles, room and ceiling height and VAV simulator dimensions. Also shown are the maximum room sizes that would be simulated in the RAT room. Consideration of the practical difficulties of working with very thin materials suggests that the scale factors of 2.5 or 3.2 would be most suitable. The model facility would be a convenient size for working in and the materials would not be overly flimsy.

Another advantage of the model approach is that the effects of ceiling and plenum height could also be examined on the model scale.

17.3 Room Shape

The room used in this work was rectangular in plan. There may be differences in sound pressure level at a given distance from a source when the room shape changes. For example, levels at 3 m from the source in a room with a square plan may be different from those in a room with a rectangular plan. This could be evaluated in a model.

17.4 Ceiling attenuation and leakage

The results showed little difference in sound attenuation for common ceiling classes. It is probable that the attenuations found in this work will give acceptable precision in any prediction scheme. On the other hand, different systems for supporting ceiling tiles, for example, concealed splines, may give quite different results. If such systems are used to a significant extent, then their properties should be investigated.

No cases were measured where the ceiling was a continuous, solid layer of gypsum board. Such systems are perhaps not too common and it may not be considered necessary to actually construct and measure them. The assumptions used to calculate the attenuations of such ceilings are described in Section 0 and may be considered adequate.

17.5 Plenum obstructions

In buildings the quantity, type and disposition of devices in the plenum will vary widely. While plenum obstructions could be investigated in the laboratory, it is not likely to be practical to try to assign a number to these obstructions for use in a prediction algorithm. Hence this factor is called unknowable in the table.

17.6 Source radiation patterns

It was concluded in this work that the lower face of the terminal unit was an important factor in determining the sound pressure level in the room below. In principle, if there is no radiation from this face, then the sound pressure level should be quite different. In practice, there may be differences in radiation patterns between sources but these are not likely to be important judging from the results obtained in this work for typical terminal units.

17.7 Improvement strategies

The importance of the lower face of the terminal unit suggests that measures taken to reduce the radiation from this face of the unit might be very beneficial in situations where noise in the room below is excessive. A small research program could look at effect of adding a heavy layer directly to the lower face or a heavy layer backed by a cavity filled with sound absorbing material. It is possible that some repair techniques would exacerbate the situation because of resonances between the added layer and the terminal unit. The benefits accruing using this technique would depend on the importance of the sound energy from the lower face of the terminal unit relative to the sound energy coming through the ceiling from the plenum. It should be borne in mind too that the space available for such measures is very limited. The research program could also look at other strategies such as the use of sound absorbing material alone or changes to the ceiling in the vicinity of the terminal unit.

Table 17-1: Factors affecting average sound pressure level in the room, <SPL>, and rate of change of sound level with distance.

Factor	Effect on <SPL>	Effect on spatial decay of <SPL>.
Plenum Depth	Unknown, but if primary source is lower face of terminal unit, probably not very important.	Unknown, but probably not significant.
Ceiling Height	Unknown.	Unknown
Room size	Unknown, range of rooms studied not wide enough.	Unknown
Room shape	Unknown	Unknown
Plenum Absorption	Increased absorption reduces <SPL>	
Room Absorption	Reduces <SPL> at and above 250 Hz	Not significant for source above the ceiling.
Distance from terminal unit to ceiling	No significant effect.	No significant effect.
Area of lower face of terminal unit	Correlates positively with <SPL>	No significant effect.
Openings in plenum	Not important when typical ceiling leakage exists.	No significant effect.
Leakage around tiles	Primarily determines the insertion loss for the ceiling.	Unknown
Plenum obstructions	Unknowable.	Unknowable
Transmission to adjacent offices	Radiation from lower face of terminal unit is not a factor in the adjacent room so <SPL> is lower due to presence of dividing wall.	NA.
Room furnishings	Hard to quantify but could be examined.	Hard to quantify but could be examined.
Source radiation pattern	May not be an issue. Are sources strongly directional?	

Table 17-2: Some important dimensions for scale modeling.

	Dimension (mm)					
Scale Factor	1	2	2.5	3.2	4	5
T-bars						
height	30	15	12	9	8	6
width	25	13	10	8	6	5
Tiles						
width	600	300	240	188	150	120
length	1200	600	480	375	300	240
Thickness, MF	16	8	6	5	4	3
Thickness, GF	50	25	20	16	13	10
Room						
Room Height	3600	1800	1440	1125	900	720
Ceiling Height	2750	1375	1100	859	688	550
VAV simulator						
height	300	150	120	94	75	60
width	600	300	240	188	150	120
length	900	450	360	281	225	180
speaker diameter	200	100	80	63	50	40
	Simulated maximum room length and width (m)					
Room Length	10	20	25	32	40	50
Room width	3.7	7	9	12	15	19

18. Proposed amendments to ARI 885

Since there is no immediate likelihood of a new type of test or rating procedure for terminal devices installed in a ceiling or for the ceilings themselves, the model established by the existing ARI 885 should continue to be used but with modifications. The proposed procedure is listed here.

1. Obtain the sound power levels of the device, $L_w(f)$.

2. Subtract the environmental correction in Table 18-1.

3. Using the corrections, *k(f),* in Table 18-2 and the area of the surface of the source closest to the ceiling tiles, A_s (m^2), calculate the value $k(f)(A_s - 0.83)$ to be subtracted from the sound power values at each frequency.

4. Select the Ceiling/Plenum attenuations, $\alpha(f)$ from Table 18-3 according to the ceiling type in use and calculate the average sound pressure level in the room.

5. For practical purposes, the sound field in the room may be assumed to be essentially uniform up to distances of about 5 m from the source.

Table 18-1: Environmental correction to be subtracted from hemi-free field sound power levels or sound power levels determined in a reverberant room using the substitution technique.

Frequency, Hz	63	125	250	500	1k	2k	4k
Environmental correction factor, dB	4	2	1	0	0	0	0

Table 18-2: Factors to be used to compensate for source area effect.

Frequency, Hz	63	125	250	500	1k	2k	4k
Area Correction factor, k, dB	4.4	4.1	2.5	0	0	0	0

The model and the data used in this section should be used in the ASHRAE handbook. The existing text in the handbook should be modified to suit.

The data for the solid gypsum board ceiling given in Table 18-3 were obtained by adjusting the data for the tile measurements using the E90 and CIL data for the taped and untaped cases of G13. The estimate for the concealed spline case is based on the data presented by Mechel [21]. The values seem somewhat high, but may be correct. Mechel did not present data for the 63 and 4000 Hz band; these values were estimated. Estimates for the solid sheets of gypsum board are based on mass law corrections applied to the data for the 13 mm gypsum board.

Table 18-3: Ceiling/Plenum attenuations for generic ceiling types in T-bar suspension systems, except as noted.

Tile Type	Approximate Density, kg/m^2	Thickness, mm	63	125	250	500	1k	2k	4k
Mineral fiber	5	16	13	16	18	20	26	31	36
Mineral fiber	2.5	16	13	15	17	19	25	30	33
Glass fiber	0.7	16	13	16	15	17	17	18	19
Glass fiber	3	50	14	17	18	21	25	29	35
Glass fiber with TL backing	3	50	14	17	18	22	27	32	39
Gypsum board tiles	9	13	14	16	18	18	21	22	22
Solid gypsum board ceiling	9	13	18	21	25	25	27	27	28
Solid gypsum board ceiling	11	16	20	23	27	27	29	29	30
Double layer of gypsum board	18	25	24	27	31	31	33	33	34
Double layer of gypsum board	22	32	26	29	33	33	35	35	36
Mineral fiber tiles, concealed spline mount.	2.5 to 5	16	20	23	21	24	29	33	34

19. References.

[1] ASTM E90 – Standard Test Method for Laboratory Measurement of Airborne Sound Transmission Loss of Building Partitions.

[2] ARI Standard 885-90, 'Procedure for estimating occupied space sound levels in the application of air terminals and air outlets', Air-Conditioning & Refrigeration Institute, Arlington, Virginia, 1990.

[3] ANSI S12.31 – Precision Methods for the determination of sound power levels of broad-band noise sources in reverberation rooms.

[4] ARI Standard 880, "Air terminals", Air-Conditioning & Refrigeration Institute, Arlington, Virginia, 1990.

[5] ASTM C423 – Standard Test method for sound absorption and sound absorption coefficients by the reverberation room method.

[6] ASTM E795 – Standard Practices for mounting test specimens during sound absorption tests

[7] Schultz, T., 'Relationship between sound power level and sound pressure level in dwellings and offices', RP-339, ASHRAE Transactions 1985, V. 91, Pt. 1.

[8] Calibration of Reference Sound Sources, M. Vorländer, G. Raabe, Acustica, **81**, p247, 1995

[9] Revised Relation between the Sound Power and the Average Sound Pressure Level in Rooms and Consequences for Acoustic Measurements., M. Vorländer, Acustica, **81**, p332, 1995

[10] Blazier, Jr., W., 'Noise rating of variable air-volume terminal devices', ASHRAE Transactions 1981, V. 87, Pt. 1.

[11] Blazier, Jr., W. E., 'Improved guidelines for application of sound rating data to the acoustical design for HVAC systems', ASHRAE Transactions 1984, V. 90, Pt. 2.

[12] Beranek, L. L., *Noise and Vibration Control*, McGraw-Hill, N. Y., 1971.

[13] Ebbing, C. and Waeldner, W. J., 'Industry standard 885: an overview, estimating space sound levels for air terminal devices', ASHRAE Transactions 1989, V. 95, Pt. 1.

[14] Smith, M. C., 'Industry standard 885 acoustical level estimation procedure compared to actual acoustic levels in an air distribution mock-up', ASHRAE Transactions 1989, V. 95, Pt. 1.

[15] Int-Hout, D., 'Verification of ADC/ARI 885 application guidelines using acoustic intensity sound measurements', ASHRAE Transactions 1989, V. 95, Pt. 1.

[16] Mariner, T., 'Theory of sound transmission through suspended ceilings over partitions', Noise Control 5 (6), pp 13-18, 1959.

[17] Hamme, R. N., 'Laboratory measurements of sound transmission through suspended ceiling systems', J. Acoust. Soc. Amer., V. 33 , pp 1523-1530, 1961.

[18] Jonasson, H., ‘The sound insulation of suspended ceilings - theory, methods of measurement and interpretation of results’, Byggmastaren, 1973, 52(1), 17-20.

[19] Andersson, N. A.,’ Sound insulated suspended ceilings - some practical aspects’, Byggmastaren, 1973, 52(2), 15-19.

[20] Vercammen, M. L. S. and Scheers, Th. W., ‘Sound transmission through suspended ceilings’, Inter-noise 93, pp 983-986.

[21] F.P. Mechel, “Theory of Suspended Ceilings”, Acustica, **81**, p491, 1995

[22] M.J. Crocker and F.M Kessler, *Noise and Noise Control*, Vol II, Chapter 2, CRC Press, 1982

[23] I.L Vér, Enclosures and Wrappings, Chap.13 in *Noise and Vibration Control Engineering*, Ed. L.L Beranek and I.L Vér, J. Wiley and Sons, 1992.

[24] Jackson, R. S., ‘The performance of acoustic hoods at low frequencies’, Acustica, V. 12, pp 139-152, 1962.

[25] Jackson, R. S., ‘Some aspects of the performance of acoustic hoods’, J. Sound Vib., V. 3, pp 82-94, 1966.

[26] Junger, M. C., ‘Sound transmission through an elastic enclosure acoustically closely coupled to a noise source’, ASME Paper No. 70-WA/DE-12, 1970.

[27] Tweed, L. W. and Tree D. R., ‘Three methods for predicting the insertion loss of close-fitting acoustical enclosures’, Noise Control Engineering, V. 10, pp 74-79, 1978.

[28] Ver, I. L., ‘Reduction of noise by acoustic enclosures’, *Isolation of Mechanical Vibration Impact and Noise*, J. C. Snowdon and E. Ungar, Eds. (ASME Design Engineering Technical Conference, Cincinnati, Ohio, September 1973).

[29] Tweed, L. W. and Tree D. R., ‘A model of close fitting acoustical enclosures’, Noise-con 77, pp 319-330.

[30] Oldham, D. J. and Hillarby, S. N., ‘The acoustical performance of small close fitting enclosures, part 1: Theoretical models’, J. Sound Vib., 150, pp 261-281, 1991.

[31] Oldham, D. J. and Hillarby, S. N., ‘The acoustical performance of small close fitting enclosures, part 2: experimental investigation’, J. Sound Vib., 150, pp 283-300, 1991.

[32]. O’Keefe, E. J. and Stewart, D. R., ‘Insertion loss measurements of small rectangular enclosures’, Noise Control Engineering, V.15, pp 20-27, 1980.

[33] I.L. Vér and E. Veres, “An Apparatus to Study the Sound Excitation and Sound Radiation of Plate-like Structures”, Proc. InterNoise 80, pp535 -540.

[34] K.P. Byrne, H.M. Fischer, and H.V. Fuchs, “Sealed, Close-Fitting, Machine-mounted Acoustic enclosures with Predictable Performance:, Noise Control Eng. J. **31**, 7-15 (1988).

[35[Keith Walker, private communication to ASTM task group.

[36] Norman Bay, ETL testing laboratories, private communication to ASTM task group.

[37] J. Watson, Watson Moss Growcott Acoustics Pty. Ltd., Private communication to ASTM task group.

[38.] ASTM E1414 – Standard Test Method for airborne sound attenuation between rooms sharing a common ceiling plenum.

[39]. Halliwell, R.E., Quirt, J.D., Warnock, A.C.C., 1993, Design and commissioning of a new sound transmission facility, Proceedings of INTER-NOISE 93, p995.